Top Curr Chem (2012) 318: 109–192
DOI: 10.1007/128_2011_211

Published online: 9 August 2011

Liquid Crystalline Crown Ethers

Martin Kaller and Sabine Laschat

Abstract In this chapter, a comprehensive review over the entire reserarch on liquid crystalline crown ethers since their discovery will be given. Monomeric and polymeric molecules containing crown ethers as well as aza crown ethers, thia crown ethers and crown ethers with several different heteroatoms will be presented. Liquid crystallinity is, in most cases, caused by the substituents attached to the crown ethers. The respective macrocycle can be surrounded by multiple substituents or attachment can take place terminally or laterally. Within the substituents, a variety of geometries, such as rods, discs or tapers have been reported, resulting in different types of mesophases. The effects of complexation will be discussed in detail as complexation has a varying influence on the properties, ranging from the induction or stabilization of a mesophase to the destabilization or even the complete loss of the mesophase, depending on the crown, the salt or the counterion of the salt. For selected examples, the synthesis of the materials will be discussed. Possible applications in sensor or membrane technology as well as in chromatography will be shown.

Keywords Crown compounds · Liquid crystals · Mesophases · Metallomesogens · Polymers · Salt effects · Self-assembly · Substituent effects · Supramolecular chemistry · Phthalocyanines · Cyclophanes

Contents

M. Kaller and S. Laschat (✉)
Institut für Organische Chemie der Universität Stuttgart, Pfaffenwaldring 55, 70569 Stuttgart, Germany
e-mail: sabine.laschat@oc.uni-stuttgart.de

1 Introduction

Since the discovery of crown ethers, cryptands, and other macrocyclic ligands by Cram, Lehn, and Pedersen, who were awarded the 1987 Nobel Prize in chemistry "for their development and use of molecules with structure-specific interactions of high selectivity" [1], a completely new research field was opened: supramolecular chemistry [2–4]. Since then, this research field has been extended in many fields such as molecular recognition, organic sensing, and liquid crystals.

The combination of crown ethers with mesogenic groups is interesting because the resulting hybrid materials possess the properties of both constructive subunits, i.e., liquid crystalline order in the mesophase and the ability to complex specific cations selectively according to the crown ether cavity size.

Since the first description of substituted aza crown ethers **1** (Scheme 1) by Lehn in 1985 [5], showing columnar hexagonal phases, many groups have entered the field and extended the knowledge on structure-property relations in these versatile hybrid systems.

Matsuda presented the first examples of liquid crystalline crown ethers **2** (Scheme 2) in 1987 [6]. In all subsequent studies, he wanted to answer two

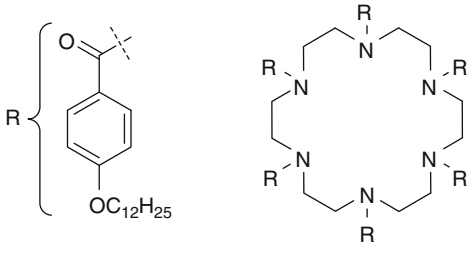

1

Cr 122 Col_h 142 I

Scheme 1 First liquid crystalline crown ether **1**

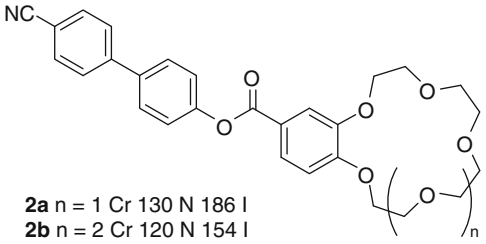

2a n = 1 Cr 130 N 186 I
2b n = 2 Cr 120 N 154 I

Scheme 2 First liquid crystalline crown ethers **2**

questions [7]: (1) what is the influence of a crown ether on the thermal properties of the liquid crystalline substituent and (2) how do complexed salts alter the thermal behavior? These fundamental questions must always be investigated when dealing with liquid crystalline crown ethers. This review discusses all substances with respect to these questions.

Until now, i.e., in 25 years of research, only two reviews on liquid crystalline crown ethers have been published [8, 9]. As both reviews cover the field only partially and, e.g., the fascinating polymeric crown ethers as well as taper-shaped liquid crystalline crown ethers are not discussed, we decided to give the first comprehensive review. The present chapter will be structured according to the molecular structure of the mesogens. The discussion of each type of crown ether mesogen will start with small molecules, continue with polymeric compounds, and conclude with possible applications (where applicable).

The present chapter will not deal with general topics of liquid crystals or crown ethers as this exceeds the scope of this volume. Interesting reviews and monographs on liquid crystals and their properties can be found in the literature [10–13]. The synthesis of crown ethers can be challenging. Most commonly, the synthetic routes are based on procedures established by Pedersen [14–17]. A review by Bradshaw [18] and a monograph edited by Patai [19] also cover the synthesis and properties of crown ethers. More recent reviews deal with the use of crown ethers as chemosensors [20, 21], potential antitumor agents [22], molecular wires [23], or carriers for the separation of metal ions in liquid membrane processes [24].

2 Mesogenic Crown Ethers

The schematic representations used to describe the molecular design of the discussed mesogens are depicted in Table 1.

For the mesophase ranges, we will use the following nomenclature:

$Phase_1$ xx °C $Phase_2$ yy °C I	Phase transitions upon heating
I yy °C ($Phase_2$ xx °C $Phase_1$)	Phase transitions upon cooling (mostly used in the case of monotropic phases)
$Phase_1$ yy °C ($Phase_2$ xx °C) I	Monotropic phase upon cooling

All phase transition enthalpies will be omitted for reasons of clarity.

2.1 Terminally Attached Crown Ethers with Rod-Like Substituents

The general design of the following crown ether mesogens is a terminal crown ether connected to a calamitic unit carrying flexible side chains and optional functional groups (Fig. 1).

Table 1 Schematic representation of the building blocks of the discussed mesogens

Symbol	Explanation
	crown ether
	disk-like unit
	flexible chain
	functional or polymerizable group
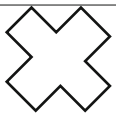	phthalocyanine
	rod-like unit
—	spacer

Fig. 1 Rod-like mesogen with terminal crown ether

2.1.1 Monomeric Compounds

Matsuda [6, 7] was the first to synthesize liquid crystalline crown ethers of this type. Benzo[15]crown-5 and benzo[18]crown-6 were attached to a cyanobiphenyl moiety via an ester (**2a**,**b**) or an ethynylene (**3a**,**b**) linker group (Scheme 3). The synthesis was straightforward starting from the respective crown ethers carrying carboxylic acid chlorides (**4a**,**b**) or ethynylene (**5a**,**b**) functional groups. Linkage was achieved by esterification with hydroxy cyanobiphenyl **6** or by Sonogashira coupling with iodo-cyanobiphenyl **7**.

Matsuda and coworkers investigated (1) the effect of a crown unit on the mesomorphic properties and (2) the behavior after complexation with suitable salts. These issues are still relevant today in current investigations.

Upon addition of a terminal crown ether to the calamitic core unit, nematic phases were observed for **2**, **3** in agreement with previous studies on substituted cyano biphenyls [25, 26].

Ester-linked crown ether **2a** with a 15C5 substituent showed a nematic phase width of 56 K (Scheme 3). For the homolog with an 18C6 unit (**2b**) it could be noted that the transitions generally occurred at lower temperatures and the phases were less stable (a range of 34 K). Ethynylene-linked crowns **3** showed a similar behavior as their ester-linked homologs **2**. For 15C5 (**3a**), melting into the nematic phase was observed at 165 °C and clearing at 202 °C while **3b** with the larger 18C6 showed melting at and clearing at significantly lower temperatures (122 °C and 162 °C,

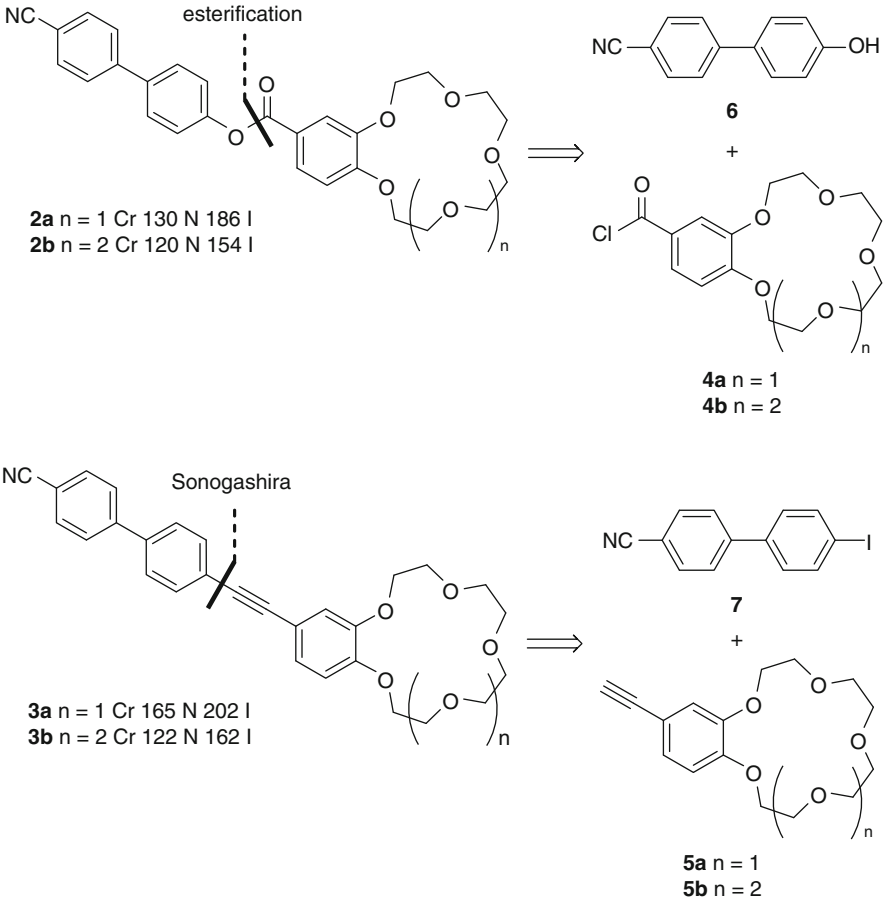

Scheme 3 Retrosynthesis of liquid crystalline crown ethers **2**, **3**

respectively). This behavior was attributed to the larger and more flexible crown in 18C6 derivatives leading to disorder and lower transition temperatures.

The complexation of ester-linked **2** with picrate salts was monitored by absorption and fluorescence spectroscopy [7, 27]. Sodium picrate doping of **2a** with a 15C5 moiety led to a red shift in UV measurements (in the mesophase) while potassium and tetramethylammonium picrate did not show this effect. This result was taken as evidence for the selective complexation of sodium cations by the crown mesogen. The uptake of sodium picrate had drastic effects on the nematic-isotropic transition which was lowered from 186 °C (without sodium picrate) to 120 °C upon complexation with 0.5 equiv. of sodium picrate. It was suggested that this result originates from the decreased anisotropy and polarizability of **2a** that leads to steric effects hindering molecular packing and thus lowering the clearing temperatures.

It is also possible to attach chiral peripheral groups to benzo[15]crown-5 as demonstrated by Shinkai [28]. In **8** (Scheme 4), a cholesteryl subunit was attached using an ester group as linker and a chiral nematic phase was observed.

For the liquid crystalline behavior, the position of the ester group was crucial. Introduction of an ethyl spacer in **9** led to the complete loss of the mesophase and

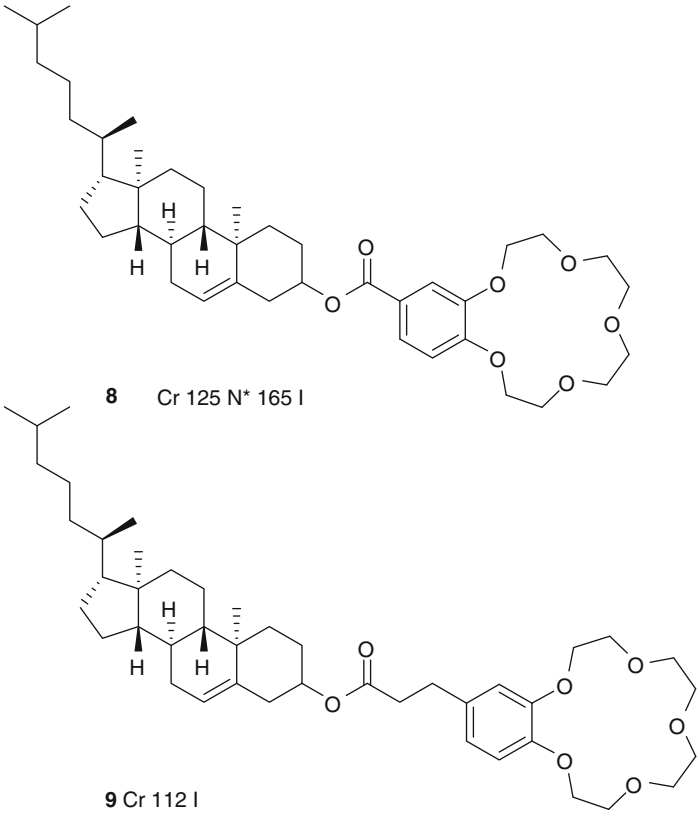

8 Cr 125 N* 165 I

9 Cr 112 I

Scheme 4 Liquid crystalline crown ethers **8**, **9** with cholesteryl subunits

only melting to the isotropic phase was observed. Most interestingly, a 1:1 mixture of **8** and **9** exhibits a liquid crystalline phase between <0 and 108 °C. The **8/9** 1:1 mixture was used to produce an ion-permeable membrane[28]. Perylene®, **8** and **9** were dissolved in $CHCl_3$, spread on a glass plate, dried in high vacuum, and tempered at 140 °C. The resulting membrane was 70 μm thick and used for ion transport studies. It was shown that both NaSCN and KSCN could be transported across the membrane. Sodium cations were transported faster than potassium cations, which is due to the perfect recognition of Na^+ by 15C5. The activation energy for the permeation of Na^+ is $E_A = 43.4$ kJ mol^{-1}, indicating an ion translocation process through the ion channels consisting of stacked crown moieties.

Subsequent studies on the chiral nematic phase of **8** and **10** showed the influence of complexed salts on the liquid crystalline properties. In the complexes (Scheme 5), the helical pitch was strongly affected by the complexed cation and the counterions [29].

For MSCN·**8**, the pitch increased with increasing radius of the cation in the order of $Li^+ < Na^+ < Cs^+ < K^+$ while the order changed for MSCN·**10** with $Li^+ < Na^+ < K^+ < Cs^+$. On investigation of the helical pitch in complexes KX·**10** it was found that the pitch increased with the size of the anion $Cl^- < SCN^- < ClO_4^- \ll B(p\text{-}Cl\text{-}C_6H_5)_4^-$. The authors proposed the use of **8**, **10** as promising host-guest sensory systems.

In a subsequent study [30], cholesteryl-substituted 18C6 derivative **11** and diaza [18]crown-6 **12** (Scheme 6) were used to create solid-supported bilayer lipids. The liquid crystalline crown derivatives **11**, **12** were dissolved in chloroform and mixed with squalene or squalene saturated with cholesterol. The solid-supported bilayers were prepared in freshly cut stainless steel wires. A 10^{-4} to 10^{-1} mol L^{-1} solution of MCl (M = Li, Na, K, Rb, Cs) or $MgCl_2$ was used as aqueous phase. Measurement of the membrane potential revealed a Nernst response to the concentration of M^+ in solution. It was possible to differentiate between the different cations which might be used for the preparation of new ion sensors. For the detection of K^+ and Rb^+, aza crown derivative **12** proved to be the most selective. A problem was the presence of traces of $Fe^{2+/3+}$ that made the measurements difficult. It was also not

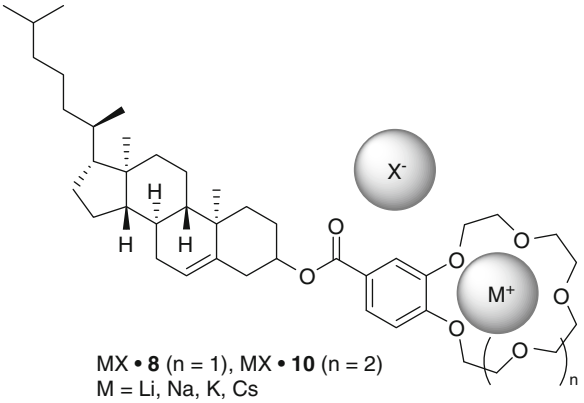

MX • **8** (n = 1), MX • **10** (n = 2)
M = Li, Na, K, Cs
X = Cl, ClO_4, SCN, $B(p\text{-}Cl\text{-}C_6H_4)_4$

Scheme 5 Complexation of chiral liquid crystals **8** and **10** with alkaline metal salts

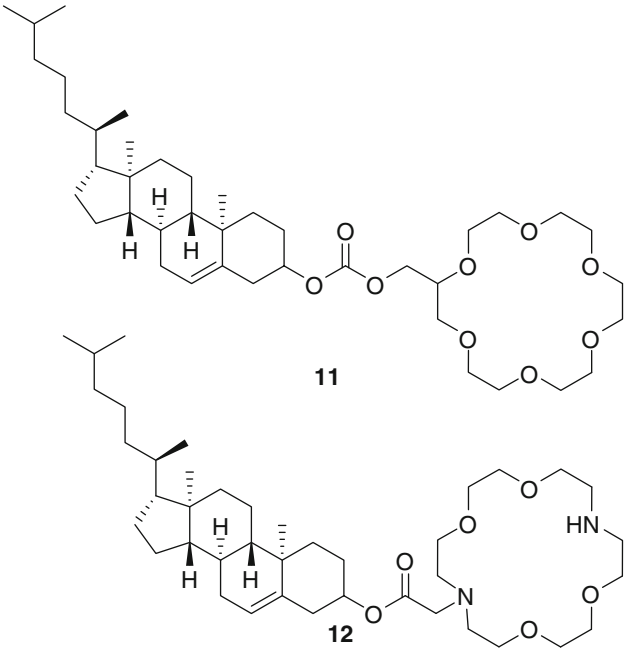

Scheme 6 Cholesteryl-substituted [18]crown-6 **11**, **12** and diaza[18]crown-6

possible to detect Li^+ and Mg^{2+} due to their low binding constants resulting from their small diameters, high charge density, and high hydration energy.

Jiang and co-workers presented a series of substituted crown ethers (Scheme 7) with the macrocycle being attached via an ester (**13a**), amide (**13b**), imine (**13c**), or aza (**13d**) spacer [31]. All compounds exhibit liquid crystalline phases (Fig. 2). The clearing points decrease in the order –N=CH– > –N=N– > –C(O)O– > –C(O)NH–. While **13a**,**b** with ester or amide linkers possess only nematic phases, smectic and nematic phases were observed for **13c**,**d** with imine or aza bridges. The reason why compounds **13c**,**d** with imine and aza spacers exhibit additional smectic phases and high clearing points is the presence of an additional double bond in the spacer. The electrons in this particular bond are delocalized into the two adjacent benzene rings leading to a large flat and conjugated system. The intermolecular attraction between **13c**,**d** is therefore higher than for **13a**,**b** where the conjugation is interrupted by the C=O bond. Thus, **13a**,**b** show nematic phases only with low clearing points (Fig. 2).

Judeinstein found that crown ethers **14** (Scheme 8) with a nematogenic unit linked via an imine bond showed monotropic mesophases upon cooling that were stable until room temperature [32]. When the aromatic core was extended by an additional benzene ring in **15a**, the melting temperatures to the nematic phase were raised to ~150 °C and the clearing temperatures to ~200 °C. Lateral substitution of the additional ring in **15b** decreased the clearing temperatures to ~90 °C. The complexation of **15a** with NaOTf and $LiBF_4$ was also investigated [32]. It was found that the phase width of the nematic phase decreased with increasing amounts

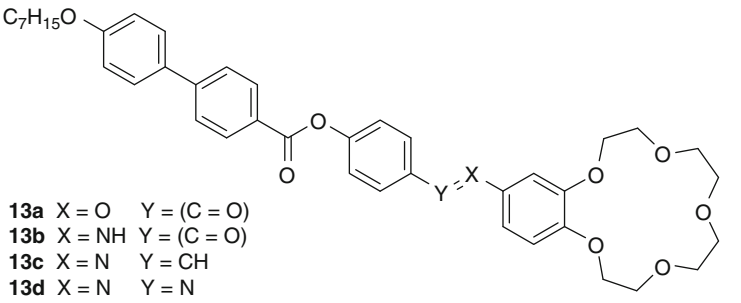

13a X = O Y = (C = O)
13b X = NH Y = (C = O)
13c X = N Y = CH
13d X = N Y = N

Scheme 7 Liquid crystalline crown ethers **13** with different spacers

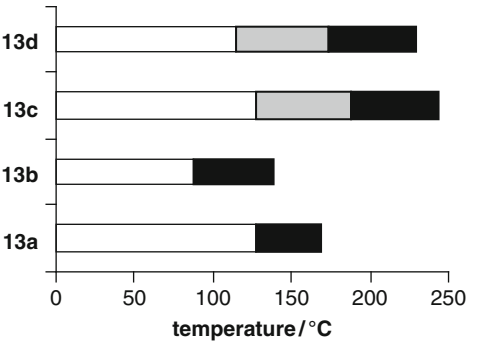

Fig. 2 Mesophases of **13a–d**; *white shade* crystalline, *grey shade* smectic, *black shade* nematic

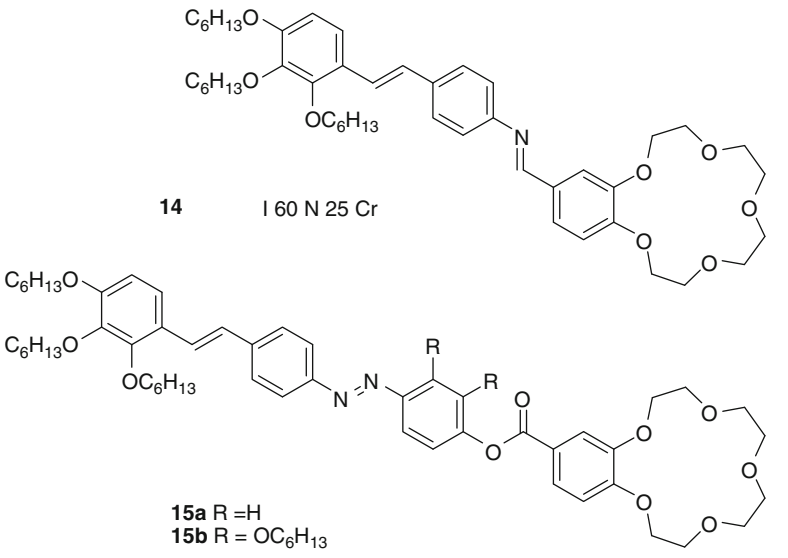

Scheme 8 Liquid crystalline crown ethers with imine **14** and aza **15** spacers

of salt, having a minimum at 0.5 equiv. of added salt due to the formation of sandwich complexes. Upon further addition of salt, a smectic phase was induced that had the maximum phase width at 1.0 equiv. of added salt. Thus, the phase type and the phase stability could be tuned by an external stimulus.

Most of the above liquid crystalline crown ethers contained a benzo[15]crown-5 unit or common [18]crown-6 as well as some aza derivatives. It was also possible to obtain liquid crystals **16** (Scheme 9) containing more unusual crown ethers such as 1,4-dithia-7-azacyclononane [33].

The dithiaazacrown was modified with a variety of rod- and disc-like substituents. With the shortest rod-like substituent carrying one terminal octyl chain (**16a**), direct melting into the isotropic state was observed. By adding an additional *p*-salicylic acid group (**16b**), a monotropic nematic phase was observed upon cooling. Attaching a second octyl chain gave **16c** but destroyed the mesomorphism and the only visible transition was isotropic melting. However, adding a third terminal alkyl chain in **16d** gave a material that exhibits a columnar hexagonal mesophase. There is a subtle relation between the molecular structure and the observed phases: clearly rod-like substituents as in **16b** exhibit a nematic phase and clearly discotic substituents as in **16d** give columnar phases. Molecules with a morphology in between (**16c** with two terminal chains) give no mesophase.

2.1.2 Polymeric Compounds

A variety of polymers containing liquid crystalline crown ethers of the molecular shape discussed in this section is known throughout the literature, most of which originate from Percec's laboratory.

One of the first published examples (Scheme 10) was the modified polymethacrylate **poly(17)** obtained from monomer **17** containing a benzo[15]crown-5 unit and a biphenyl linked via an ester group [34]. The synthesis was

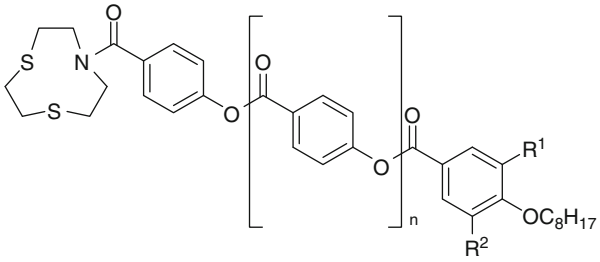

16a	n = 0	$R^1 = R^2 = H$	Cr 108 I
16b	n = 1	$R^1 = R^2 = H$	I 114 N 96 Cr
16c	n = 1	$R^1 = C_8H_{17}$ $R^2 = H$	Cr 90 I
16d	n = 1	$R^1 = R^2 = C_8H_{17}$	Cr 37 Col_h 48 I

Scheme 9 Liquid crystals **16** bearing thiaaza crown ethers

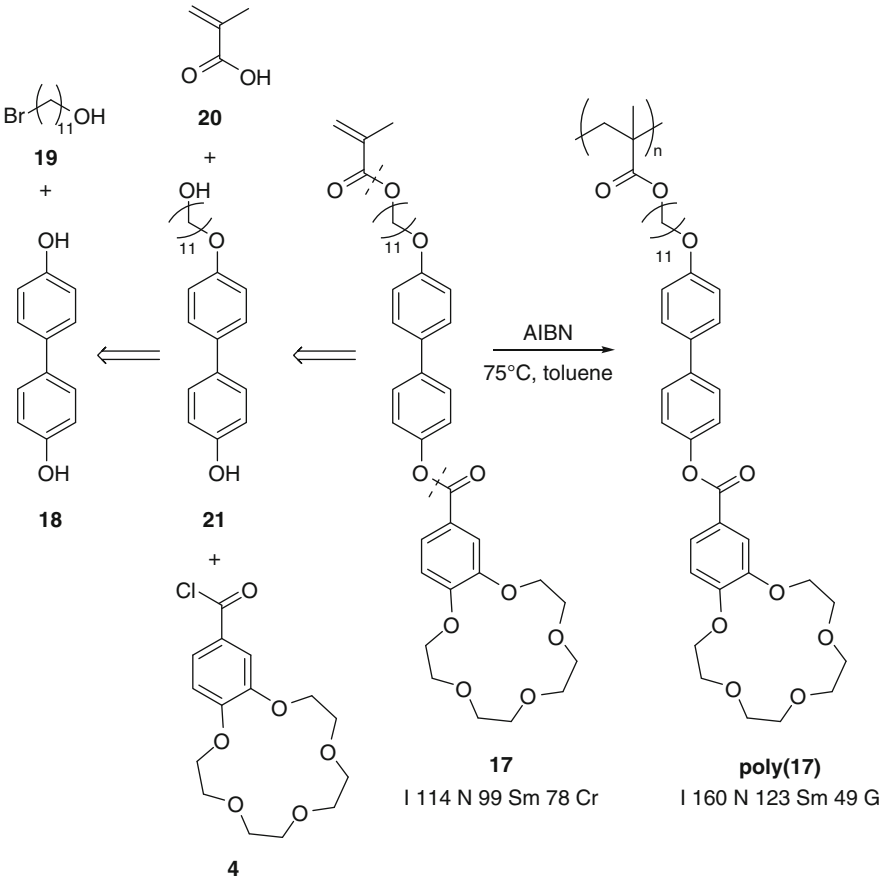

Scheme 10 Liquid crystalline polymer **poly(17)** and its precursors

straightforward starting from 4,4′-dihydroxybiphenyl **18** and 11-bromoundecan-1-ol **19**. Addition of a methacrylic acid moiety gave monomer **17**. Living radical polymerization was initiated with AIBN and carried out in toluene to give **poly(17)**. Monomer **17** and **poly(17)** display mesophases. Monomer **17** displays a monotropic nematic phase upon cooling which is stable for 15 K while **poly(17)** displays enantiotropic smectic and nematic mesophases stable for 111 K. Detailed X-ray scattering experiments [35] revealed the presence of SmA and SmC phases for **poly(17)**. It is remarkable that polymerization could turn a monotropic phase into an enantiotropic phase with a higher range of stable mesophases. The reason why the transition temperatures for the polymers are higher than for the monomers is a loss of degrees of freedom due to the limited free volume within the polymer.

When one of the phenyl groups in **poly(17)** was changed to a *trans*-1,3-dioxane ring (Scheme 11), the mesophase of the resulting **poly(22)** became smaller and the clearing transition was lowered by 33 K due to the loss of rigidity in the molecule [36].

Scheme 11 Liquid crystalline crown ether polymer **poly(22)**

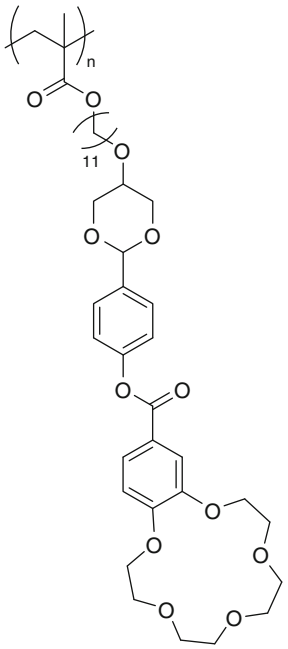

poly(22)
I 127 N 85 Cr

Percec and co-workers not only developed monomers suitable for radical polymerization but also presented systems suitable for the introduction into poly(methylsiloxane)s [34] via hydrosilylation (Scheme 12). Monomer **23** with a terminal double bond was added to the poly(methylsiloxane) using Cp_2PtCl_2 as a catalyst to give **'poly'(23)**. The trends observed for **'poly'(23)** were also found for **poly(17)** as polymerization improves the mesophase stability significantly.

Another mechanism to obtain polymers is cationic polymerization. Monomeric **24** which already displays a broad nematic phase could be polymerized to **poly(24)** (Scheme 13) which displays an even broader phase [37]. Neither the triple bond nor the crown ether moiety in **24** was affected by the harsh conditions for polymerization ($EtAlCl_2$, SMe_2).

A variety of other liquid crystalline crown ether containing polymers were synthesized, all possessing the same mesophase-stabilizing effect of polymerization (polymer effect) [38, 39].

Most interesting are the effects of salt complexation on the mesomorphic behavior of liquid crystalline crown ethers and liquid crystalline crown ether polymers. Sodium triflate was added to **poly(17)** [34] and **poly(25)** (Scheme 14) [39]. The enantiotropic nematic and smectic phases of **poly(17)** were changed dramatically [40]. With increasing amounts of salt, the clearing temperatures are shifted to higher values while the melting transition increases only slightly.

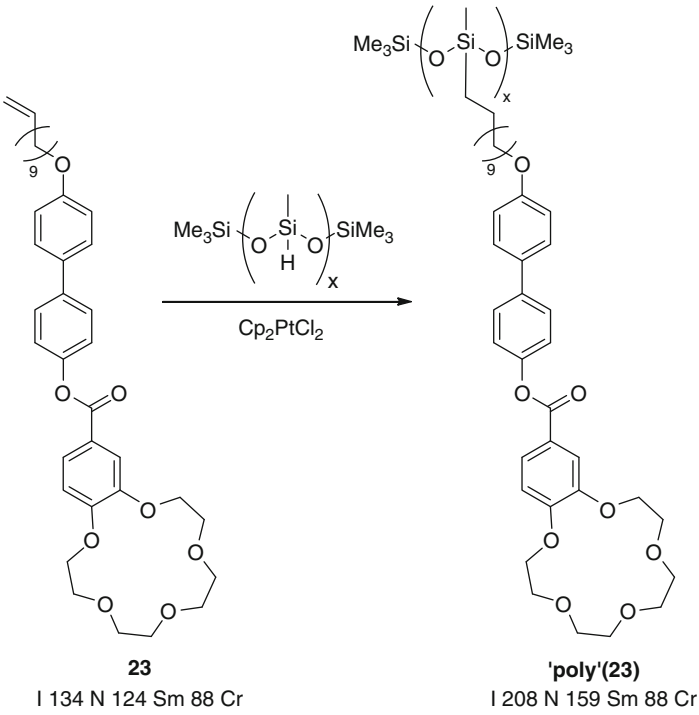

Scheme 12 Synthesis of crown-containing liquid crystalline polysiloxane **'poly'(23)**

Additionally, the smectic phase is lost and only nematic phases are being observed. One of the reasons for the increase in the mesophase stabilities upon complexation is the increased polarity of the crown moiety leading to stronger microsegregation. Also, the complexed crown is more rigid than the neat crown. The more polar the crown ether fragment, the higher the isotropization temperature. Uncomplexed **poly(25)** with a triple bond instead of a biphenyl group is crystalline. Complexation induced a smectic phase. Further experiments on similar polymers could confirm the observations and also revealed the stabilizing effect of complexation [41].

Bobrowsky prepared copolyacrylates **26**–**28** (Scheme 15) containing the nematogenic phenylmethoxybenzoate group as well as different crown ether substituted fragments [42]. The aim of the study was to obtain multifunctional materials. It is known that the incorporation of azobenzene groups into polymers leads to light-controllable films that might have uses in data recording and storage. In previous studies on crown ethers containing azobenzene groups, it could be shown that only the *Z*-isomer of the azobenzene group was able to form complexes with alkali metals whereas the *E*-isomer was unable to form complexes [43, 44]. Combination of both properties could yield novel polyfunctional materials. Unfortunately, the study revealed that the crown ether substituents are too bulky and prevent photoorientation of the azobenzene groups diminishing the photoinduced order. Another observation was the decrease in phase stability upon uptake of

Scheme 13 Cationic polymerization of **24**

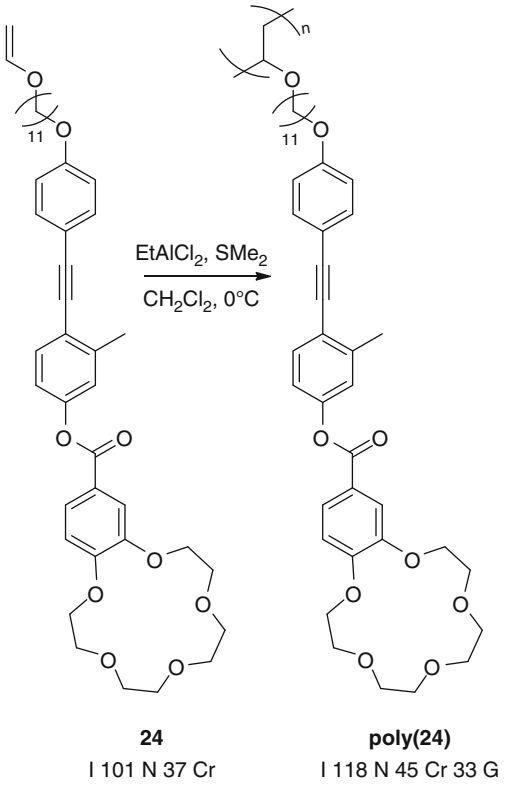

potassium perchlorate. This was attributed to the reduction of the side group anisotropy, mainly due to the presence of the perchlorate anion. Taking Percec's results from complexation experiments using sodium triflate [40] into account, it would be interesting for further investigations how **26**–**28** behave upon complexation of other salts with smaller anions.

2.1.3 Applications

Crown ethers of the type discussed in this section have been used as sensors, membranes, or materials for chromatography. Shinkai used cholesterol-substituted crown ether **10** as a sensor for chirality in chiral ammonium compounds (Scheme 16). It was found that the pitch of the cholesteric phase exhibited by **10** was changed upon addition of the chiral salt. As the wavelength of reflection for incident light depends on the pitch, a color change was observed that was visible to the naked eye [45, 46]. Such chirality sensing systems were known before but chromophores had to be bound to the crown ether in order to observe color changes [47]. This problem could be overcome by **10**, which uses intrinsic properties of the chiral nematic phase.

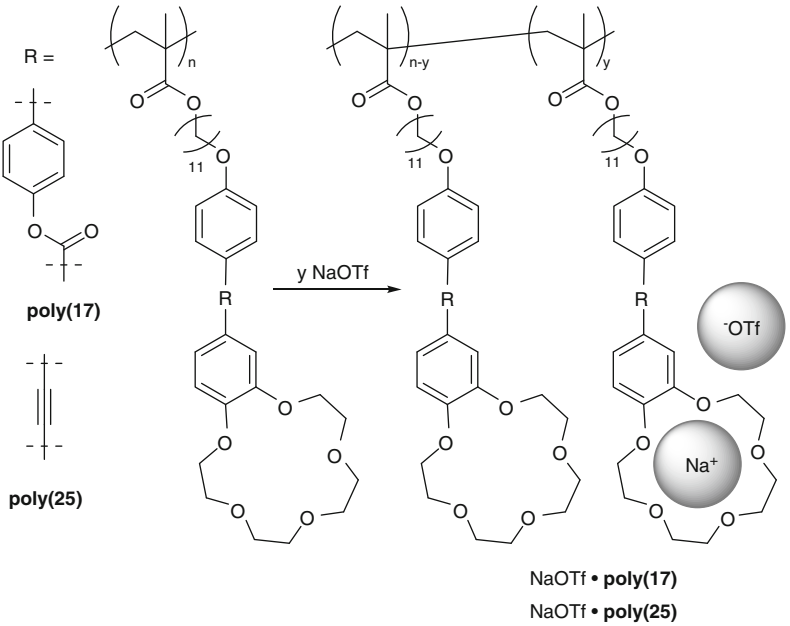

Scheme 14 Complexation of liquid crystalline crown ether polymers **poly**(**17**, **25**)

Kimura used the cholesterol-substituted [15]crown-5 **8** in ion sensing membranes. It was found that the addition of the crown ether affects the sensor properties, especially the ion specificity, and it was possible to obtain sensors with extremely high sensitivities [48]. The performance could be further increased by using perfluoroalkyl side chains instead of cholesterol [49].

Zeng used a silica monolith modified with the liquid crystalline crown ether **29** as a column material in capillary electrochromatography (Scheme 17) [50]. Polycyclic aromatic compounds, benzenediols, pesticides, and steroids were successfully separated on the column. Introduction of the liquid crystalline crown ether led to a significant improve of the electrochromatographic performance.

2.1.4 Summary

In most cases, the addition of a rod-shaped molecule to a crown ether leads to the formation of a nematic phase. In the case of addition of a chiral unit, such as cholesterol, chiral nematic phases can be observed. Some molecules can also show smectic phases when the attached rod shaped unit is long and inflexible.

Polymerization of liquid crystalline crown ethers leads to an increase in phase transition temperatures due to the loss of degrees of freedom.

Complexation can have different effects. In some cases, the phase widths were decreased upon complexation while stabilizing effects were observed in complexed

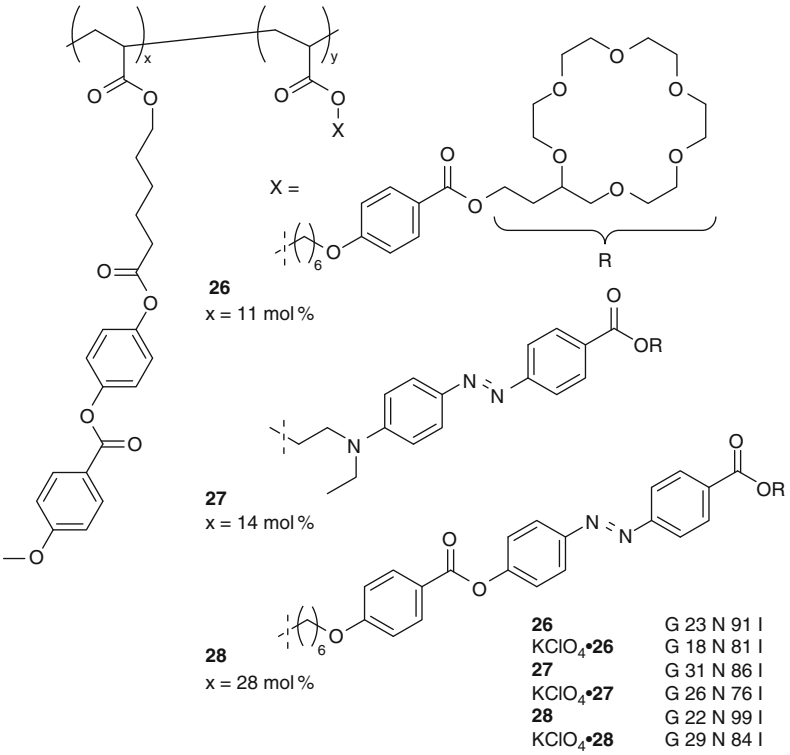

Scheme 15 Liquid crystalline polymethacrylates **26**–**28** containing [18]crown-6

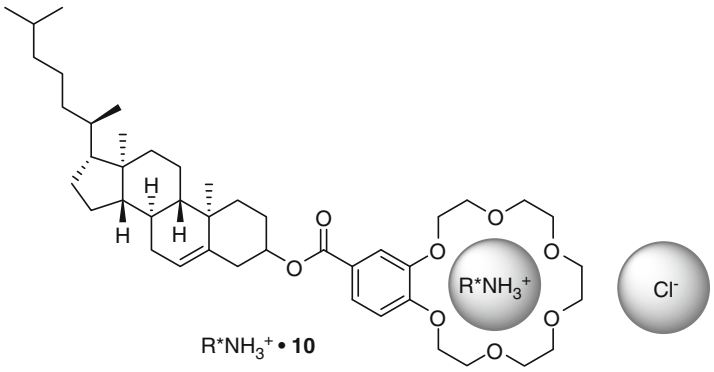

Scheme 16 Liquid crystalline crown **10** as chiral sensor

polymeric crown ethers. An exception to this behavior was found when perchlorate was used as the counterion – due to the size, the anisotropy of the complexes was decreased and the phase width decreased, too.

Scheme 17 Novel material **29** for capillary electrophoresis

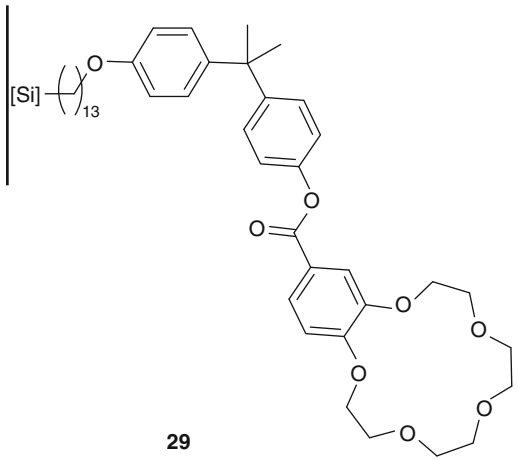

29

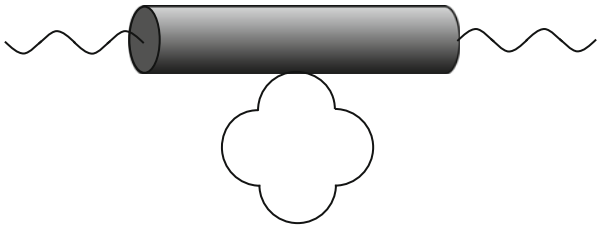

Fig. 3 Rod-like molecules with laterally attached crown ethers

2.2 Rod-Like Molecules with Laterally Attached Crown Ethers

The general design concept for liquid crystalline crown ethers discussed in this section consists of a rigid core with terminal chains and a laterally attached crown ether unit (Fig. 3).

2.2.1 Monomeric Compounds

Tschierske developed a variety of molecules containing a *p*-terphenyl unit as backbone equipped with two terminal decyloxy chains and laterally attached crown ethers of different sizes [51–53]. The synthesis was straightforward starting from methyl-2,5-dibromobenzoate **30** that was coupled with [4-(decyloxy)phenyl]boronic acid **31** in a subsequent Pd^0-catalyzed Suzuki reaction. The 2-hydroxymethyl crown ethers **32** were attached in the last step (Scheme 18) to yield mesogenic **33**.

In the crown ether derivatives **33**, only monotropic phases were observed. All compounds exhibited a very small nematic phase with a relatively broad smectic phase. Decreasing the size of the crown ether unit resulted in higher clearing points

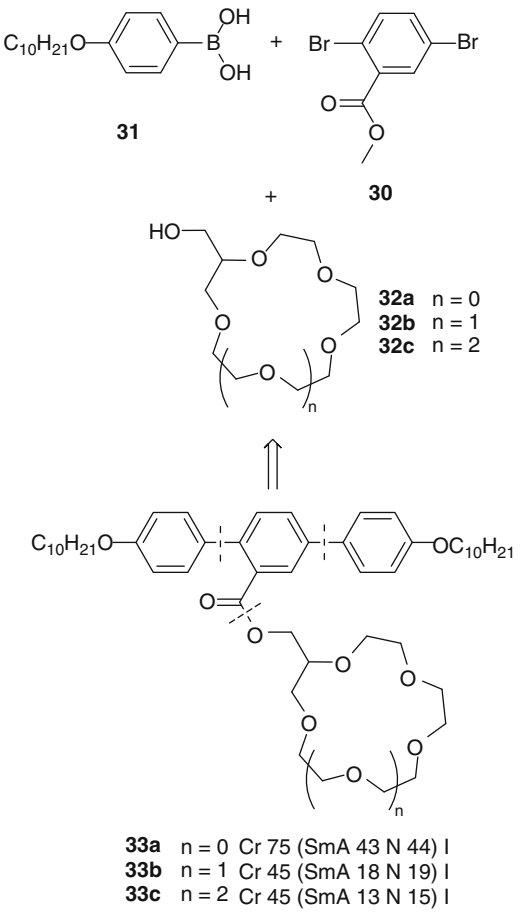

Scheme 18 Synthesis and mesogenic properties of crown ethers **33** with a lateral *p*-terphenyl group

and stability of the smectic phase. The bulky crown ether groups are normally prone to suppress smectic phases and induce nematic phases. It is likely that the crown ether units force micro-segregation between the rigid *p*-terphenyls and the alkyl chains. In conclusion, steric disturbance caused by the crown ether competes with layer-stabilizing micro-segregation and causes the observed phase behavior [54]. It is worth mentioning that crown ethers **33** form Langmuir films at the air-water interface. The properties of these films are strongly dependent on the nature of dissolved salt in the aqueous phase [53]. The most surprising and interesting effects of complexation on the mesophase behavior were observed in the system **33c** ($n = 2$)/water/MX [51]. First, it was observed that the lyotropic system MX/water/**33c** exhibits a columnar rectangular mesophase instead of a smectic phase for neat **33c**. Complexation with a salt can change the phase type. A ribbon-type model was proposed for the mesophase with the *p*-terphenyl units packed parallel to each other and separated by the complexed crown ether moiety with the solvent molecules. The space between the ribbons should be filled with the molten alkyl

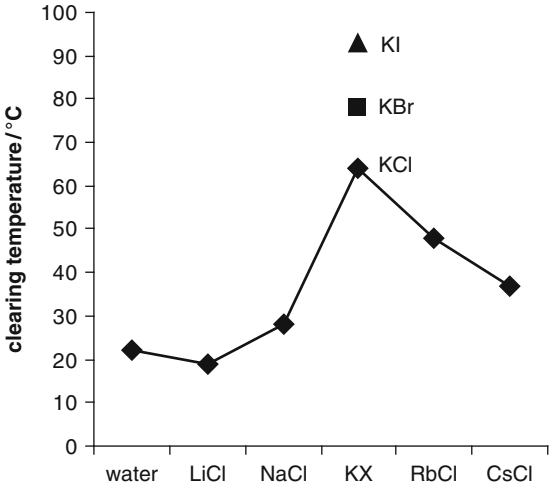

Fig. 4 Mesomorphic properties of the lyotropic system **33c**/water/MX

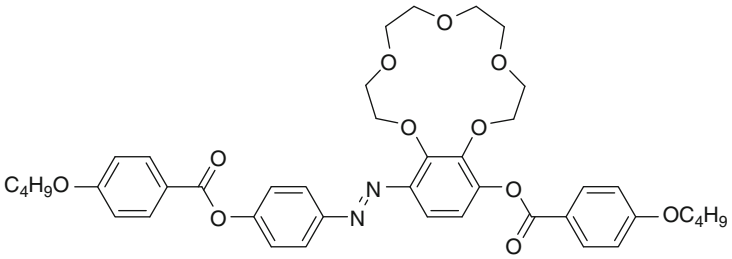

34
Cr 133 N 229 I

Scheme 19 Liquid crystalline properties of **34**

chains. The clearing points of the lyotropic columnar mesophases vary with the size of the cation. For cations which are smaller than the diameter of the [18]crown-6 unit (Li^+, Na^+), low clearing points are exhibited (Fig. 4). The same issue arises for Rb^+ and Cs^+, which are larger than the cavity. The highest clearing points were observed for K^+, which fills the crown perfectly. Another observation was the dependence of the clearing point on the anion of the complexed salt. For potassium halides, T_{clear} increases with increasing size of the counterion with $I^- > Br^- > Cl^-$ (Fig. 4). Ion pairing could be a reason for the increase in thermostability [55].

Bayle presented liquid crystal **34** (Scheme 19) bearing four aromatic units linked by ester and azo functional groups [56]. Two butyloxy groups are attached at the ends of the molecule and the crown ether is bound at the side of the molecule. The nematic phase exhibited by **34** is quite broad ($\Delta T = 96$ K). Upon complexation with $LiBF_4$, the nematic range diminishes with increasing amounts of added salt and disappears completely at 0.5 equiv. of added $LiBF_4$ which is most likely due to the formation of a 2:1 crown:lithium complex. From 0.2 equiv. of salt, a smectic

Scheme 20 Symmetric substitution on benzo[15] crown-5 and physical properties of **35**

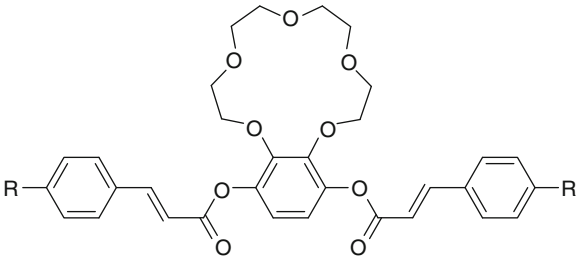

35a	R = $O(CH_2CH_2O)_1CH_3$	Cr 127 N 141 I
35b	R = $O(CH_2CH_2O)_2CH_3$	Cr 73 N 85 I
35c	R = $O(CH_2CH_2O)_3CH_3$	Cr 32 I
35d	R = $O(CH_2CH_2O)_1C_4H_9$	Cr 75 N 90 I
35e	R = $O(CH_2CH_2O)_2C_4H_9$	Cr 65 I
35f	R = OC_7H_{15}	Cr 122 N 147 I
35g	R = $OC_{11}H_{23}$	Cr 102 N 125 I

phase appears which gains in stability upon further addition of $LiBF_4$. Upon further (>0.5 equiv.) addition of salt, the smectic range stays almost constant. This is another example of molecular recognition that can change the type of mesophases.

The symmetric derivatives **35a–g** with lateral crown ethers prepared by the same group (Scheme 20) were used for three purposes: (1) to find out about the geometry of the lateral ring in the mesophase, (2) to examine the effect of different side groups, e.g., poly(ethylene glycol) chains, and (3) the further elucidation of the effects of $LiBF_4$ complexation [57]. The molecules prepared possess a mirror plane in the molecule to ease the assignment of the NMR signals observed in the ^{13}C 2D-SLF method used to elucidate the structure of the ring. The NMR experiments revealed that the crown ether moiety is far from being flat and the conformation changes significantly upon temperature changes. The most stable nematic phases were observed for **35f**,**g** with alkyloxy chains. When ethylene glycol fragments are included (**35a–e**) in the side chains, the clearing temperatures and nematic ranges decrease. If the number of $–OCH_2CH_2–$ fragments is too high, the nematic phase is lost (**35c**,**e**). Most surprising and in contrast to what was observed for $LiBF_4$·**34** [56], the mesophase was lost in $LiBF_4$·**35a–g**. A possible reason for this behavior could be the presence of the two ester groups that might form a peculiar cavity together with the crown macrocycle that is unsuitable for the uptake of Li^+. Another reason might be the presence of only three aromatic rings. This mesogenic unit is probably not powerful enough to overrule the geometry change upon complexation.

Ziessel and co-workers presented the "three block" crown ethers **36** (Scheme 21) [58] consisting of the aromatic part, the crown ether fragment, and the alkyl chains. Columnar rectangular mesophases were observed in X-ray experiments. The geometry of the phases is always *p2mm* and the columnar range is very broad ($\Delta T = 120$ K for **36a**) but decreases with increasing chain length as the melting points increase and the clearing points decrease. In the mesophase, microsegregation can be observed as the alkyl chains form a continuum while the molecules are disposed

Scheme 21 Liquid crystalline crown ethers **36**

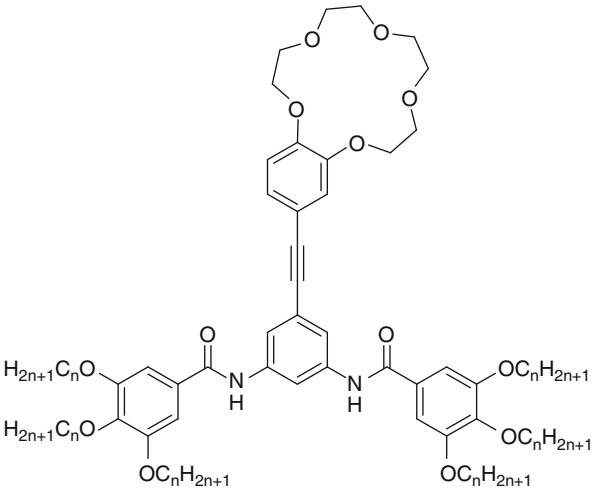

36a	n = 8	Cr 89 Col_r 209 I
36b	n = 12	Cr 109 Col_r 177 I
36c	n = 16	Cr 131 Col_r 175 I

alternately within the *p*2*mm* phase. In the third dimension, microsegregation will be maintained and the molecules are stacked over each other – probably in an alternating manner – allowing hydrogen bonds to stabilize the structure.

2.2.2 Polymeric Compounds

There is only one example that fits into this section and it uses a spectacular way to form the crown ether in the polymer that is worth noting (Scheme 22). In contrast to all other procedures that use crown ethers pre-formed in the monomers, this example by Percec forms the crown ether [13]crown-4 during the polymerization reaction [59]. Cationic cyclocopolymerization of 1,2-bis(2-ethenyloxyethoxy)benzene **37** with the mesogenic cyano biphenyl unit **38** gave copolymer **39** with a 1:1 ratio of **37**:**38** displaying a smectic phase.

2.2.3 Summary

There have been only a few reports on crown ethers laterally attached to rod-like molecules in the last few years. Nevertheless, very interesting compounds have been synthesized in the past. The general problem of this compound class is the flexible crown ether itself that can destroy the mesomorphic properties when attached laterally. Making the rigid rod longer can circumvent this problem. Another way to obtain stable mesophases is the complexation with suitable salts.

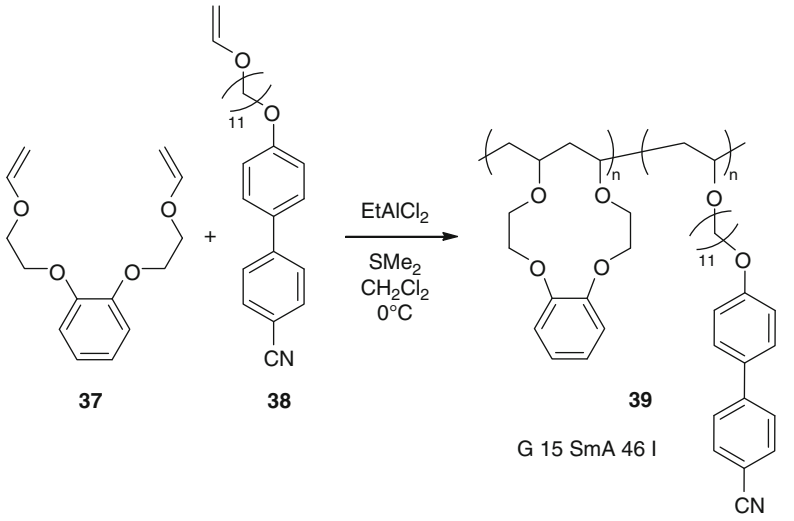

Scheme 22 Crown formation during polymerization

Examples were presented where the uptake of the salt led to a change of the mesophase geometry.

Future research in this field should concentrate on the effect of ion complexation and possible applications.

2.3 Central Crown Ethers with Terminally Attached Rod-Like Substituents

In this section, molecules will be discussed that have a crown ether in the center of the molecule which is substituted by two rigid rod substituents equipped with terminal flexible chains (Fig. 5). Attaching functional groups is also feasible.

2.3.1 Monomeric Compounds

Most of the liquid crystals discussed in this section bear a diaza[18]crown-6 **40**, a 4,4′-diaminodibenzo[18]crown-6 **41**, or a thia crown ether **42** in their center (Scheme 23). Substitution in **40** and **41** is conveniently feasible on the nitrogen atoms by formation of a Schiff base or an aza compound (in the case of **41**) or by N-alkylation or -acylation (in the case of **41**). *O*-Alkylation and -acylation of **42**, which are difficult to obtain, open a path to thia crown centered liquid crystals.

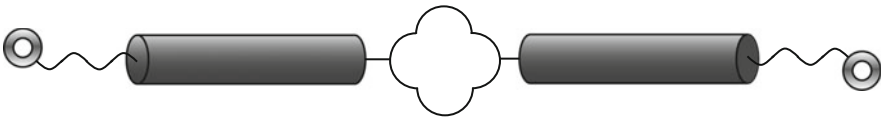

Fig. 5 Schematic representation of crown ethers with two rod-like substituents

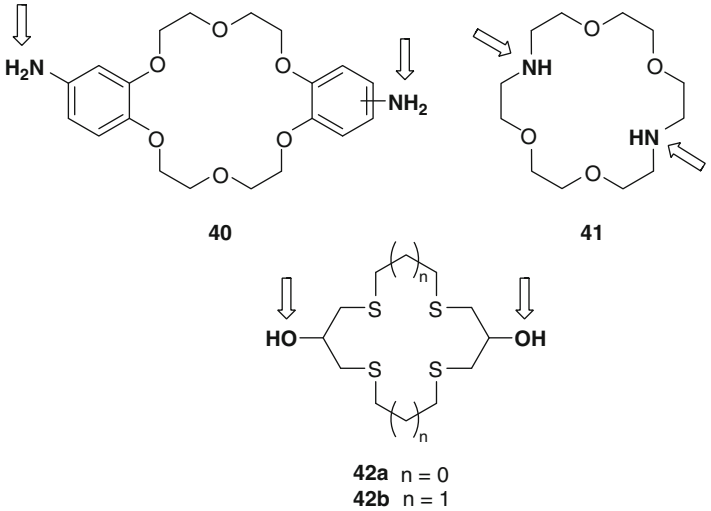

Scheme 23 Common precursors **40–42** for terminal attachment of mesogenic groups

Schiff Bases and Azo Compounds

The Schiff base (**43c**,**d**) and azo (**43a**,**b**) linked liquid crystalline crown ethers were synthesized (Scheme 24) by Xie [60] starting from dibenzo[18]crown-6 **44** which was nitrated with 68% nitric acid. Subsequent reduction with hydrazine and catalytic amounts of palladium gave 4,4′-diaminodibenzo[18]crown-6 **40**. The amino groups are either *cis* or *trans* and the products can be obtained separately according to literature procedures [61]. The Schiff bases **43c**,**d** were obtained by coupling **40a**,**b** with aldehyde **45**. In order to obtain the azo-linked compounds **43a**,**b**, **40a**,**b** (*cis* and *trans* refer to the positions relative to the crown ether, not to the geometry of the —N=N— double bond) was diazotizated followed by azo coupling with phenol and intermediate **46a**,**b** was finally esterified with acid chloride **47**.

The liquid crystalline properties of **43a–d** were interesting as all derivatives showed very stable mesophases with phase widths of 57–109 K. It is remarkable that Schiff bases **43c**,**d** are stable at temperatures above 300 °C. It also strikes that, in contrast to conventional calamitic liquid crystals, the Schiff bases **43c**,**d** possess significantly higher phase transition temperatures compared to azo linked **43a**,**b**. Additionally, the *trans* compounds tend to possess higher clearing temperatures due to the elongated shape of the molecules.

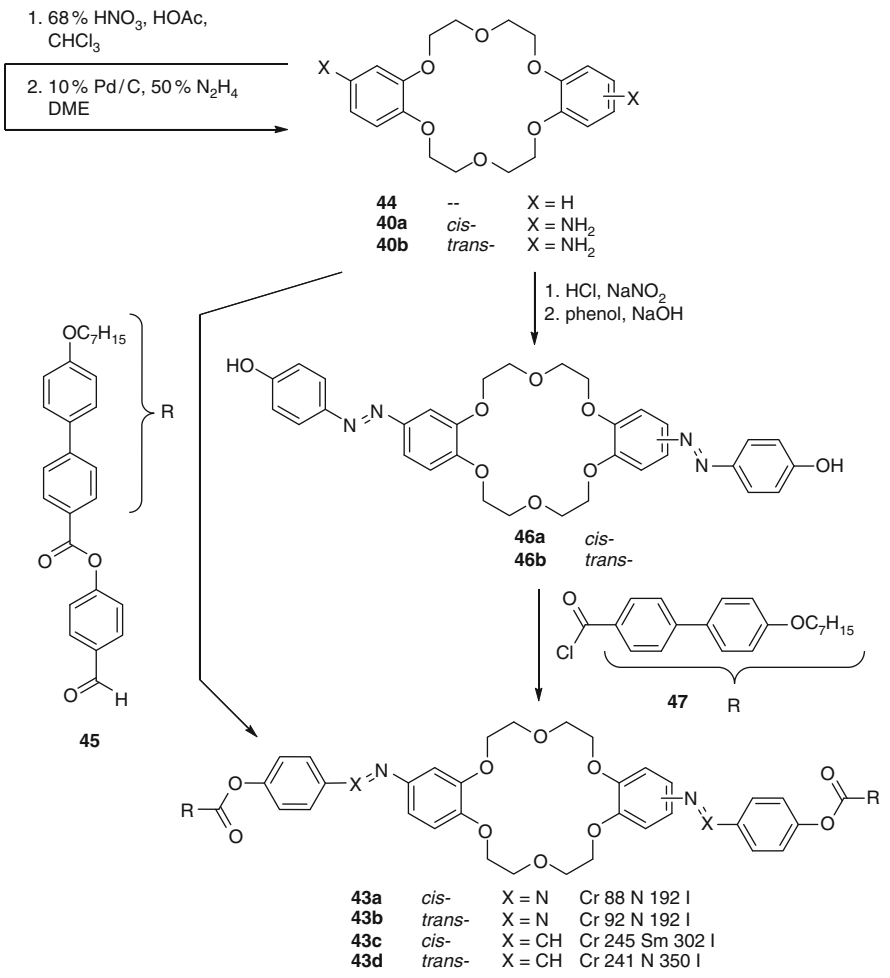

Scheme 24 Synthesis and properties of Schiff base and azo-linked liquid crystals **43**

Li and co-workers investigated derivatives of **43c**,**d** [62]. Instead of the terminal heptyl chains, chiral (*S*)-2-methylbutyl or dodecyl chains were used. For the methylbutane side chain, a chiral smectic and a chiral nematic phase were observed and the clearing points were higher than in **43c**,**d** due to the shorter chain while they were lower for the longer dodecyl side chains. It was also observed that the *trans*-compounds possess higher clearing temperatures compared to their *cis*-derivatives.

Menon presented a set of interesting liquid crystals **48** (Scheme 25) based on dibenzo[18]crown-6 modified with 2-hydroxy-3-methoxybenzene (**48a**), 3,4,5-trimethoxybenzene (**48b**), thiophene (**48c**), and pyrrole (**48d**) linked via a Schiff base [63]. All compounds are lacking long alkyl chains in the periphery. Nonetheless, broad mesophases with different geometries (SmC, SmA, N) were observed.

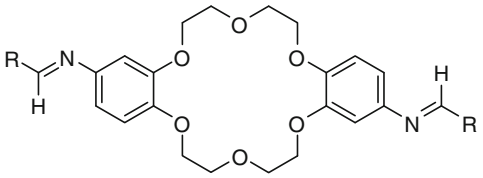

48a Cr 123 SmC 153 SmA 225 N 244 I
48b Cr 92 SmA 132 N 300 I
48c Cr 155 SmC 196 I
48d Cr 171 N 210 I

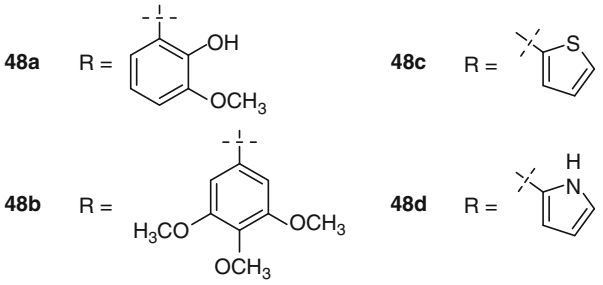

Scheme 25 Liquid crystals **48** devoid of peripheral chains

Diazacrowns

The first azacrowns with two mesogenic 4-[(4-(heptyloxy)benzyl)oxy]benzoic acid side groups bound to the crown ether *N*-atoms were presented by Xie [64] (Scheme 26). Neat **49** exhibits a nematic phase with a small ($\Delta T = 16$ K) range. Upon complexation with KCl, KI, and $KClO_4$, the nematic phase is lost while the clearing temperature is almost constant. Upon complexation with potassium picrate, the clearing point is lowered while the melting point is increased, resulting in a smaller mesophase. Complexation with thiocyanates also results in smaller mesophases as the melting points are increased while the clearing points remain virtually unchanged. Once more, complexation decreases the tendency to form mesophases.

Heiney [65] investigated Langmuir films formed by Xie's liquid crystalline crown ether **49** and improved the synthesis towards higher purity of the final product. It was found that **49** self-assembles at the air-water interface as depicted in Scheme 27. The crown ether part of the molecule is located at the aqueous side while the arms of the molecule are bent by the angle φ, which is small but different from zero, and point into the air.

Xie [66] also investigated derivatives of diaza[12]crown-4 (**50a**) and diaza[18]crown-6 (**50b–d**) with terminal cholesterol moieties (Scheme 28). While **50a** with the smaller ring is not liquid crystalline, the derivatives **50b–d** with the larger diaza[18]crown-6 center show remarkably stable smectic phases as observed under the POM. Comparing **50b–d** with each other, no specific tendency is observed. Derivative **50b** with the side groups added via a urethane group has a smectic range

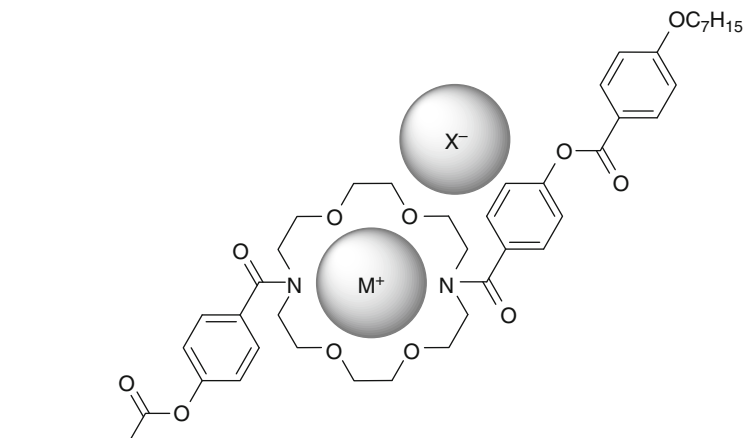

49 • free	Cr 113 N 129 I
49 • MX = KCl	Cr 128 I
49 • MX = KI	Cr 125 I
49 • MX = $KClO_4$	Cr 127 I
49 • MX = K-picrate	Cr 115 N 125 I
49 • MX = KSCN	Cr 120 N 129 I
49 • MX = NH_4SCN	Cr 119 N 130 I
49 • MX = NaSCN	Cr 119 N 130 I

Scheme 26 Effect of complexation on **49**

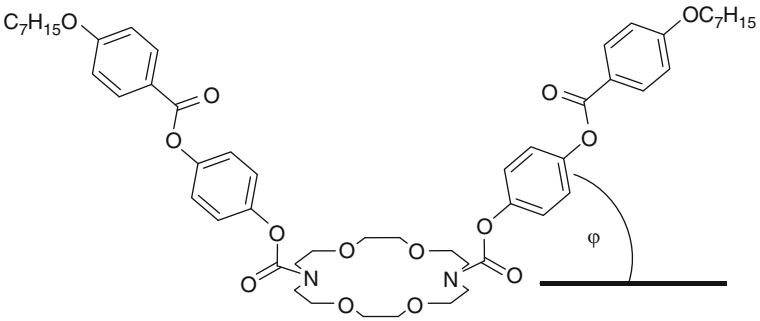

49

Scheme 27 Geometry of **49** at the air-water interface

of 66 K while derivative **50c** with a CH_2 spacer between the ester and the amino group has a much broader phase (133 K) and **50d** with an ethyl spacer has the smallest phase (31 K).

Goodby presented a series of substituted diaza crown ethers **51**–**53** (Scheme 29, Table 2) containing three aromatic rings on each attached arm and studied the effects of different central ring sizes (6-, 12- and 18-membered rings), different

Scheme 28 Aza crown ethers **50** modified with cholesterol

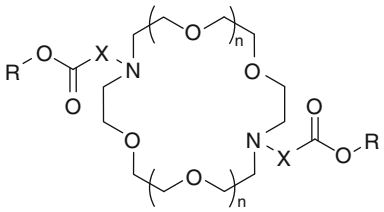

50a	n = 0	X = --	Cr 260 I
50b	n = 1	X = --	Cr 149 Sm 215 I
50c	n = 1	X = CH_2	Cr 125 Sm 258 I
50d	n = 1	X = C_2H_4	Cr 173 Sm 204 I

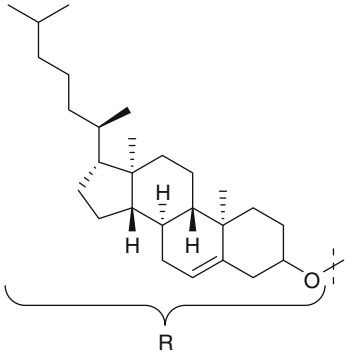

substitution patterns at the termini (dicatenar, tetracatenar, and hexacatenar), and different heteroatoms in the crown ether macrocycles (oxygen and sulfur) [67, 68].

First, the effects of different sized central rings and different heteroatoms in the crown ether of dicatenar compounds **51** with octyloxy chains in the periphery were investigated [67]. It was found that the mesomorphic behavior is strongly dependent on the size of the central ring (Table 3). While compound **51a** with a piperazine central unit possesses a clearing point at 322 °C (accompanied by decomposition), **51b** possessing a diaza[12]crown-4 central unit exhibits a clearing point which is 150 K lower. For **51c**, with the largest examinated central unit (diaza [18]crown-6), the isotropization temperature is on a par with **51b**. The reason for the huge differences in the phase transition temperatures is the flexibility of the crown ethers: small rings behave like a rigid core while larger rings behave like a flexible linker of the two mesogenic side groups. Concerning the phase types, it was found that the larger the crown, the less probable is the occurrence of smectic phases. On replacing the oxygen atoms by sulfur (**51d**) the mesogenity is almost lost, which is surprising as one would expect the opposite effect due to increased van-der-Waals interaction between the S-containing molecules.

For **51c**, temperature-dependent NMR experiments were carried out [67] that suggest the presence of a variety of conformers in solution. It was assumed that the same conformers will be present in the mesophase, too. The U- and zigzag-shaped

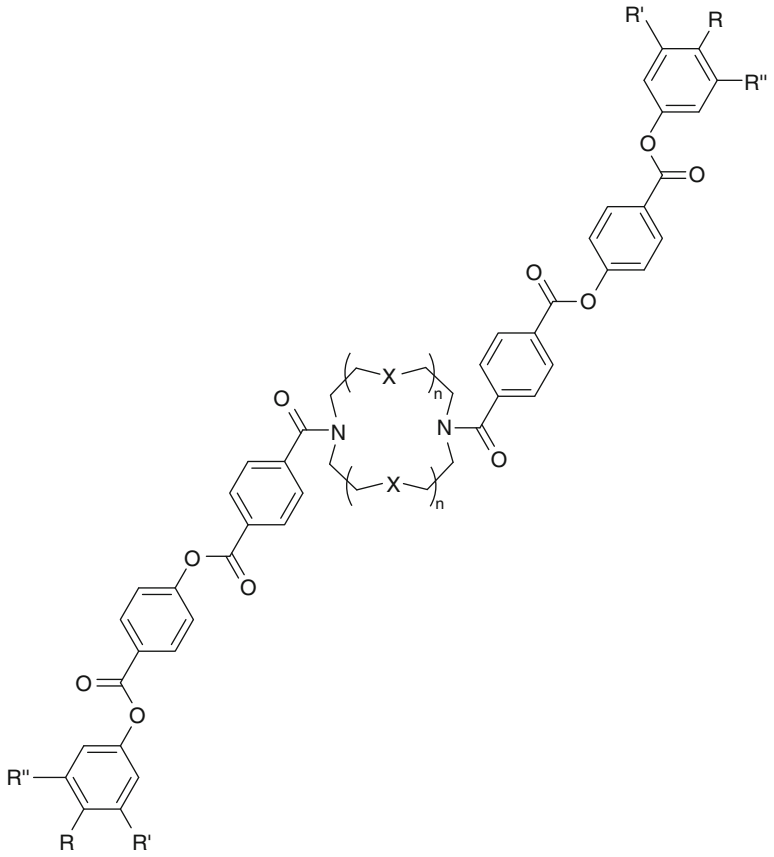

Scheme 29 Diaza crown ethers **51**–**53** of different sizes and with different terminal substituents

Table 2 Ring sizes and terminal substituents in **51**–**53**

Compound	X	*n*	R	R′	R″
51a	O	0	OC_8H_{17}	H	H
51b	O	1	OC_8H_{17}	H	H
51c	O	2	OC_8H_{17}	H	H
51d	S	2	OC_8H_{17}	H	H
52a	O	2	$OC_{10}H_{21}$	$OC_{10}H_{21}$	H
52b	O	2	$OC_{14}H_{29}$	$OC_{14}H_{29}$	H
52c	O	2	$OC_{16}H_{33}$	$OC_{16}H_{33}$	H
52d	O	2	$OC_{18}H_{37}$	$OC_{18}H_{37}$	H
53	O	2	$OC_{10}H_{21}$	$OC_{10}H_{21}$	$OC_{10}H_{21}$

conformers were discussed to be the most stable ones and were used to explain packing within the smectic layers (Fig. 6). Folding of this type of molecules was also observed by Heiney [65].

Table 3 Mesomorphic properties of **51**–**53**

Compound	Transition temperatures (°C)
51a	Cr 205 SmX 211 N 322 I decomp
51b	Cr 156 N 157 SmA 175 I
51c	Cr 170 N 184 I
51d	Cr 172 N 173 I
52a	Cr 138 (SmC ≈ 88) I
52b	Cr 134 (SmC 130) I
52c	Cr 120 (Col_h 90) I
52d	Cr 79 Col_h 86 I
53	G −6 Col_h 46 I

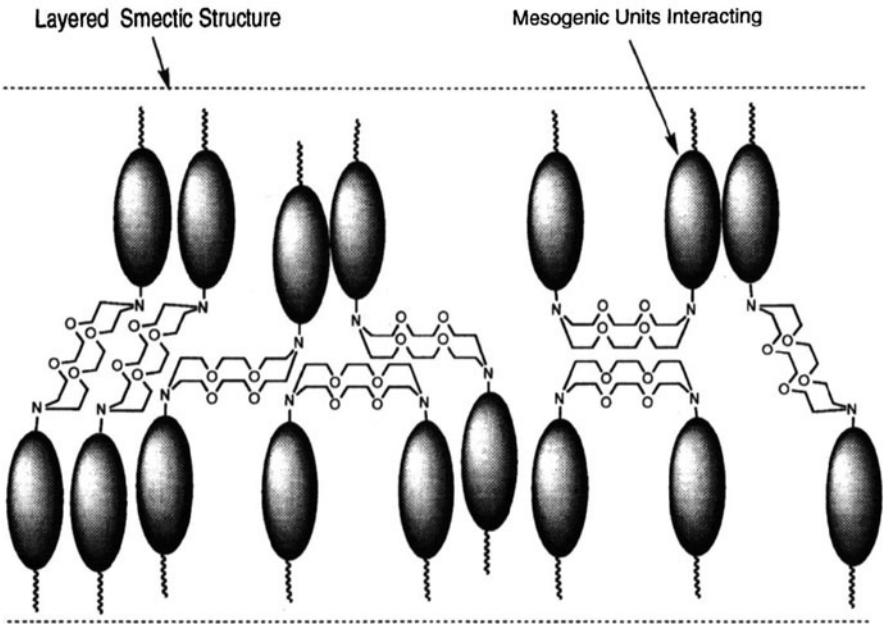

Fig. 6 Proposed layered structure of **51c**. Reproduced by permission of The Royal Society of Chemistry from [67]

Further investigations revealed the dependence of the mesomorphic properties on the number of terminal alkyloxy substituents [68]. While **51** and **52** are not directly comparable due to the different lengths of the terminal chains, the trend is clear: with increasing number of alkyl chains, the clearing temperatures are shifted to lower temperatures. This becomes more obvious on comparing **52a** with four decyloxy chains that clears at 138 °C with **53** carrying six decyloxy chains which clears at 46 °C. Overall, all examined compounds do not possess broad mesophases. Interestingly, tetracatenar derivatives **52c**,**d** possess columnar phases instead of smectic phases in the case of **52a**,**b**. Compound **53** also possesses a columnar phase as deduced from POM (Fig. 7) which can be explained by the presence of the terminal gallic acid group.

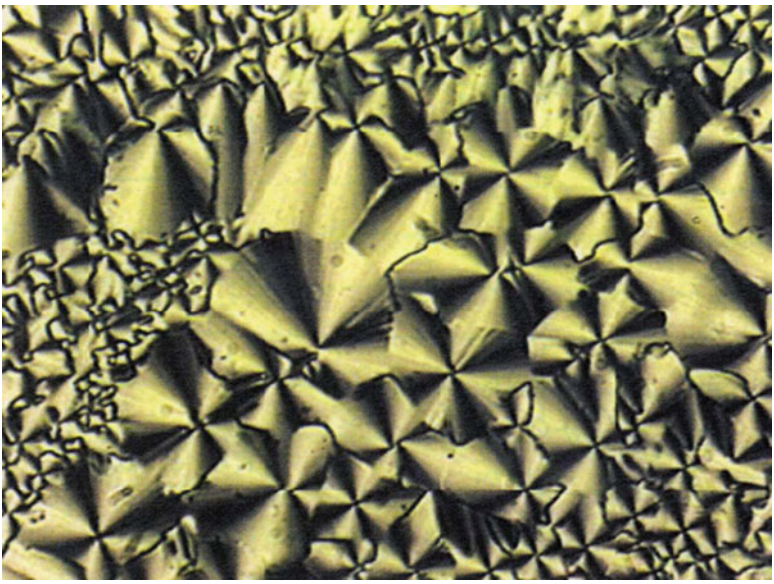

Fig. 7 Texture of **53** as observed under POM. Reproduced by permission of The Royal Society of Chemistry from [68]

The columnar order in **52a**,**b** was explained by molecular folding: the molecules are assumed to be in their U- (or wedge-) shaped conformation and six molecules self-assemble to a supramolecular disc. These discs are stacked in columns and arranged within a columnar hexagonal lattice (Fig. 8). Folding of similar mesogens was also seen by Heiney [65].

It has to be emphasized that all assumptions on the mesophase geometries and packing models made by Goodby are based on observations made under the POM; X-ray experiments were not carried out. Thus, the observations still have preliminary character [67, 68]. Similar compounds were also studied by Neve, also with respect to complexation. Copper [69] and palladium [70] complexes of derivatives of **51d** were found to form mesophases.

Lanthanide-containing mesophases are known with phthalocyanines and porphyrins [71–77] and possess interesting properties for bio-analyses and materials science due to their photochemical properties and the magnetic anisotropy of the complexed cations. It could be possible to obtain materials with properties that can be tuned by magnetic fields [78]. Bünzli investigated the first liquid crystalline crown ether complexes of lanthanide salts. The liquid crystalline and photoluminescence properties of **54** and its complexes with $Eu(NO_3)_3$ and $Tb(NO_3)_3$ [79, 80] (Scheme 30) were studied in detail. It was found that a broad Col_h mesophase ($\Delta T \approx 115$ K) could be induced by complexation of $Ln(NO_3)_3$ (Ln = Eu, Tb) with the non-mesomorphic host **54**. This is surprising as, up to now, mesophase induction and stabilization by complexation was only known for liquid crystalline polymers – not for low mass materials. The columnar hexagonal arrangement

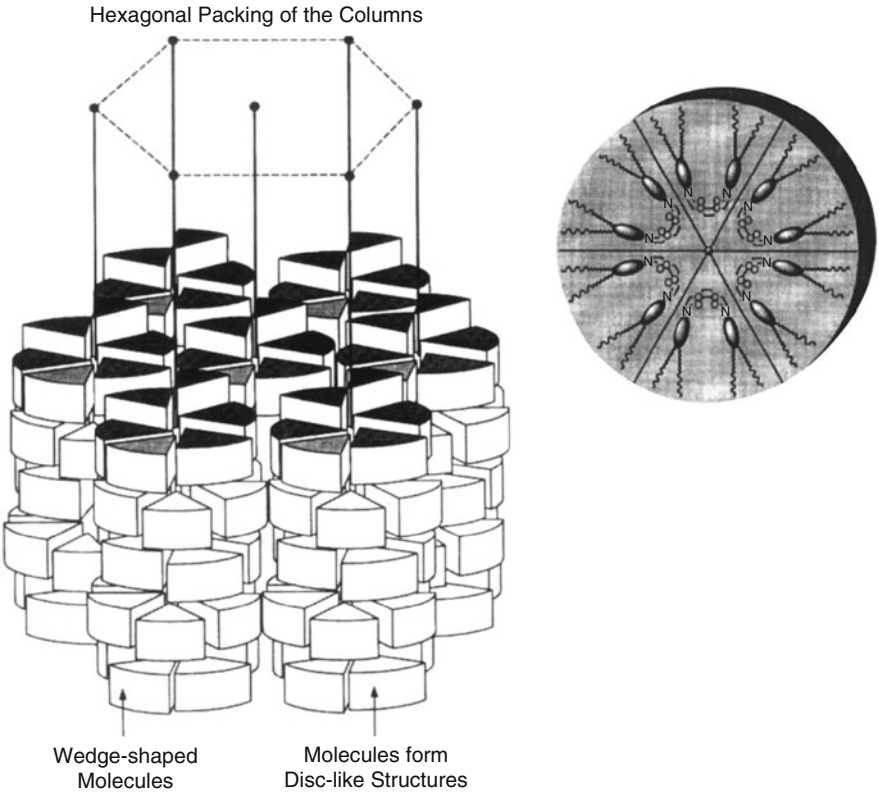

Fig. 8 Schematic representation of the formation of supramolecular discs from six molecules of **52** and their assembly into columnar phases. Reproduced by permission of The Royal Society of Chemistry from [68]

(as demonstrated by SAXS) is made possible through the increased microsegregation between the aliphatic chains and the polar crown upon complexation. The presence of the anions also disturbs the structure leading to mesomorphic behavior.

The complex with Eu^{3+} contained 0.25 equiv. of water while 1 equiv. of THF was included in the Tb^{3+} complex as deduced by elemental analyses. The $^5D_0 \rightarrow {}^7F_2$ emission for Eu^{3+} and the $^5D_4 \rightarrow {}^7F_5$ emission for Tb^{3+} were monitored. At the $Cr \rightarrow Col_h$ transition, both the lifetime and the intensity of both transitions were changed. Thus, it was possible to determine the melting point with a high level of accuracy using photoluminescence. The melting points observed in this way agree with the values obtained by conventional methods (DSC, POM), which further demonstrates the usefulness of this method.

In a further study, the effects of side chain length and lanthanide salt were investigated [78]. It was found that the chain length only plays a minor role and that the phase transition temperatures to the Col_h and the isotropic phase remain

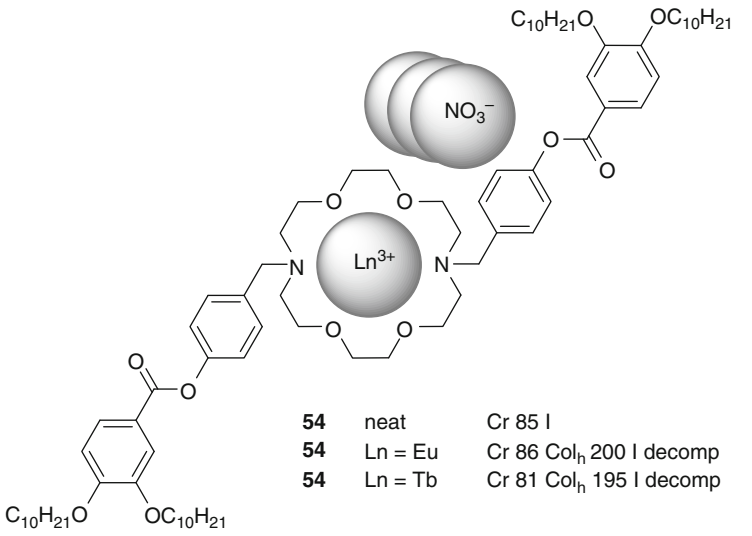

Scheme 30 Complexation of lanthanide salts by **54**

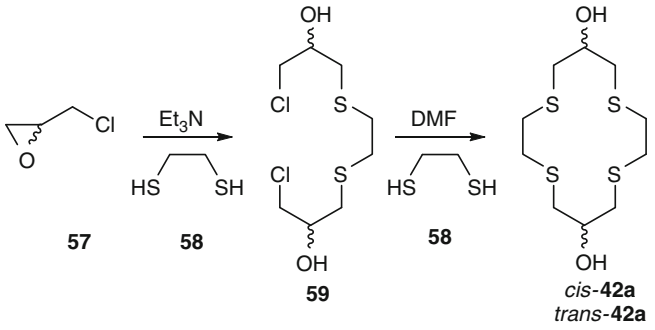

Scheme 31 Synthesis of crown thioether **42a**

fairly unchanged. Moreover, the anion of the lanthanide salt is not very important. The complexes with $LnCl_3$ are slightly less stable compared to the corresponding nitrates, which possess the most stable mesophases. When comparing $Ln(NO_3)_3$·**54** (Ln = La, Nd, Eu, Tb) it was found that uptake of $La(NO_3)_3$ gives the most stable columnar phase ($\Delta T = 147$ K) while $Eu(NO_3)_3$ as well as $Tb(NO_3)_3$ (both $\Delta T \approx 115$ K) and $Nd(NO_3)_3$ ($\Delta T \approx 90$ K) give smaller phases. Summarizing, these systems could be exploited for the design of new luminescent (in the case of Eu^{3+}, Tb^{3+}) liquid crystalline materials. Yet the antenna effect must be optimized and the transition temperatures should be lowered in order to obtain materials that work at room temperature.

Scheme 32 Liquid crystalline thia crown ethers **55**, **56**

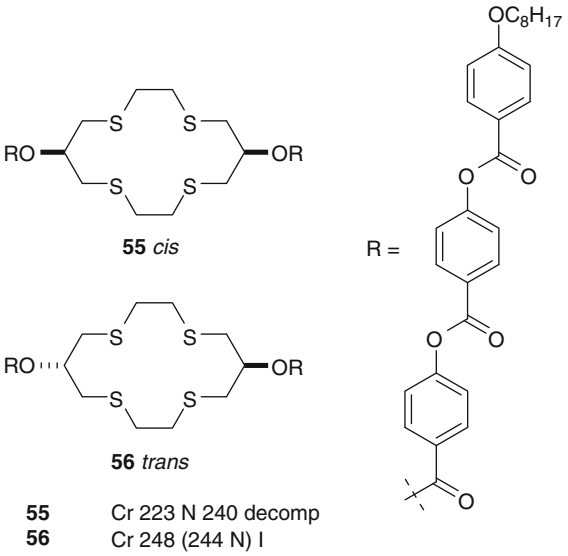

Crown Thioethers

The first examples of homoleptic thio crown ether liquid crystals (**55**, **56**) were presented by Bruce and Schröder [81] (Scheme 32). The synthesis and especially the separation of *cis*-(**42a**) and *trans*-(**42b**) forms of the macroheterocyclic diol were challenging. Reaction of (±)-epichlorohydrin **57** with 1,2-ethanedithiol **58** gave intermediate dichloride **59** that was finally reacted with 1,2-ethanedithiol **58** to give the *cis*/*trans* mixture of **42a** (Scheme 31). Separation of *cis*- and *trans*- and **42a** was carried out by flash chromatography followed by several recrystallization and fractional crystallization steps.

After DMAP-catalyzed esterification of **42a** with tri-benzoate esters, liquid crystals **55**, **56** (Scheme 32) were obtained, which both displayed narrow nematic phases as identified by their typical *Schlieren* texture. The melting and clearing points are high and, in the case of **55**, accompanied by decomposition. Compounds with shorter arms were also synthesized but found to be crystalline.

In a subsequent study, the influence of complexes with Pd^{2+} was examined in detail (Scheme 33) [82]. All uncomplexed crown ethers **60–62** only show a transition to the isotropic melt. For longer side arms ($n = 1$), transition temperatures are higher than for the related compounds with shorter ($n = 0$) substituents. Complexation changes this situation dramatically: upon uptake of $Pd(BF_4)_2$, all *cis*-complexes $Pd(BF_4)_2$·**60a**,**b** still showed isotropic melting as the only transition, while $Pd(BF_4)_2$·**61a**,**b** and $Pd(BF_4)_2$·**62a**,**b** showed monotropic smectic C ($n = 0$) phases or nematic ($n = 1$) phases. All phase transition temperatures were shifted to significantly higher temperatures. Still, longer substituents lead to higher phase transition temperatures.

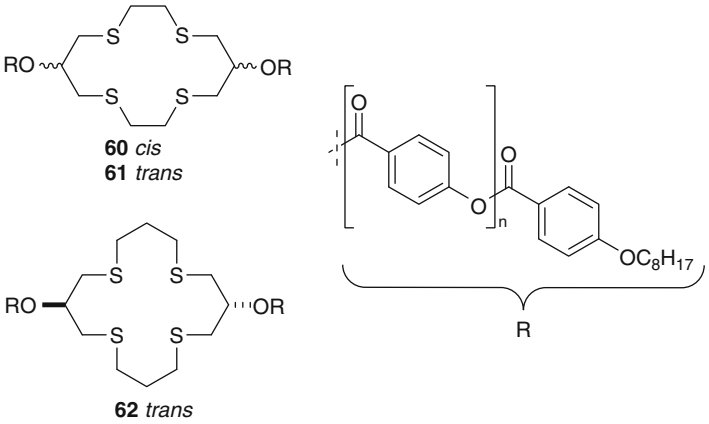

	60a	*cis*	n = 0	Cr 108 I
$Pd(BF_4)_2$ •	**60a**	*cis*	n = 0	Cr 242 decomp
	60b	*cis*	n = 1	Cr 192 I
$Pd(BF_4)_2$ •	**60b**	*cis*	n = 1	Cr 244 decomp
	61a	*trans*	n = 0	Cr 117 I
$Pd(BF_4)_2$ •	**61a**	*trans*	n = 0	Cr 222 (164 SmC) I
	61b	*trans*	n = 1	Cr 192 I
$Pd(BF_4)_2$ •	**61b**	*trans*	n = 1	Cr 280 (242 N) I
	62a	*trans*	n = 0	Cr 101 I
$Pd(BF_4)_2$ •	**62a**	*trans*	n = 0	Cr 244 (144 SmC) I
	62b	*trans*	n = 1	Cr 171I
$Pd(BF_4)_2$ •	**62b**	*trans*	n = 1	Cr 260 (238 N) I

Scheme 33 Effect of $Pd(BF_4)_2$ uptake by **60–62**

Mesophase induction by complexation was explained with the help of single crystal X-ray diffraction (Fig. 9). In the crystalline state, $Pd(BF_4)_2$·**61** and $Pd(BF_4)_2$·**62** adopt a zigzag conformation with the Pd^{2+} ion located in the inversion center of the molecule and hence in the exact center of the S_4 plane. Hereby, the crown ether loses some flexibility. It can now be considered as rigid core that interlocks the two attached substituents which promotes mesogenity. Crystal structures of the corresponding $Pd(BF_4)_2$·**60** suggest the presence of a U-shaped conformation with the Pd^{2+} slightly out of the S_4 plane. This arrangement seems to disfavor the existence of liquid crystalline phases.

2.3.2 Polymeric Compounds

Percec and Rodenhouse presented the first main-chain liquid crystalline polymer with a crown ether moiety in the backbone of the polymer [83]. Liquid crystalline polyethers **63** were obtained by phase transfer catalyzed polyetherification of

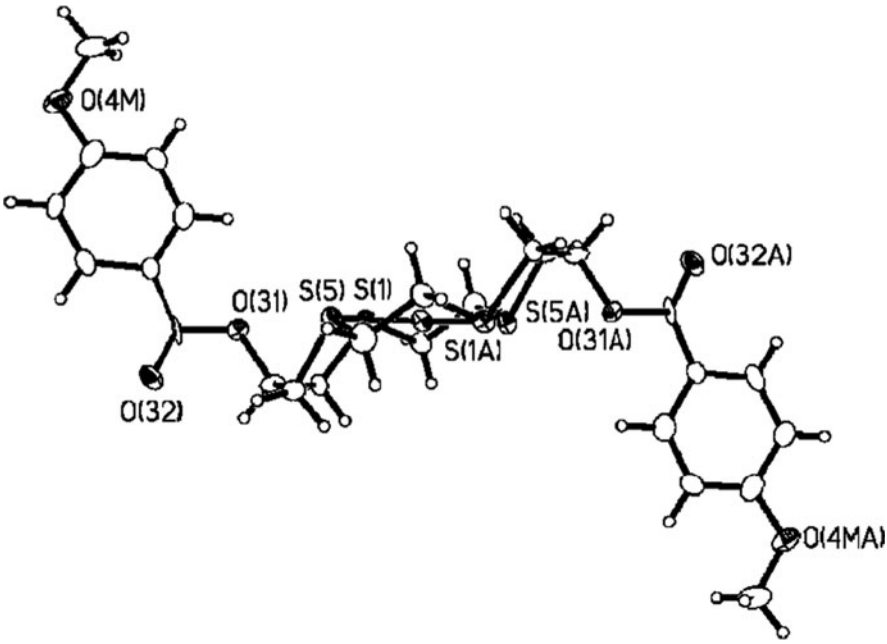

Fig. 9 Zigzag conformation of $Pd(BF_4)_2$·**61a** in the crystalline state. Reproduced by permission of The Royal Society of Chemistry from [82]

bis(8-bromooctyl)dibenzo[18]crown-6 **64** with 1,11-dibromoundecane **65** and the mesogenic unit 4,4′-dihydroxy-α-methylstilbene **66** (Scheme 34). The copolyethers **63** with ratios of **64/65** exhibit monotropic nematic phases for compositions between 80/20 to 40/60. The I→N transition upon cooling was influenced by the amount of crown ether: for a molar ratio of 80/20, $T_{I\rightarrow N}$ was at 95 °C and decreased to 65 °C for a 40/60 ratio.

2.3.3 Summary

Liquid crystals with a central crown ether and lateral rod-like substituents are very versatile compounds. Plenty of possibilities for variation of the structure were presented. All materials exhibit a multitude of phase geometries, including nematic, smectic, and columnar. The mesomorphic properties can be tuned by complexation. Thia- and aza crown ethers offer the interesting possibility to complex transition or f-block metal salts. Due to their interesting magnetic or luminescence properties, novel light emitting or magneto-responsive liquid crystalline materials for analytics or material science could be obtained.

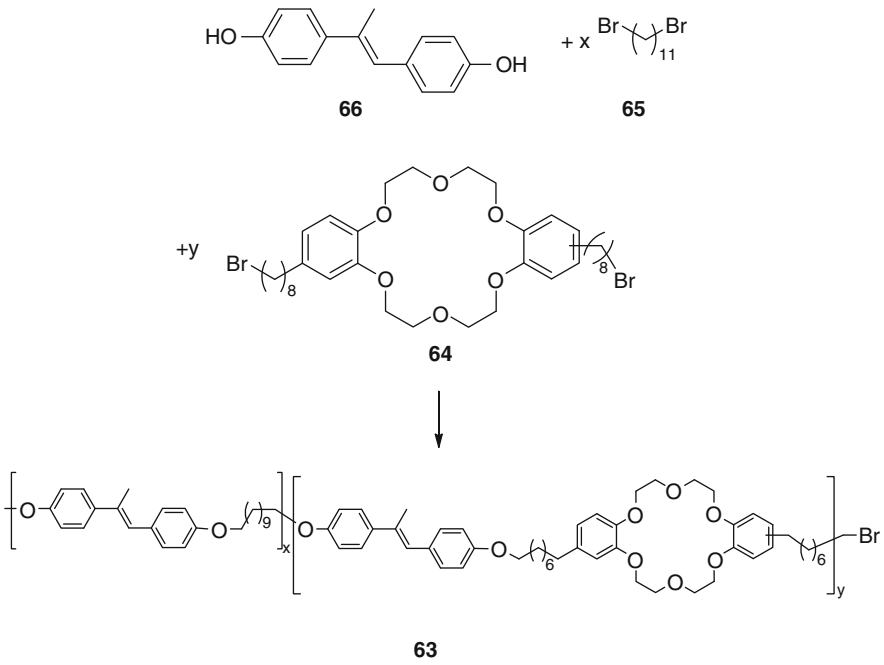

Scheme 34 Main chain liquid crystalline polymer **63**

2.4 Terminal Crown Ethers with One Taper-Shaped Substituent

In this section, crown ethers will be discussed which are equipped with one taper-shaped substituent (Fig. 10). Columnar hexagonal mesophases are the most commonly observed phases in this kind of molecule.

2.4.1 Monomeric Compounds

Percec studied taper-shaped molecules like **67** and **68** (Scheme 35) and investigated their liquid crystalline properties upon complexation with NaOTf and KOTf [84, 85]. It was found that the neat materials exhibit only crystalline phases with **67** melting at 60 °C and **68** melting at 94 °C. The increased melting point in the latter system can be explained by the presence of an additional aromatic ring. Both **67** and **68** consist of an *endo*-receptor (the [15]crown-5 macrocycle) and an *exo*-receptor (the taper-shaped 3,4,5-tris(*p*-dodecyloxybenzoate)).

Upon addition of NaOTf, columnar hexagonal mesophases could be induced. For **68**, 0.4 equiv. of salt were needed while for **67**, only 0.2 equiv. of NaOTf were needed for mesophase induction. Upon complexation, the complexed crown ether moieties and the anions self-assemble within a supramolecular tube and the taper-shaped side groups stack over each other in the periphery. X-Ray scattering

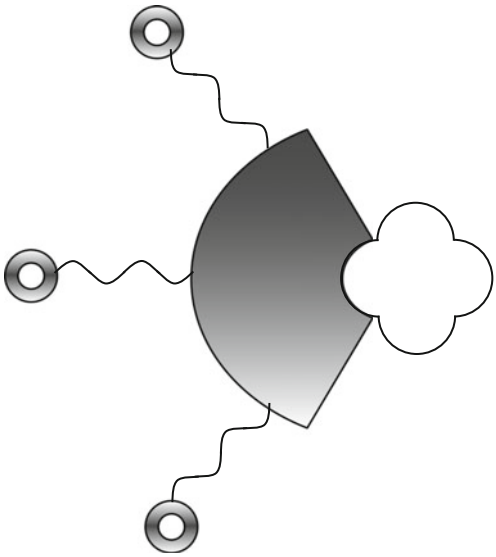

Fig. 10 General design of liquid crystalline crown ethers with a taper-shaped substituent

experiments were carried out to elucidate the structure of the mesophase. It was found that a supramolecular disc within the columns consists of approximately six molecules (Fig. 11). The interesting mechanism of this molecular recognition-mediated self-assembly is related to that observed in the tobacco mosaic virus [85].

Another finding was that, in contrast to the observations made for most crown ether modified rod-like molecules, the uptake of a salt led to an increase in the mesophase stability (Fig. 12). While neat crown ether **67** recrystallized at 12 °C, a transition from the isotropic melt to a columnar hexagonal phase was observed at 39 °C for 0.4 equiv. of NaOTf·**67**. At higher concentrations of salts, the clearing point was shifted to higher temperatures and reached its maximum at 2.0 equiv. of salt. Interestingly, the Col_h phases were stable far below room temperature upon cooling and maintained the columnar order even in the subsequently observed glassy or crystalline phases (Fig. 12).

The DC conductivity of NaOTf·**68** was measured to be in a range of 10^{-6} to 10^{-7} S cm^{-1}, a value typical for ionic conductors [84]. The authors proposed that the crown ethers stack over each other to form six parallel ion channels within the tube.

The electric conductivity was also measured for complexes of taper-shaped mesogens with oligo(ethylene oxide) central groups. The DC conductivity is in a range of 10^{-9} to 10^{-6} S cm^{-1} and shows a step-like increase at the crystal-columnar phase transition [86]. It was also shown that taper-shaped molecules adjacent to different endo-receptors such as crown ethers or oligo(ethylene oxide) chains were miscible with a poly(methacrylate) matrix and formed isomorphic phases [87]. Applications as columnar reaction media for polymerizations were foreseen. Comprehensive summaries of Percec's taper-shaped molecules can be found in the literature [88, 89].

Scheme 35 Taper-shaped crown ethers **67**, **68**

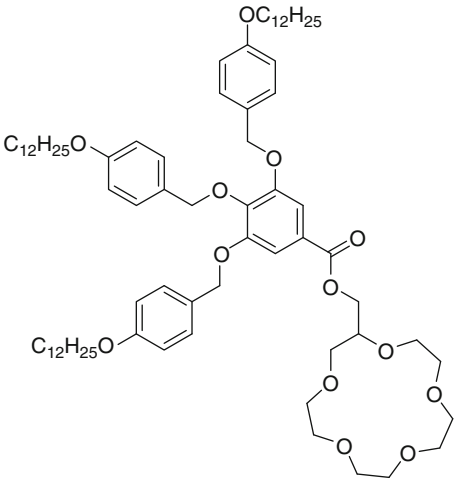

67 Cr 60 I

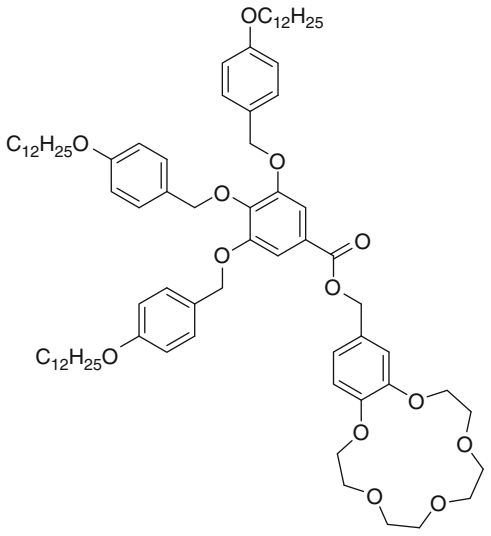

68 Cr 94 I

The effects of fluorinated side chains were also investigated [90]. Replacing the dodecyloxy chains from **67** and **68** with heptadecafluorododecyloxy chains resulted in taper-shaped **69** and **70** (Scheme 36). While **69** exhibited an enantiotropic columnar hexagonal phase, **70** showed a cubic phase solely upon cooling. This shows impressively that fluorination enhanced the self-assembly of the materials as the corresponding alkyl-substituted derivatives **67** and **68** are non-mesomorphic. The geometry of the columnar hexagonal phase is the same as discussed above with the crown ethers side by side in the center of the column and the melted taper-shaped

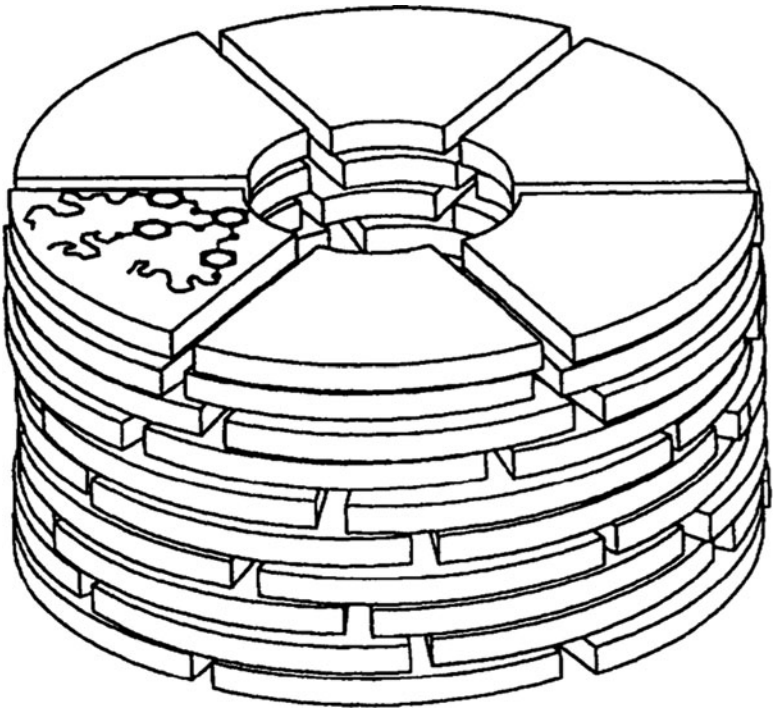

Fig. 11 Molecular recognition directed self-assembly of NaOTf·**67**, NaOTf·**68** to supramolecular discs which further self-assemble to supramolecular tubes. Reproduced by permission of The Royal Society of Chemistry from [85]

groups in the periphery. The fluorinated segments are microsegregated via the fluorophobic effect from the hydrogenated and aromatic units. More interestingly, the mesophase range and stability are higher for neat fluorinated **69** than for complexed hydrogenated NaOTf·**69**. This means that the fluorophobic effect overrules the ion-mediated self-assembly.

A detailed study on the elastic behavior of **69** based on the POM textures and observations under the TEM were carried out by Jung [91].

Percec published a detailed and elaborated study about monodendritic crown ethers based on benzo[15]crown-5 modified with parallelepiped (**71**), tapered (**72**), conic (**73**), and half-disc (**74**) shaped substituents [92] (Scheme 37) and the effects of complexation of NaOTf by these crown ethers (Scheme 38). Some general trends of NaOTf complexation were found. First, SmA phases formed by parallelepiped monodendrons (**71**) are stabilized upon complexation. While neat **71** exhibits an SmA phase range of only 7 K, 0.8 equiv. NaOTf·**71** leads to a smectic phase which is stable for 101 K (Table 4). This was explained by the interdigitated bilayer structure derived from X-ray measurements. The crown ether moieties are located in the middle of the bilayer and uptake of a salt leads to ionic interactions stabilizing the bilayer and hence increasing the clearing point and mesophase range.

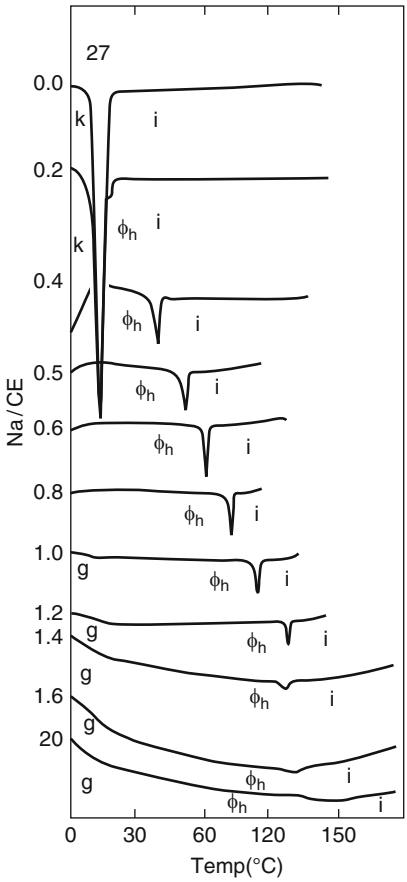

Fig. 12 DSC traces of NaOTf·**67** upon cooling from the isotropic phase. *k* crystalline, *g* glass, ϕ_h columnar hexagonal, *I* isotropic, *CE* crown ether **67**. Reproduced by permission of The Royal Society of Chemistry from [85]

Second, the mesophase behavior observed for taper shaped monodendrons (**72**) is also significantly influenced by the complexation with NaOTf. While neat **72** is crystalline, the complex 1.0 equiv. NaOTf·**72** exhibits a columnar hexagonal phase which is stable for 67 K (Table 4). The possible reason for the induction of a mesophase and the mechanism of self-assembly of taper-shaped molecules has already been discussed above for **67**, **68** and is shown in Scheme 38. Third, cubic phases as observed in spherical monodendrons **73** are also stabilized by the presence of NaOTf. Uncomplexed **73** exhibits a cubic phase as broad as 39 K while 0.4 equiv. NaOTf·**73** possesses a cubic phase range of 141 K and is stable until −26 °C (Table 4). Conic monodendrons self-assemble to spheric dendrons that organize in cubic lattices (Scheme 38). As the crown ether is located at the center of the spheres, the uptake of NaOTf and the associated ionic interactions lead to the drastic improvement of the liquid crystalline properties. Fourth, the columnar hexagonal mesophases observed for half disc-shaped molecules **74** are being destabilized upon complexation. Neat **74** has a columnar phase range of 131 K.

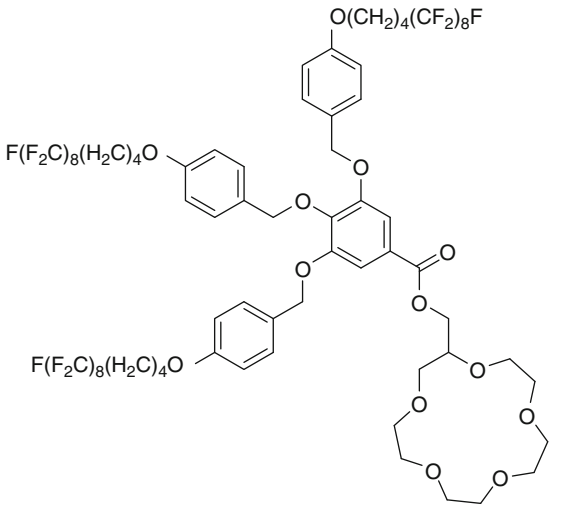

69 I 132 Col_h 30 Cr

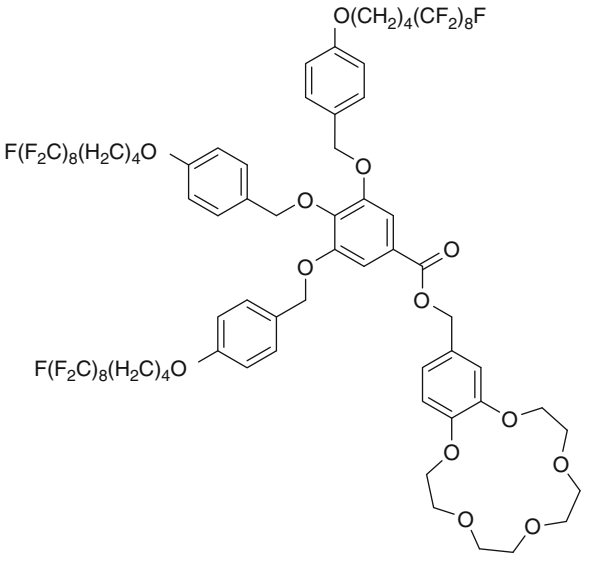

70 I 112 Cub 20 G

Scheme 36 Liquid crystalline crowns **69**, **70** with fluorinated side chains

In contrast, complexation of **74** with 0.4 equiv. NaOTf yielded a phase which is only 110 K stable (Table 4). As complexation leads to a side by side arrangement of the crown ethers, induction of columnar phases is most effective for taper-shaped molecules that do not disturb each other when being placed close to each other.

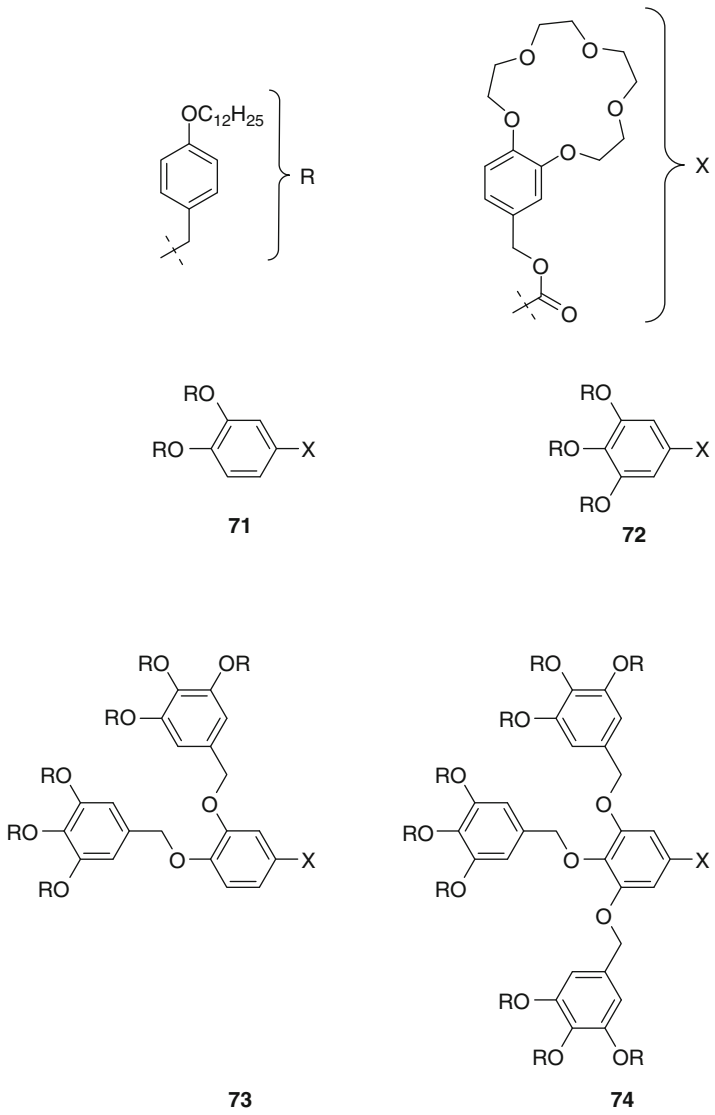

Scheme 37 Monodendritic crown ethers **71**–**74** with differently shaped substituents

Molecules possessing a half disc shape cannot be placed side by side to form a supramolecular disc as the half disc molecules disturb each other, which ultimately leads to smaller mesophase ranges.

Gitsov presented a series of poly(benzyl ether) monodendrimers capable of cation complexation lacking alkyloxy side chains which were non-mesomorphic [93].

Laschat followed a different route to obtain disk-like liquid crystals equipped with crown ether moieties. The crown ether was not attached to the mesogenic

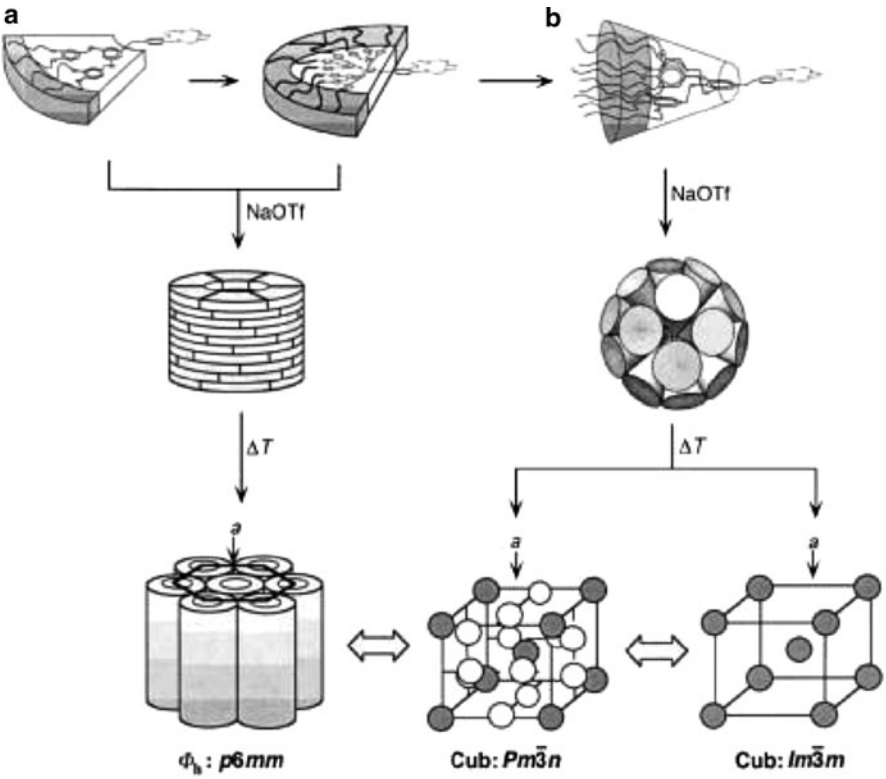

Scheme 38 (**a**) Self-assembly of taper- and half disc-shaped molecules to form tubes that self-organize into Col_h (Φ_h) phases; (**b**) self-assembly of monodendrons of conic shape into spherical dendrimers that self-organize in Cub phases. Copyright Wiley-VCH Verlag GmbH & Co. KGaA. Reproduced with permission from [92]

Table 4 Mesomorphic properties of **71**–**74**

Phase transition temperatures (°C) of **71**–**74** and their complexes with NaOTf upon first cooling	
71	I 50 SmA 43 G
0.8 equiv. NaOTf·**71**	I 117 SmA 16 G
72	I 34 Cr
1.0 equiv. NaOTf·**72**	I 98 Col_h 31 G
73	I 78 Cub 40 Cr
0.4 equiv. NaOTf·**73**	I 115 Cub −26 Cr
74	I 107 Col_h −24 Cr
0.4 equiv. NaOTf·**74**	I 85 Col_h −25 Cr

group by a methylene linking group but was directly attached to the *o*-terphenyl side group [94–96]. The effects of different substituents adjacent to the *o*-terphenyl substituent (alkyloxy **75**, acyloxy **76**, or gallic esters **77**, Scheme 39) as well as the influence of NaI complexation were studied.

Scheme 39 Liquid crystalline [15]crown-5 ethers **75**–**77** with differently substituted *o*-terphenyl units

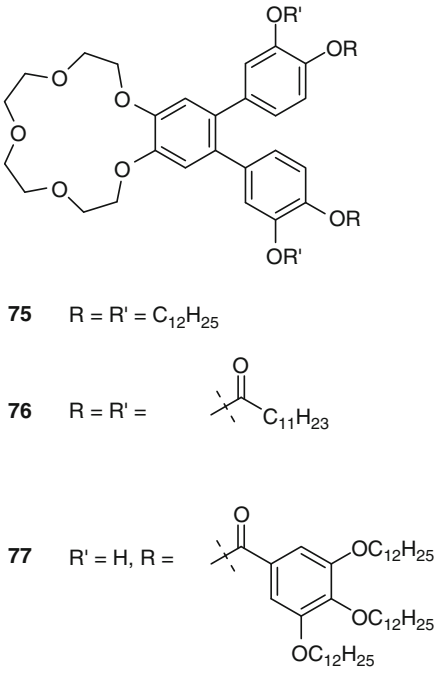

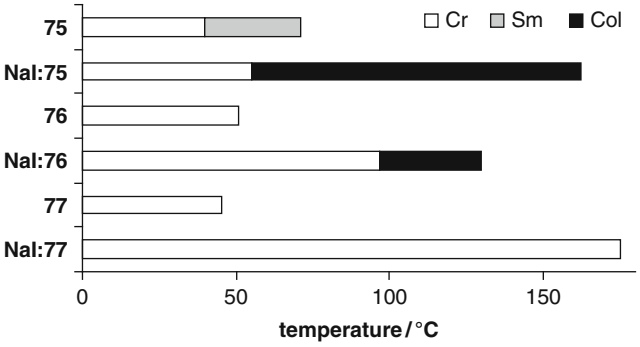

Fig. 13 Liquid crystalline properties of **75**–**77**

While alkyloxy-substituted **75** exhibits a smectic phase from 40–71 °C (Fig. 13), NaI induces a change in the phase geometry as complex NaI·**75** exhibits a columnar rectangular phase which is significantly more stable than the smectic phase of **75** [94, 96]. As deduced from single crystal X-ray analysis, ion channels form in the liquid crystalline state with the molecules being aligned antiparallel. The introduction of acyloxy groups in **76** changes the behavior [95, 96]. Neat compounds **76** are crystalline. Introduction of NaI leads to the presence of

a columnar phase, which is smaller compared to NaI·**75**. The introduction of gallic esters in **77** finally results in disappearance of the liquid crystalline properties. Neither **77** nor NaI·**77** show any mesophases. Nevertheless, complexation still leads to a drastic increase in the clearing point. The reason for the loss of mesomorphism might be the large number of alkyl chains. The tendency to nanosegregate is much lower for **77** because the polar crown ether plays a minor role as compared to the number of alkyl chains.

2.4.2 Polymeric Compounds and Possible Applications

Beginn developed Percec-type dendrimers, which are known to form supramolecular channels, with polymerizable acrylate groups in order to obtain ion-permeable membranes [97–99]. First, the dendron **78** (Scheme 40) was dissolved in a polymerizable acrylate mixture that does not shrink on polymerization. The second step was the thermo-reversible gelation of the acrylate mixture, which was followed by the last step, polymerization to fix the supramolecular channel structure (Scheme 40). In the first experiments, compounds with only one polymerizable group were used but it turned out that the gelating properties were not sufficient [100, 101] so threefold modified **78** had to be developed.

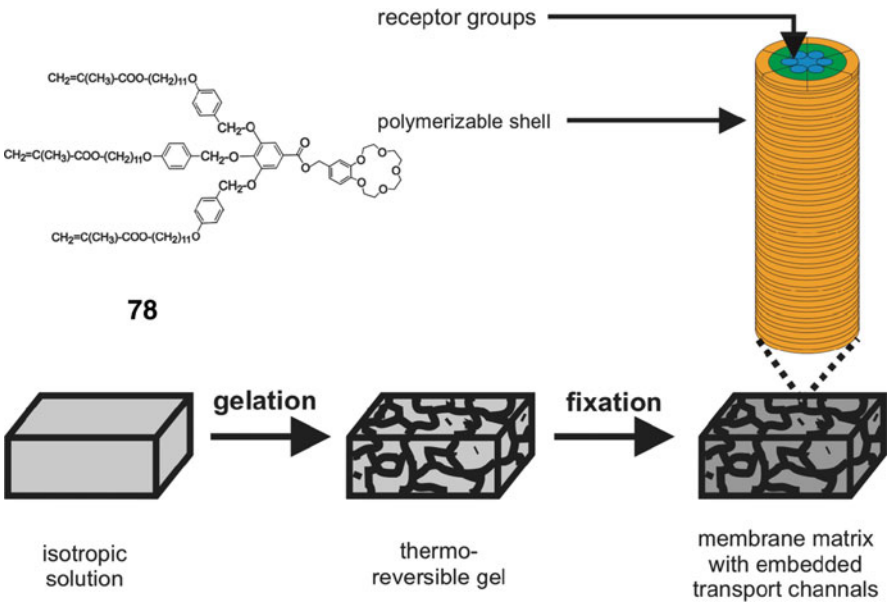

Scheme 40 Formation of membrane-fixed supramolecular channels from **78**. Copyright Wiley-VCH Verlag GmbH & Co. KGaA. Reproduced with permission from [98]

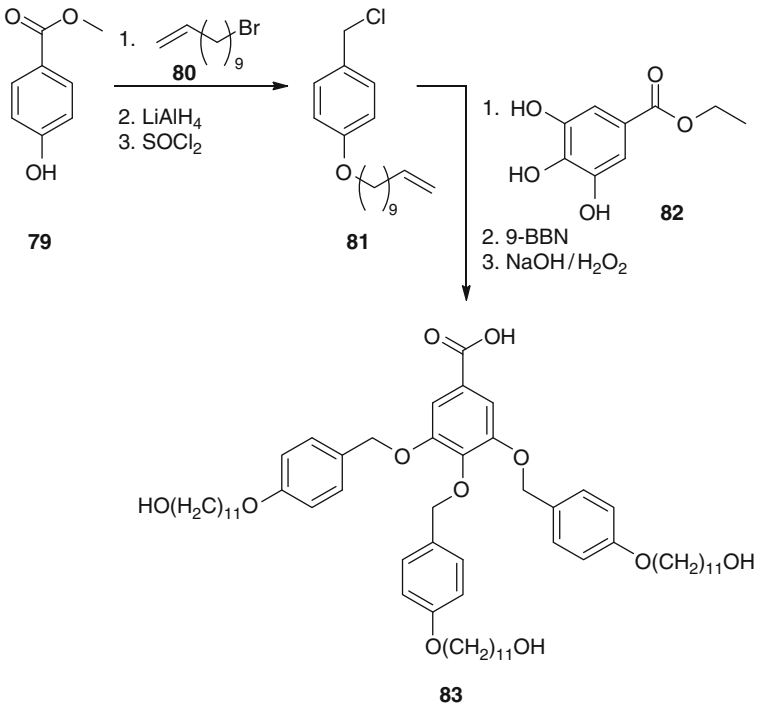

Scheme 41 Synthesis of precursor **83** for monodendritic crown ether **78**

The synthesis of **78** [97] started from methyl-4-hydroxbenzoate **79** that was alkylated with 11-bromoundec-1-ene **80**. The ester group was reduced with $LiAlH_4$ and the resulting alcohol was reacted to chloride **81** using $SOCl_2$. Coupling with **82** followed by hydroboration of the terminal double bonds and oxidation accompanied by ester cleavage yielded monodendron **83** with three alcohol units (Scheme 41).

Reaction of **83** with methacryloyl chloride **84**, followed by cleavage of the intermediate acid anhydride with pyridine and subsequent coupling with crown fragment **85**, gave the desired final product **78** [97] (Scheme 42).

Compound **78** as well as the complex NaOTf·**78** (Scheme 42) forms columnar hexagonal disordered mesophases [97]. While neat **78** exhibits a columnar phase range of 11 K, NaOTf·**78** increases the clearing temperature and stabilizes the mesophase resulting in a phase range of 20 K. Furthermore, it was shown that the columnar phase of **78** accepts up to 10 wt% of polymerizable methacrylates while leading to gelation of the added methacrylates.

The properties of the gels were investigated in detail [102] and it was found that well-defined cylinders built up from **78** are present in the transparent gels offering the possibility of ion transport. Closer investigation of the membranes [98, 99] revealed that MNO_3, MCl, and $MClO_4$ (M = Li, Na, K) can pass the membranes.

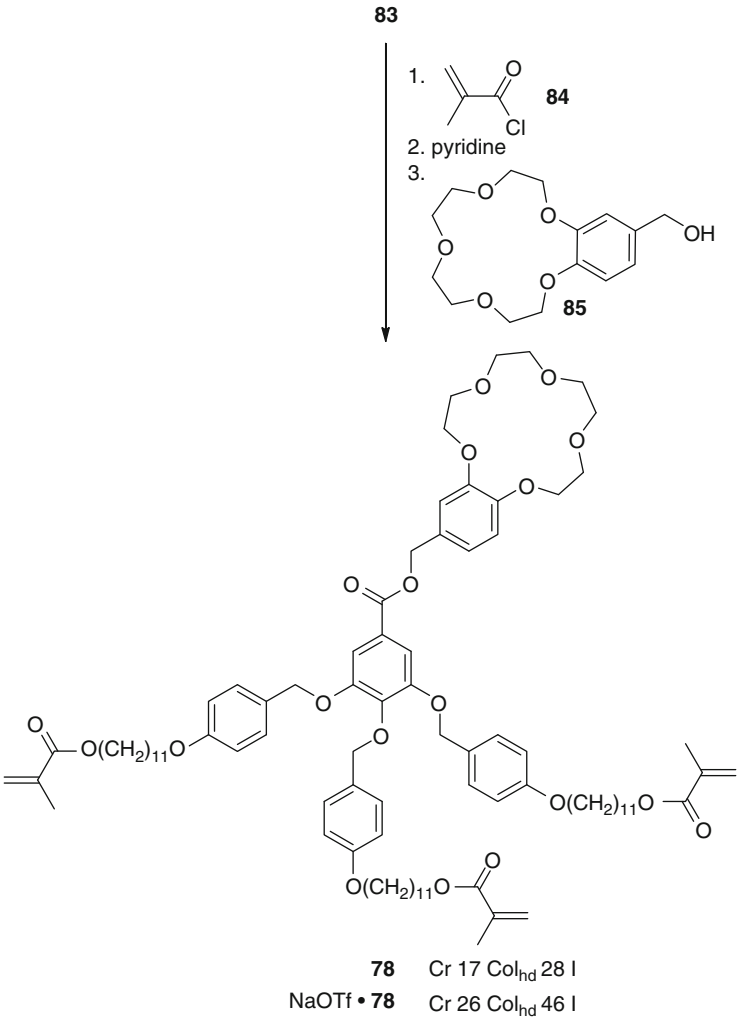

Scheme 42 Synthesis of polymerizable liquid crystalline crown ether **78**

The transport velocity of Li^+ is faster than that of Na^+ and K^+ due to the size of the cation. The data are consistent with a hopping transport mechanism of the cations accompanied by a non-specific co-transport of the anions. The transport rates for $NO_3^- > Cl^- > ClO_4^-$ are related to the adjacent hydrate shell and not yet fully understood. Anyway, a path in the center of the supramolecular tubes, where the crown ethers assemble, must exist and allow for the co-transport of the anions. By forming the membranes in the pores of track-etched membranes, the transport rates could be improved by an order of magnitude due to the orientation of the channels perpendicular to the membrane surface.

2.4.3 Summary

Terminal crown ethers with taper-shaped substituents often possess columnar phases. Sometimes, the columnar order is only observed after the complexation of specific salts. The uptake of salts often results in the crown ethers assembling side by side forming supramolecular cylinders with the crown moieties on the inside and the alkyl chains on the outside leading to possible ion-conducting arrangements within an insulating jacket. Indeed, it was shown that matrix-fixed tubular arrangements are ion conductors.

2.5 Central Crown Ethers with More than One Peripheral Substituent

Crown ethers discussed in this section possess rod-like substituents all around them or flat substituents at either end (Fig. 14). The former was the structure of the first liquid crystalline crown-like molecules and will be discussed first. The latter one comprises molecules with taper- or disk-shaped terminal groups.

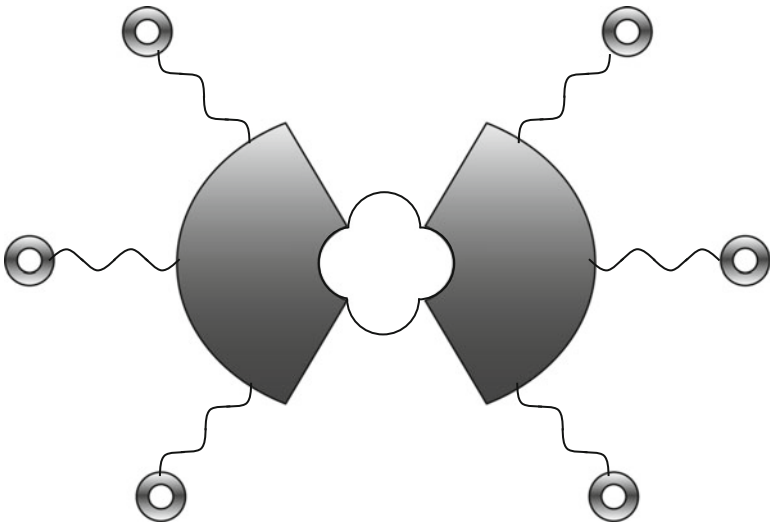

Fig. 14 Schematic representation of crown ethers with several taper- or disc-shaped substituents

2.5.1 Polysubstituted Macrocyclic Polyamines

Lehn presented the first crown-like liquid crystals (Scheme 43) in 1985 [5]. The core was built up from several polyamines, e.g., hexacyclen in **1** (termed [18]-N_6 due to the similarity to [18]crown-6). The larger [24]-N_6O_2 in **86** and [27]-N_6O_3 in **87** were also investigated. Substitution with *p*-dodecyloxybenzoyl (R) moieties was performed at all nitrogen atoms. All substances display columnar hexagonal mesophases as deduced from X-ray scattering, which were also termed "tubular" due to the hollow channels formed by the crown molecules upon stacking. While **1** exhibits an enantiotropic Col_h phase with a phase width of 20 K, **86** and **87** exhibit small (< 5 K) monotropic columnar phase widths. The reason for the reduced clearing points and phase stabilities for the larger macrocycles is probably due to the increased flexibility of the ring. For the 24- and 27-membered rings, the conformation is too far away from a disc-like arrangement to form stable mesophases.

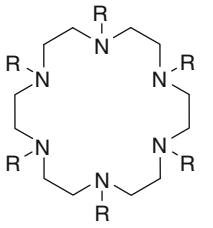

1 Cr 122 Col_h 142 I

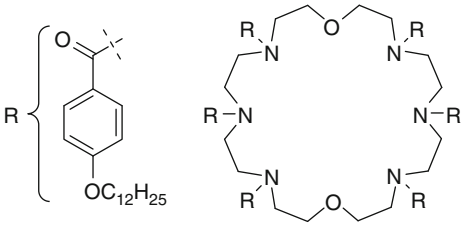

86 Cr 101 (Col_h 98) I

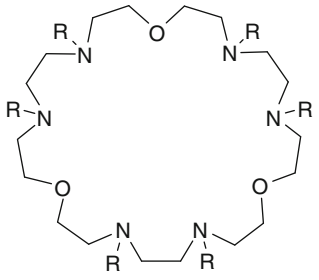

87 Cr 85 (Col_h 80) I

Scheme 43 First liquid crystalline crown ethers **1**, **86**, **87**

Table 5 Phase transition temperatures (°C) of [14]-N_4 and [18]-N_6 derivatives **88**, **89**

	R =	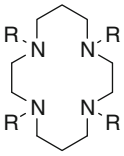 **88**	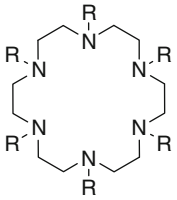 **89**
a		Cr 114 I	Cr 107 I
b	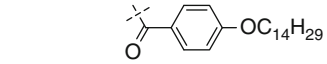	Cr 196 I	Cr 106 Col_{hd} 136 I
c	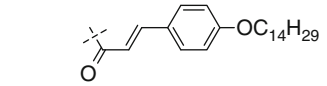	Cr 168 I	Cr 217 Col_{hd} 233 I
d	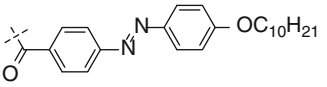	–	Cr 237 Col 245 I
e	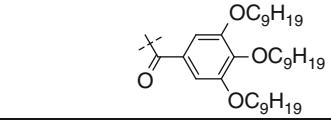	glassy	glassy

Also, **86** forms monolayers at the air-water interface as deduced from surface pressure vs surface concentration measurements [103]. It was observed that the macrocycles and the amide linkage touch the water surface while the aromatic and aliphatic substituents are tilted upright and point towards the air.

Ringsdorf also investigated derivatives of [14]-N_4 and [18]-N_6 **88** and **89** with aliphatic (**a**), rod-like aromatic (**b**–**d**) or taper-shaped aromatic (**e**) substituents [104] (Table 5). While none of the smaller macroheterocycles **88** were found to be liquid crystalline, most of **89** exhibit enantiotropic columnar hexagonal mesophases as deduced from X-ray measurements[1] and optical textures. Exceptions are the hexadecanoic acid substituted **89a** as well as the gallic acid substituted **89e**. The observed mesophases of derivatives **89c**,**d** occur at far higher temperatures as compared to **89b** which might be due to the extended aromatic core in **89c**,**d** resulting in increased interactions between neighboring molecules. It was concluded that the sixfold symmetry and the presence of a rod-like substituent attached via an sp^2-carbon are essential for the formation of stable columnar phases.

[1] It has to be noted that only the (001) reflection accompanied by a wide-angle halo was observed which would also account for a smectic phase. Yet, the textures indicate a columnar order.

Scheme 44 The first liquid crystalline [14]-N_4 derivative **90**

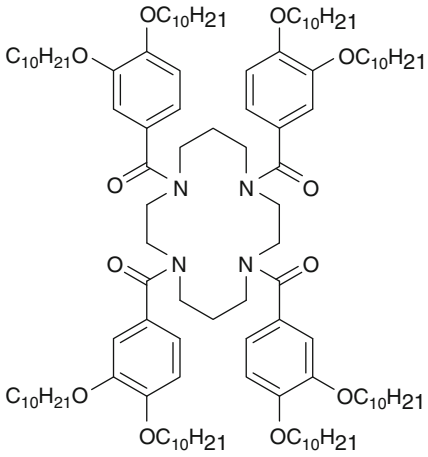

90

Lattermann found that the sixfold symmetry is not important for the presence of columnar mesophases in [14]-N_4 when appropriate peripheral groups are chosen [105]. As substituents with one terminal alkyl (**88a–d**) chain and with three terminal alkyl chains (**88e**) are not able to induce liquid crystalline behavior in **88** (Table 5) [104], a substituent with two alkyl chains, namely 3,4-bis(alkyloxy) benzoyl, was chosen since it has been known to induce liquid crystalline phases in other systems. A mesophase (most likely Col_h due to the texture) was observed between 96 and 132 °C for **90** (Scheme 44).

Based on the observations by Lehn that large polyamine rings do not exhibit stable mesophases [104] and the previous finding that 3,4-bis(alkyloxy)benzoyl substituted [14]-N_4 **90** shows columnar mesomorphism [105], Lattermann synthesized [18]-N_6, [12]-N_3, [9]-N_3 [106], and piperazine ([6]-N_2) [107] derivatives **91**–**94** with 3,4-bis(decyloxy)benzoyl substituents (Scheme 45). It was found that compounds **91**–**93** exhibit columnar mesophases while **94** exhibits a monotropic smectic phase. Derivatives **92**, **93** with 12- and 9-membered rings do not crystallize from the first cooling cycle onwards. The columnar phases (deduced from their POM textures) supercool and are stable even below room temperature. Interestingly, the clearing points decrease with decreasing ring size (with the exception of **94**).

Lattermann [106] and Ford [108] showed that the presence of water can change the properties of liquid crystalline polyamines like **91** and explained the different phase transition temperatures obtained by different groups by the presence of one to four water molecules in derivatives of [18]-N_6 as deduced from elemental analysis.

As all cyclic polyamines presented up to now were assigned to be columnar hexagonal based on their high viscosity, the typical texture or X-ray measurements devoid of the (110) or any higher reflection, Heiney and Smith [109] reinvestigated Lehn's [5] polyamine **1**. Scattering experiments were carried out using laboratory

Scheme 45 Liquid crystalline cyclic polyamines **91–94** with different ring sizes

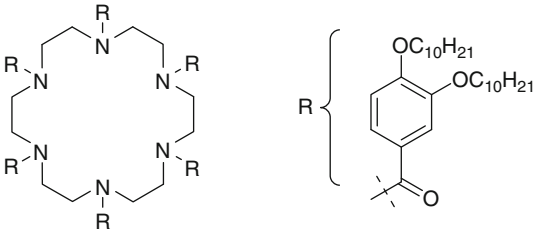

91 Cr 104 Col 140 I

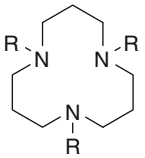

92 Col 60 I

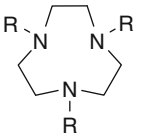

93 Col_1 44 Col_2 66 I

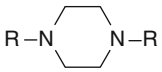

94 Cr 102 (45 Sm) I

and synchrotron X-ray sources and were found to show only the (001) reflection accompanied by a broad wide-angle halo accounting for a smectic A or C phase. There are arguments for columnar as well as for smectic structures and neither of them could be ruled out. In a later study, Lehn [110] probed the columnar hexagonal structure of the mesophase based on X-ray and miscibility (with other Col_h mesogens) experiments.

Mori [111] removed one alkyl chain from derivative **92** to obtain **95** (Scheme 46). Removal of one side chain changed the mesophase type from columnar to smectic A with an interdigitated jellyfish-like arrangement of **95**. The addition of tropolone side arms in **96** led to the formation of cubic *Pn*3*m* phases as suggested by X-ray diffraction. In the cubic phase, the molecules are arranged in a disk-like conformation with overlapping cores. The columns are branched and undulated leading to the three-dimensional skeleton of the cubic phase with the alkyl chains arranged around the skeleton. It was interesting to observe that in **95** the mesophase stability increases with increasing chain length

Scheme 46 Liquid crystalline [12]-N_3 **95**, **96**

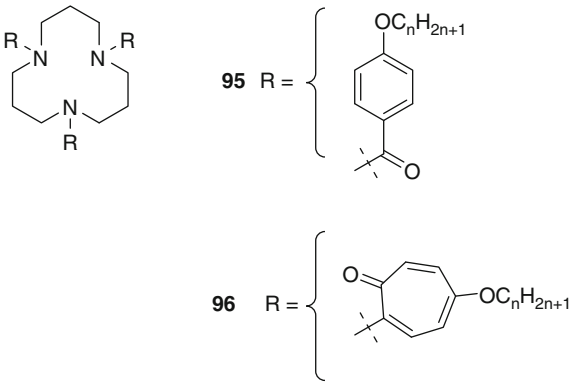

Table 6 Liquid crystalline properties of **95**, **96**

	n	Phase transitions		*n*	Phase transitions
95a	12	Cr 98 Cub 118 I	**96a**	12	Cr 63 I
95b	14	Cr 94 Cub 111 I	**96b**	14	Cr 64 SmA 79 I
95c	16	Cr 92 Cub 107 I	**96c**	16	Cr 70 SmA 81 I
95d	18	Cr 88 Cub 98 I	**96d**	18	Cr 69 SmA 87 I

Scheme 47 Non-mesomorphic amine-substituted cyclic [18]-N_6 **97**

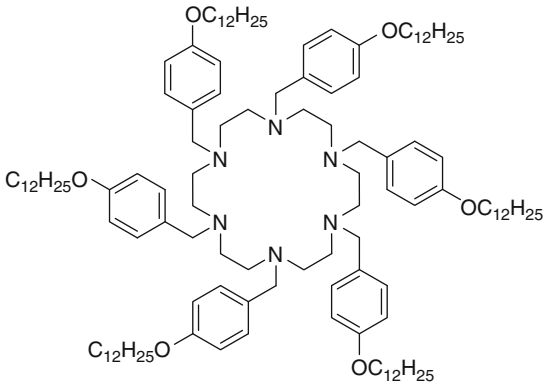

97

while for **96** the mesophase stability decreases with increasing chain length (Table 6). The authors concluded that, for longer alkyl chains, a more efficient space filling is possible, destabilizing the cubic phase. It was proposed that for even longer chains, **96** should also exhibit smectic phases.

Heiney and Smith removed the carbonyl groups from Lehn's system **1** by reduction with $LiAlH_4$ in order to find out about the necessity of amide links for the presence of mesophases [109]. Compound **97** (Scheme 47) with amine instead of amide links show no mesomorphism.

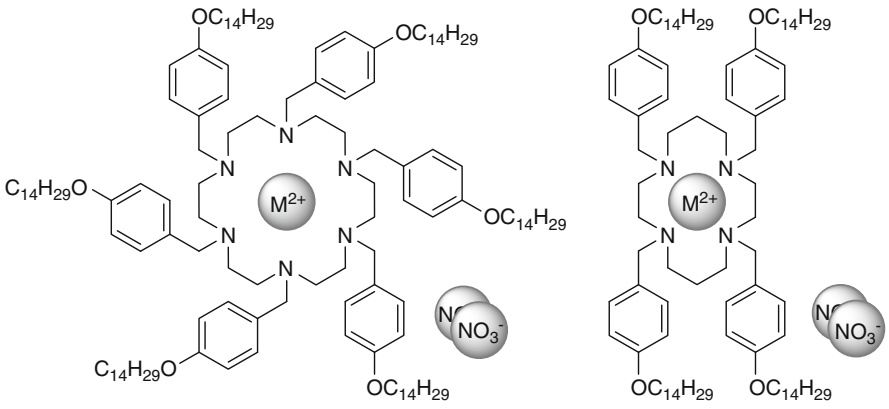

Scheme 48 Complexation of transition metal nitrated by **98**, **99**

Table 7 Mesomorphic properties of complexes **98**, **99**

Complex	Ratio host/guest	Phase transition temperatures (°C)
$Co(NO_3)_2$·**98**	2:1	Cr 30 N_D 60 I
$Ni(NO_3)_2$·**98**	1:1	Cr 29 M_X 95 I
$Cu(NO_3)_2$·**99**	1:1	Cr 18 M_X 160 decomp

Ringsdorf investigated the complexation of $Co(NO_3)_2$, $Ni(NO_3)_2$, and $Cu(NO_3)_2$ on the mesomorphic behavior of amine-linked **98** and **99** [112] (Scheme 48). Complexation induced mesomorphism in both substrates (Table 7).

Cobalt(II) nitrate induces a columnar nematic phase in the 1:2 complex with **98** (Table 7) as deduced from X-ray scattering which is stable for 30 K. Also, nickel(II) nitrate turned **98** into a liquid crystal with an unknown phase. The complex between **99** and copper(II) nitrate showed the same unknown mesophase. The phase range was ~140 K but the samples decompose before clearing. A possible reason for the induction of a mesophase by complexation is the stiffening of the crown and the adjacent flexibly linked groups [112].

By reduction of **93** [106] with BH_3·THF, Lattermann was able to obtain tridentate [9]-N_3 derivative **100** [113] (Scheme 49). While the host system **100** is only crystalline, complexation with $Ni(NO_3)_2$ induced a columnar rectangular phase as confirmed by X-ray scattering experiments.

Complexation of **100** with carbonyl complexes of chromium, molybdenum, and tungsten yielded liquid crystalline complexes **101a–c** [114] (Scheme 50). All derivatives **101** melted at similar temperatures into the columnar rectangular mesophase (deduced from WAXS and SAXS measurements). However, the clearing points were strongly dependent on the metal center and increased with increasing atom number. Upon complexation, the aza crown macrocycle loses its flexibility, with the metal carbonyl fragment located above the crown leading to a cone-shaped

Scheme 49 Induction of columnar phases in **100** by complexation of $Ni(NO_3)_2$

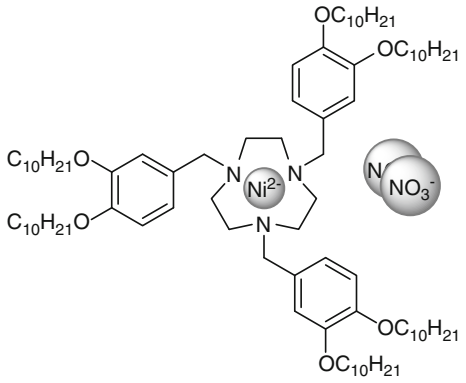

$Ni(NO_3)_2$ • **100** Cr 140 Col_{rd} 168 I

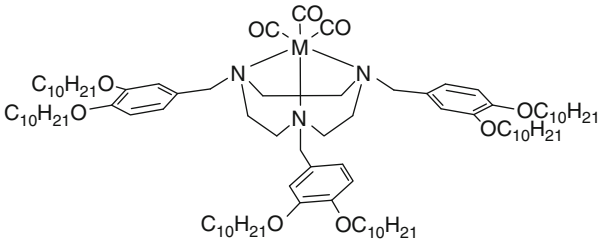

101a	M = Cr	Cr 63 Col_r 175
101b	M = Mo	Cr 67 Col_r 195
101c	M = W	Cr 63 Col_r 228

Scheme 50 Uptake of group six metal carbonyl complexes by **100**

molecule. The molecular cones can be stacked over each other and the resulting columns are comfortably accommodated within a rectangular phase.

Interesting effects were not only found upon complexation of amine substituted aza crowns, but also upon protonation. Lattermann reduced piperazine amide derivative **94** which showed a monotropic smectic phase to obtain crystalline **102** (Scheme 51). Subsequent protonation with various acids gave **103** [107] showing mesophases with broken focal-conic textures suggesting columnar phases (Scheme 51). Under the conditions of SAXS measurements, the compounds decomposed so that a clear assignment of the mesophase was not possible. Interestingly, with increasing size of the anion, the melting and clearing points decreased.

Ringsdorf investigated the photochemical properties of **89c** carrying six cinnamoyl substituents around the [18]-N_6 core [115]. Upon irradiation of *E*-**89c** in its liquid crystalline state with UV light, the mesomorphism was lost after a short time due to isomerization of the double bond (way A in Scheme 52). This showed

Scheme 51 Piperazine-based ionic liquid crystals **103** and the effects of anion exchange

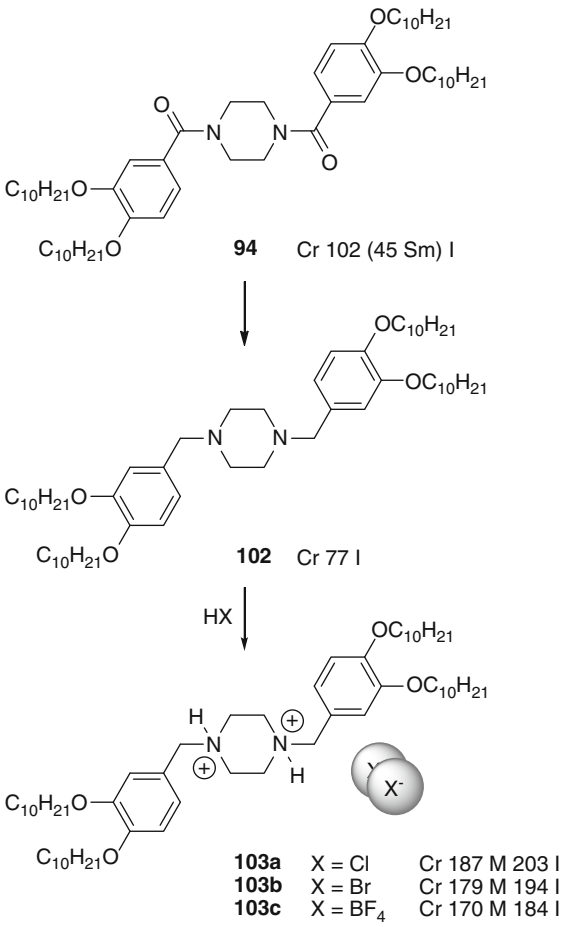

that the *Z*-isomer of the side chain suppresses mesomorphism. Upon irradiation of *E*-**89c** in cyclohexane solution, *E*/*Z*-isomerization (way A in Scheme 52) was observed until a steady state was reached. Upon further irradiation, [2+2] photocycloaddition (way B in Scheme 52) was observed. GPC analysis showed the presence of dimers, trimers, and higher aggregates (up to 20-mer) of **89c** in a tube-like array. The cycloaddition reaction is strongly dependent on the solvent – in chloroform various unidentified side-reactions took place. The cycloaddition is another way to lock the columnar alignment of the molecules and feasible only in non-polar solvents.

2.5.2 Crown Ethers with Several Taper- or Disc-Shaped Substituents

Hirose studied liquid crystal **105** consisting of a central dibenzo[18]crown-6 macrocycle and Percec-type side group dendrons (Scheme 53) [116].

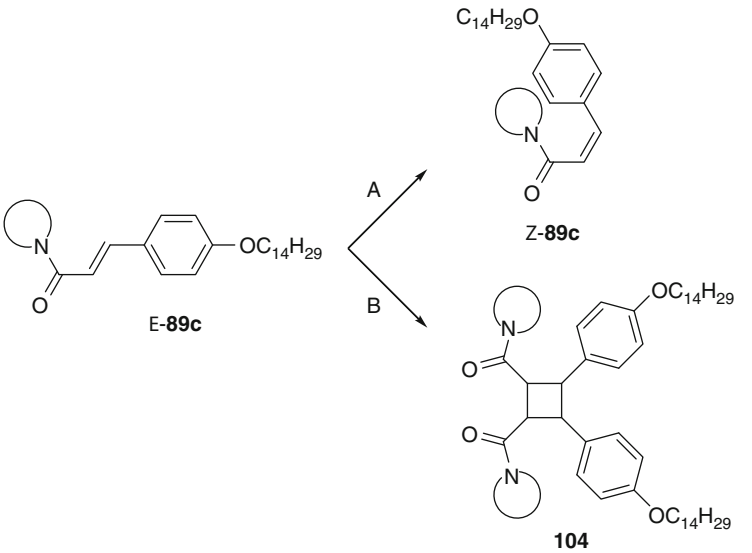

Scheme 52 Possible reaction pathways of *E*-**89c** upon UV irradiation. A: *E*/*Z* isomerization, B: [2+2] cycloaddition

Scheme 53 Dibenzo[18] crown-6 **105** modified with Percec-type dendrons

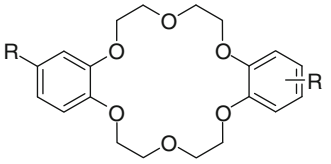

105

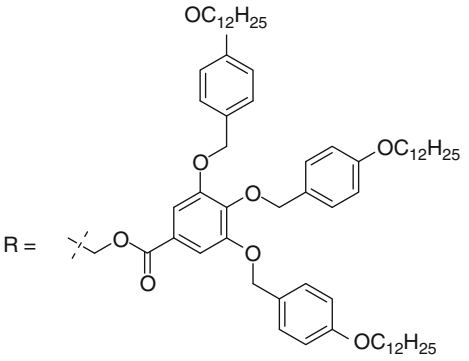

The mesophase of **105** could not be clearly identified due to missing X-ray experiments but it was considered to be a columnar phase as deduced from polarizing optical microscopy. It was found that complexation with $LiClO_4$ and $NaClO_4$ leads to a decrease of the melting and clearing point but increasing the

Table 8 Phase transition temperatures of **105** and $MClO_4$·**105**

Compound	Phase transition temperatures (°C)
105	Cr 125 M_{X1} 135 M_{X2} 145 I
$LiClO_4$·**105**	Cr 95 M_{X1} 102 M_{X2} 112 M_{X3} 117 I
$NaClO_4$·**105**	Cr 109 M_{X1} 121 M_{X2} 137 I
$KClO_4$·**105**	Cr 124 M_{X1} 129 M_{X2} 134 M_{X3} 144 I

Scheme 54 Dibenzo[30] crown-10 derivative **106** carrying four Percec-type dendrons

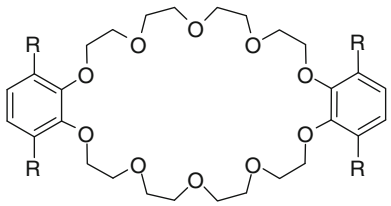

106

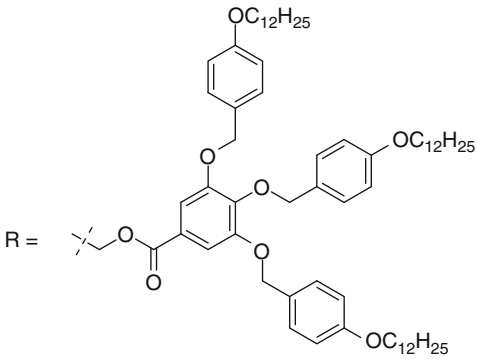

phase range slightly. Complexation with $KClO_4$ did not change the transition temperatures or the phase range (Table 8). The ionic conductivity of **105** and $KClO_4$·**105** was measured and it was found that complexation increases the ionic conductivity by ~1.5 orders of magnitude to be ~10^{-7} S m^{-1}.

Very recently, Chen published dibenzo[30]crown-10 fourfold substituted with first generation Percec-type dendrons **106** (Scheme 54) [117]. Liquid crystalline properties were not described for dry **106** but it was demonstrated that **106** is a powerful gelator of *n*-dodecane. For concentrations of **106** >0.1% (w/v), a gel with columnar rectangular lattice (*c*2*mm*) was formed upon cooling from the isotropic solution. The authors gained a deeper understanding of the mechanism of gelation: in the first step, the molecules self-assemble into cylindrical micelles. Upon further cooling, the micelles grow and form fibers which entangle and lead to a solid-like gel. Furthermore, the authors accomplished the solubilization of the cationic dye rhodamine B in *n*-dodecane. The solvent, the dye, and **106** were heated until all constituents were dissolved. Upon cooling, a gel was formed with rhodamine B included in the crown ether cavities. Possible practical applications of such functional gels were seen in drug delivery, filtration, or separation.

Scheme 55 Liquid crystalline derivative **107** of dibenzo[18]crown-6 stabilized by internal hydrogen bonds

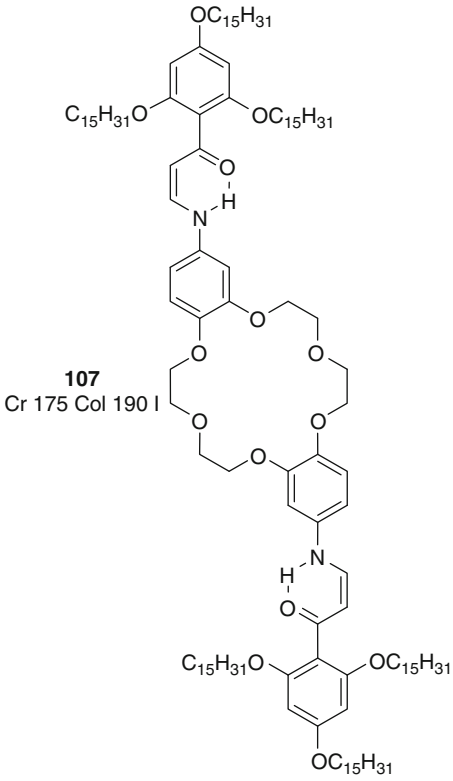

Akopova synthesized enamine ketone derivative **107** of dibenzo[18]crown-6 (Scheme 55) which exhibits columnar mesomorphism [8]. An interesting feature of compound **107** is the hydrogen-bond mediated stabilization within the side group.

Laschat developed a method by which a variety of liquid crystalline crown ethers of different ring sizes with two *o*-terphenyl or triphenylene substituents are conveniently accessible. Derivatives with *o*-terpenyl substituents of [12]crown-4 **108a** [118], [18]crown-6 **108b** [55, 119], and [24]crown-8 **108c** [118] were synthesized from the respective 4,4′,5,5′-tetrabromodibenzo[18]crown-6 **109a–c** and boronic acid **110** in a Suzuki coupling reaction (Scheme 56). Oxidative cyclization using $FeCl_3$ as oxidant gave the corresponding triphenylene-substituted crown ethers **111a** [118], **111b** [120], and **111c** [118] (Scheme 56). Compounds **108** and **111** were studied with respect to their liquid crystalline properties.

An essential part of the studies was also to gain insight into the effects of complexation of salts on liquid crystalline phases. Crown ethers **108a**, **111a** with ring sizes of 12 atoms were complexed with LiI [118] (Scheme 57). The homologs **108b**, **111b** with central [18]crown-6 cores were complexed with a variety of potassium salts (e.g., KCl, KI, KSCN) [55, 120] in order to obtain information

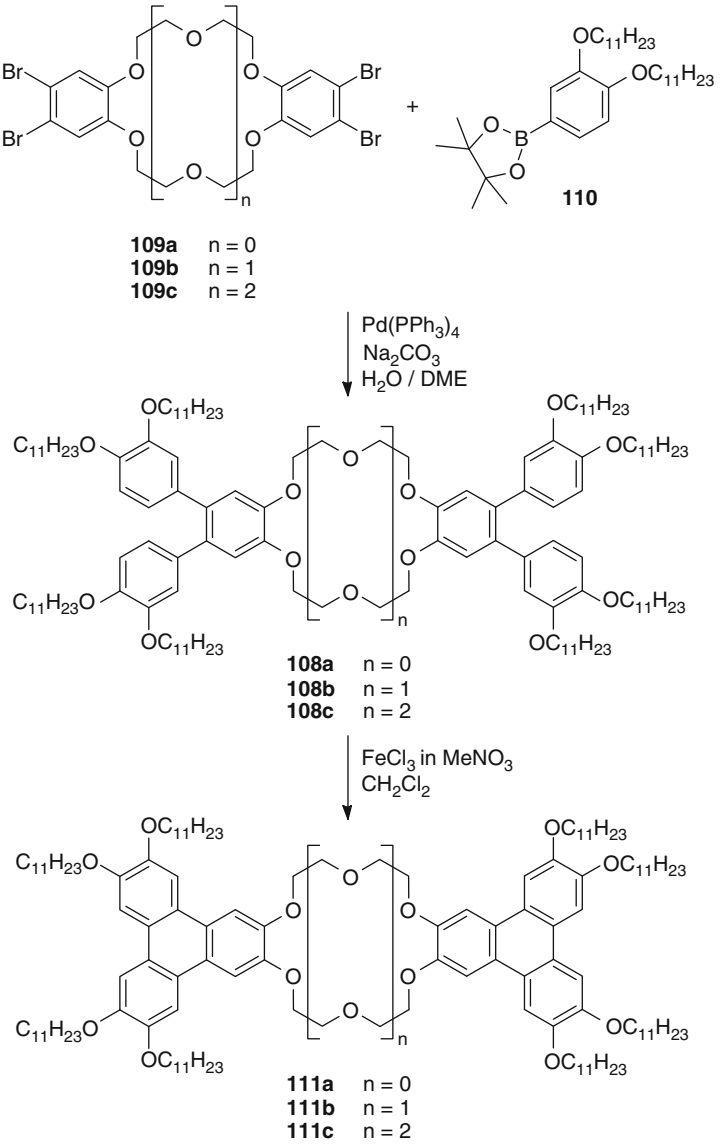

Scheme 56 Synthesis of substituted crown ethers **108**, **111** with varying ring size

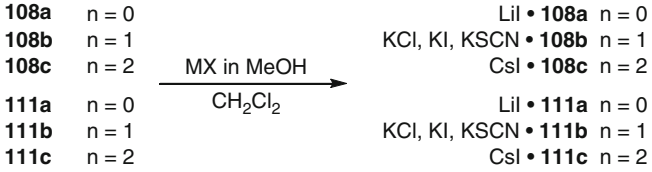

Scheme 57 Synthesis of crown ether complexes

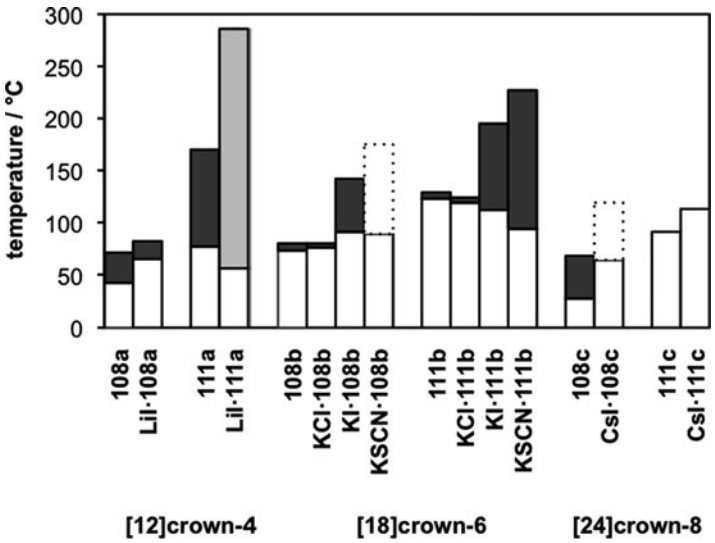

Fig. 15 Mesomorphic behavior of **108**, **111** and their metal complexes; *white shade* crystalline, *grey shade* columnar hexagonal ordered, *black shade* columnar, – plastic

about the influence of the different counterions (Scheme 57). Crown ethers **108c**, **111c** with a 24-membered macrocycle were complexed with CsI (Scheme 57) [118].

Several interesting trends were observed comparing the different compounds (Fig. 15[2]). First, triphenylene-substituted crown ethers **111** generally possess higher clearing temperatures compared with *o*-terphenyl-substituted **108**. The reason can be seen in π–π-stacking, which is stronger in **111** than in **108**. Second, the clearing temperatures and phase widths are dependent on the size of the macrocycle, especially for the series **111a–c**. While **111a** possesses a columnar hexagonal phase with a range of 93 K clearing at 170 °C, **111b** clears at 129 °C possessing a columnar rectangular range of 6 K. Finally, **111c** clears at 91 °C and is devoid of a mesophase. Third, complexation with salts possessing hard counterions (e.g., KCl) leaves the mesomorphic properties virtually unchanged (KCl·**108b** possesses a columnar rectangular phase range of 4 K compared with 7 K observed for **108b**) while salts with soft counterions (e.g., LiI, KI, and KSCN) lead to a significant increase in the mesophase range (51 K for KI·**108b**, 133 K for KSCN·**111b**). It was concluded from NMR experiments that tight ion pairs are present in these complexes and are responsible for the increase of the clearing points [55, 120].

[2] A variety of phase geometries (*p6mm*, *p2mg*, *p2gg*, *c2mm*) was observed depending on lateral substituent and complexed salt. Details can be found in [55, 118–120].

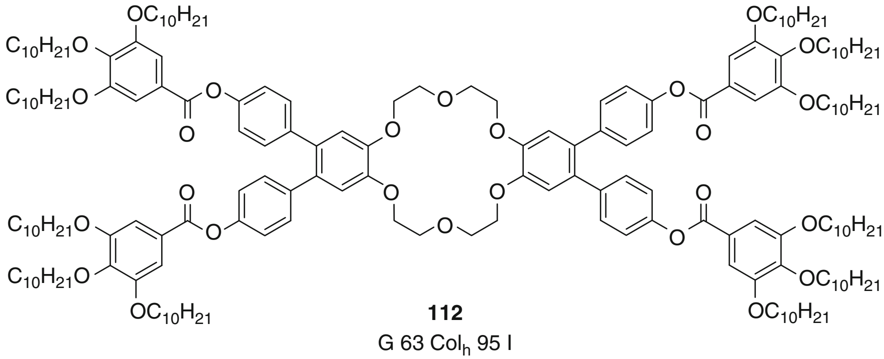

112

Scheme 58 Dibenzo[18]crown-6 **112** modified with four gallic acid groups

In the case of KSCN·**108b**, the interactions are too strong, leading to a plastic phase. In the case of LiI·**111a**, columnar hexagonal ordered phases were observed.

Summarizing, it can be stated that for the neat compounds, broad mesophases can be observed for small rings with rigid substituents (**111a**). If the ring is too large (**111c**), mesophases are absent. For complexation, a different picture emerges: as complexation can lead to the formation of ion pairs, the crown ether should be of medium size (**108b**, **111b**) in order to obtain broad mesophases. For smaller crowns, complexation rigidifies the crown too much leading to ordered phases (LiI·**111a**). If the crown is too large and flexible (**108c**, **111c**), complexation cannot induce mesophases.

When the lateral substituents were changed from ether to gallic ester groups, a columnar hexagonal phase was observed for **112**, while complexation with KI destroyed the mesomorphic behavior [121] (Scheme 58). The presence of ion pairs in the complex presumably leads to unfavorable interactions between neighboring molecules leading to non-mesogenity.

He and Cammidge prepared liquid crystal **113** (Scheme 59) with a central [27] crown-9 moiety, three attached triphenylene units carrying a total of 12 hexyloxy chains and exhibiting a columnar hexagonal mesophase [122].

2.5.3 Summary

The compounds presented in this section possess, in most cases, columnar phases as expected from their molecular shape. Aza crown ethers and conventional crowns offer a multitude of possibilities to add functional groups. Possible applications can be seen in the field of sensors or functional channels. Unfortunately, no applications have been reported yet. Addition of polymerizable groups might lead to functional membranes as shown in Scheme 40.

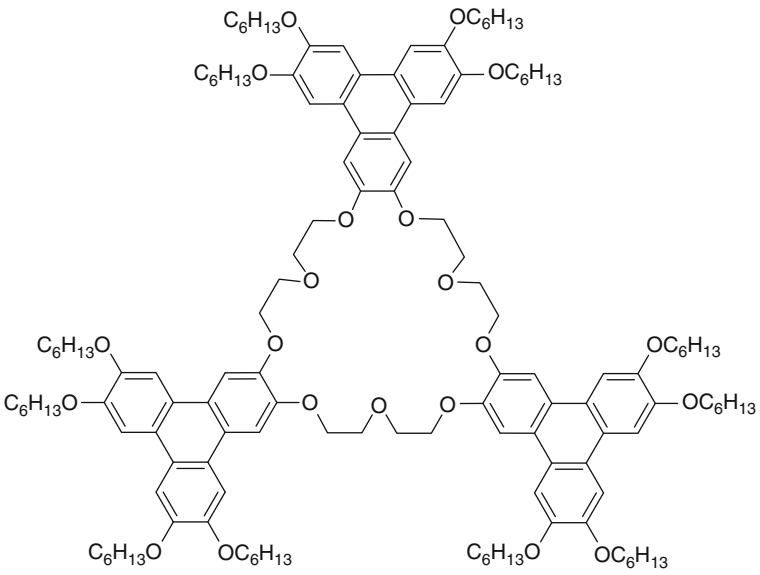

113

Cr 148 Col_h 176 I

Scheme 59 [27]crown-9 **113** with three triphenylene substituents

2.6 Crown Ethers with a Central Phthalocyanine

Possessing a flat shape, phthalocyanines are predestined to form columnar mesophases. The addition of crown ethers (Fig. 16) can yield interesting materials that can complex two different salts (one in the crown, one in the phthalocyanine) leading to interesting columnar channel structures.

Nolte synthesized the first liquid crystalline phthalocyanine **114a** bearing crown ether moieties in the periphery (Scheme 60). In total, eight decyloxy chains were present in the molecule [123]. The phthalocyanine was also equipped with a dihydroxy silicon group in the center in order to obtain polymerizable **114b** [124].

Compound **114a** showed a columnar hexagonal mesophase that was confirmed by X-ray scattering experiments [123]. The mesophase appeared at 170 °C while the isotropic phase could not be observed as **114a** decomposed above 320 °C. Despite the high number of alkyl chains, **114a** was insoluble in most organic solvents. Only boiling chloroform and toluene could dissolve it. Chloroform solutions of **114a** with a minimum concentration of 7 mg mL^{-1} turned into a gel upon cooling. TEM photographs showed the presence of a network of fibers. The fibers were several micrometers in lengths and consist of bundles of strands. The strands themselves are of molecular thickness (~50–60 Å). Within one fiber, the surprisingly high number of approximately 10^4 molecules is accommodated

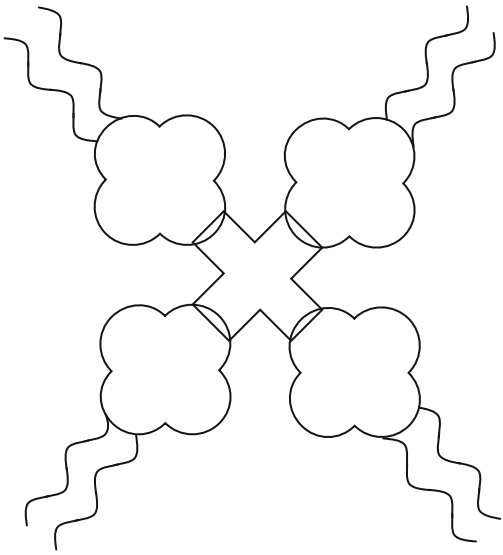

Fig. 16 Schematic representation of liquid crystalline crown ethers with a central phthalocyanine core

[123]. Compound **114b** can be regarded as multifunctional molecular cable with the central electron conducting phthalocyanine surrounded by the ion channels formed by the crown ethers and isolated by the alkyl chains.

For **114b**, a completely different behavior was found [124]. This compound is crystalline, polymerizing at 178 °C. The axial hydroxy groups prevented stacking of the molecules within a columnar phase. The behavior of **114b** at the air-water interface was examined and it was found that monolayers are formed. The phthalocyanine entity is lying flat on the water while the crown ethers and the alkyl chains point into the air. Addition of KCl changed the shape of the molecule leading to the crown ethers also lying flat on the water. It was possible to join the monolayers onto a glass substrate in order to obtain a Langmuir–Blodgett film [124].

Copper complex **114c** also shows columnar hexagonal phases [125]. Copper leads to an increase in the columnar phase range. The melting point is lowered to 94 °C while the decomposition does not occur before 345 °C.

Compound **114d** possesses significantly lower transition temperatures (Scheme 60) due to the branched side chains [126]. A columnar phase is present even below room temperature. At 14 °C, a new chiral columnar phase was observed while above 111 °C, an achiral columnar rectangular phase was observed. The spiral-pattern texture of **114d** in the chiral Col* mesophase is shown in Fig. 17.

Three possible arrangements of **114d** leading to the Col* phase are shown in Fig. 18. The molecules are either in a spiral staircase arrangement (left), staggered against each other at constant staggering angles (middle), or tilted and gradually rotated (right) as the most likely arrangement.

Interesting aggregation behavior was found for **114d** [128]. In chloroform, gel formation was also observed. The gel consists of long, left-handedly twisted fibers of nanometer diameter and micrometer lengths (Fig. 19a, b). These fibers

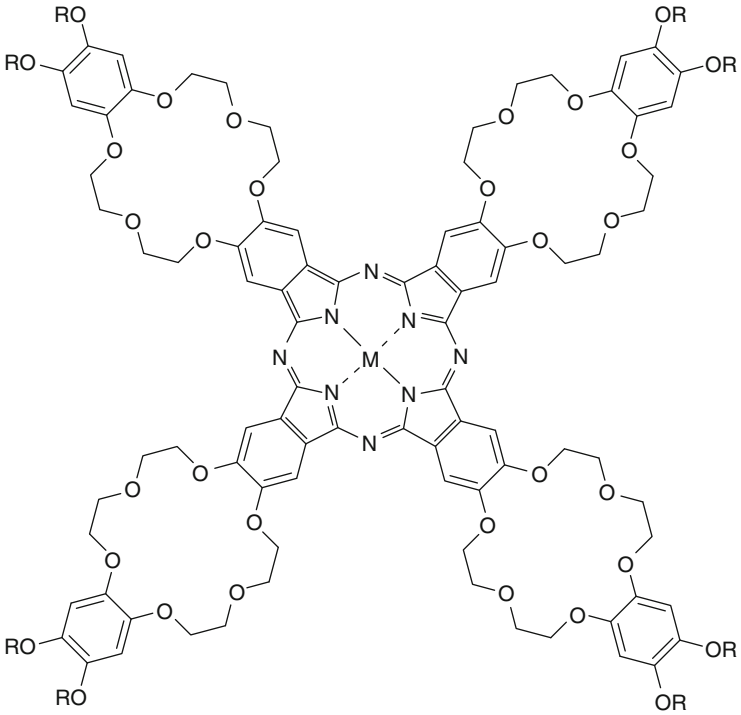

Scheme 60 Crown ether phthalocyanines **114** with different substituents in the central core

themselves consist of up to 25 fibers possessing the diameter of a single **114d** (~60 Å) (Fig. 19a, b).

Addition of potassium ions to the fibers leaves the fibrous structure intact but destroys the helicity [128]. Sandwich complexes between the cation and **114d** are observed. With higher concentrations of potassium, the sandwich complexes break down and isolated $4K^+$·**114d** are observed (Scheme 61). In both complexed forms the salt blocks the chirality transfer from the side chains to the supramolecular assemblies. Such fibers with controllable chirality can be interesting materials for molecular switches or in sensors devices.

At the gel-graphite interface, **114d** forms hexagonal (side-on arrangement of **114d** on the surface) and lamellar (edge-on arrangement) phases [129]. It could also be shown that **114a** can be oriented in high magnetic fields [130].

Ahsen synthesized liquid crystalline phthalocyanine complexes **115** equipped with four monoaza[15]crown-5 moieties substituted with substituted gallic acids

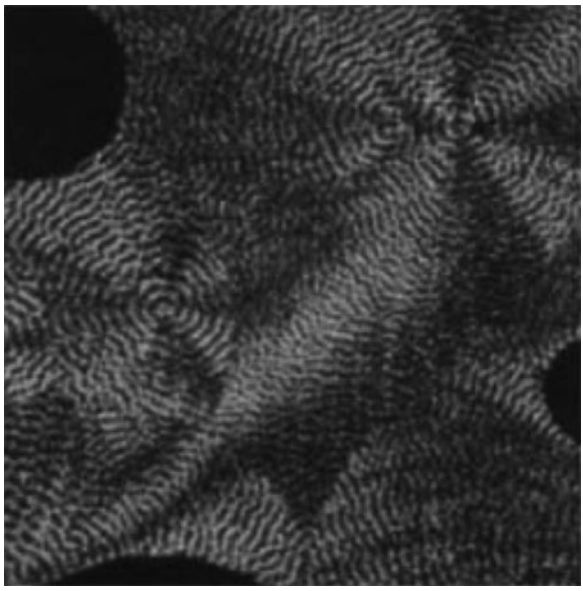

Fig. 17 Spiral-pattern texture of **114d** in the Col* phase. Reproduced by permission of Taylor & Francis (www.informaworld.com) from [127]

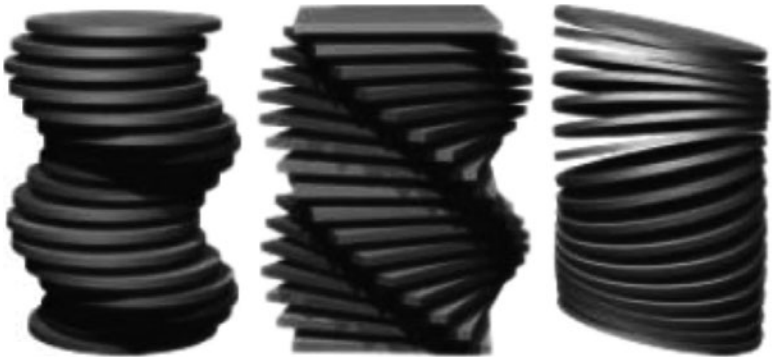

Fig. 18 Spiral staircase (*left*), staggered (*middle*), or tilted and rotated (*right*) arrangement of **114d** in the Col* phase. Reproduced by permission of AAAS from [128]

via amide linkages [131] (Scheme 62). From ~110 °C, both the zinc (**115a**) and the nickel complex (**115b**) exhibit a columnar hexagonal mesophase. Transition to the isotropic phase could not be observed as decomposition started at temperatures exceeding 320 °C.

Akopova reported liquid crystalline phthalocyanines **116a–c** (Scheme 63) with eight peripheral crown ethers devoid of alkyl chains [132]. Nonetheless, discotic nematic phases could be observed as derived from miscibility experiments with the discotic nematogen hexa(cyclohexanebenzoyloxy)triphenylene and optical textures. In the case of metal-free **116a**, a phase width of 43 K was found. Complexation with Zn(II) (**116b**) decreased the phase range to 35 K and with

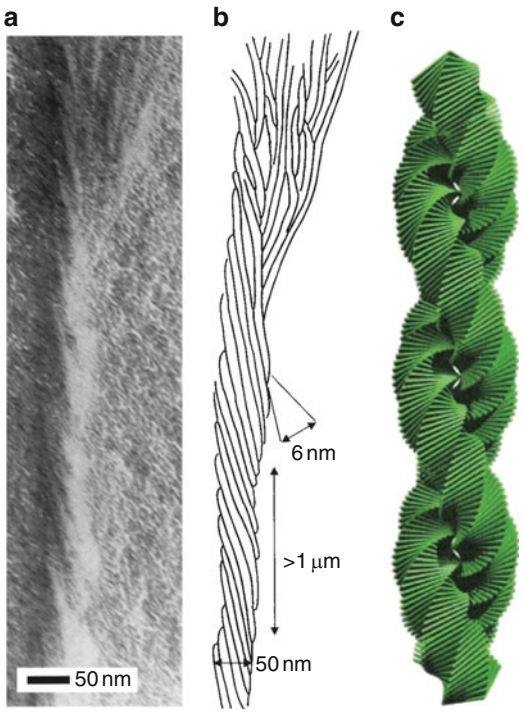

Fig. 19 TEM micrographs of gels of **114d** in chloroform showing left-handed coiled-coil aggregates (**a**) and schematic representation thereof (**b**). (**c**) Calculated model of the coiled coils. Reproduced by permission of AAAS from [128]

Scheme 61 Schematic representation of the formation and breakdown of sandwich complexes between K^+ and **114d**. Reproduced by permission of AAAS from [128]

Ni(II) (**116c**) displayed a mesophase for only 5 K. Complexation of the phthalocyanine seems to increase the interaction between the molecules leading to higher ordered systems with high melting points into the subsequently small mesophases.

The combination of a phthalocyanine ring with crown ether moieties and redox-active tetrathiafulvalenes gave compound **117** (Scheme 64) and was described by Zou as a good candidate for a redox-active Na^+ sensor [133].

Crown ether-phthalocyanines **118** ($n = 0, 1, 2$) (Scheme 65) were used as gas sensors for NO_2. They were found to be superior to the previously used materials

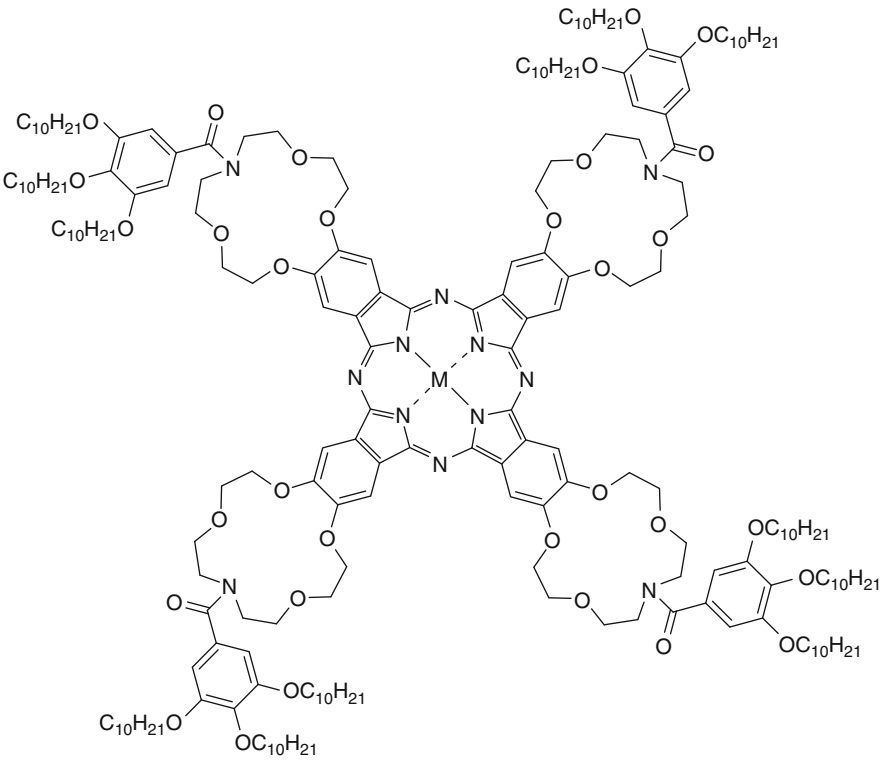

115a M = Zn(II) Cr 117 Col_h >320 decomp
115b M = Ni(II) Cr 109 Col_h >320 decomp

Scheme 62 Zn(II) and Ni(II) complexes of crown ether-modified phthalocyanine **115**

based on phthalocyanines without crown ethers. They offer faster responses and reversal times and can sense NO_2 even at ppb levels [134].

In summary, phthalocyanines modified with crown ethers are interesting synthetic targets as they are prone to form columnar phases. Their electron conductivity and complexation properties make them interesting candidates for the design of sensor materials or supramolecular switches.

2.7 Crown-Like Cyclophanes

Stoddart synthesized biphenylophane derivatives **119** depicted in Scheme 66 [135]. Compared with conventional biphenyl derivatives, the series of **119a–e** exhibits high melting and clearing temperatures. The incorporation of two mesogenic units into a macrocycle seems to be a powerful approach towards mesophase induction

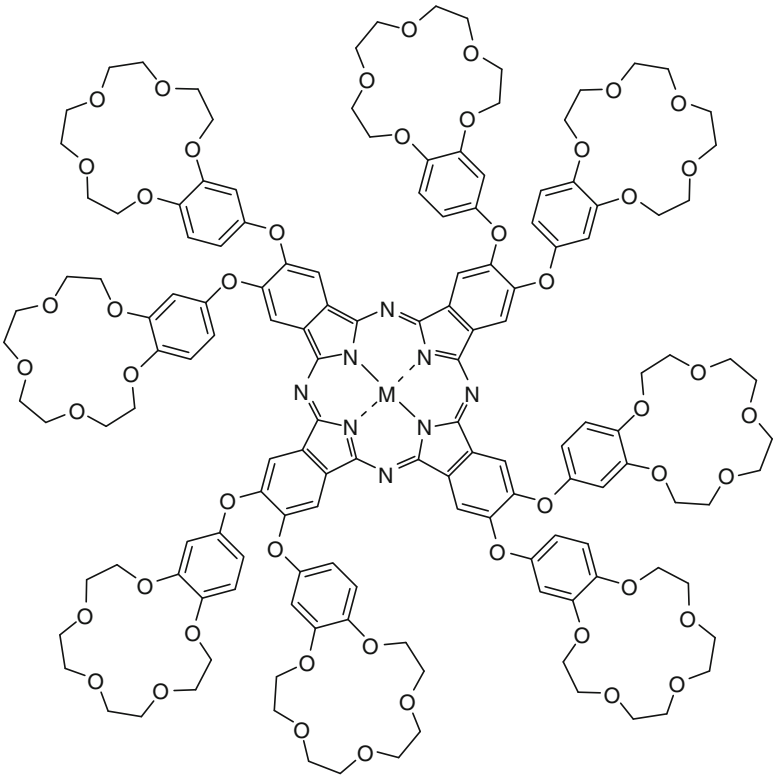

116a	M = 2H	Cr 255 N_D 298 I
116b	M = Zn(II)	Cr 254 N_D 289 I
116c	M = Ni(II)	Cr 293 N_D 298 I

Scheme 63 Liquid crystalline crown ether phthalocyanine **116** without peripheral alkyl chains

and stabilization. Shortening one bridging chain (**119b**) increases the melting and clearing temperature. Lengthening of the linking chain (**119c**) lowers the phase transition temperatures. Compound **119c**, a constitutional isomer of **119a**, contains one longer and one shorter polyether chain. As expected, this "desymmetrization" leads to a depression of the melting and clearing point and the smectic phase range. The mesophase type, namely smectic E and smectic A [136], remains unchanged upon variation of the spacer chains.

Tschierske anticipated that the mesophase type and range is not only dependent on the spacer chains but also on the mesogenic units within the macrocycle. Cyclophane derivatives **120a–d** (Scheme 67) were synthesized and examined [136]. Indeed, the calamitic units have a strong impact on the mesomorphic properties. Phenyl benzoates **120a**,**b** exhibit nematic phases with significantly lower phase transition temperatures as compared with biphenylophane derivatives **119**. Compared with open-chain analogs, the mesophase stabilizing effect of

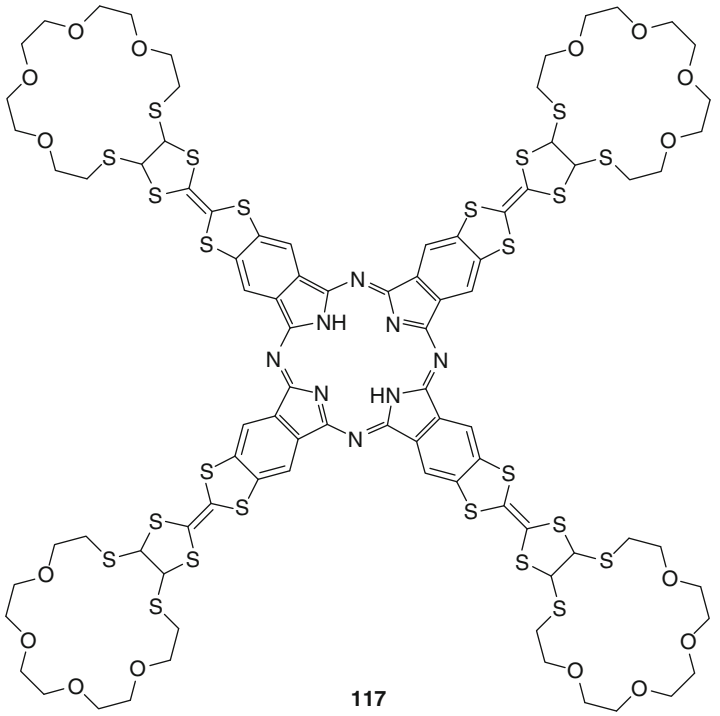

117

Scheme 64 Crown ether phthalocyanine **117** with redox-active tetrathiafulvalene groups

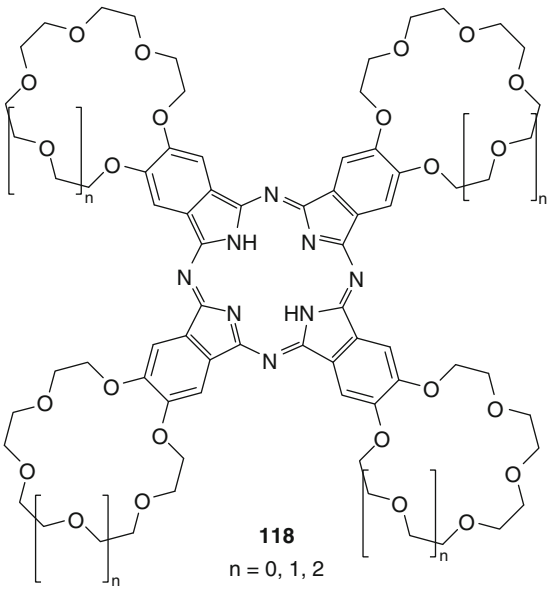

118

n = 0, 1, 2

Scheme 65 Crown ether phthalocyanines **118** as sensor materials for NO_2

Scheme 66 Liquid crystalline biphenylophane derivatives **119**

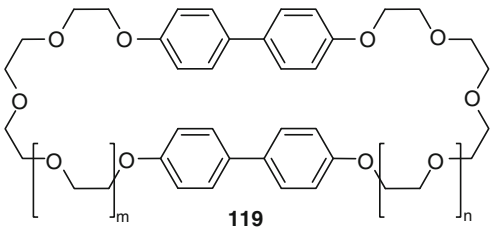

119

119a	m = n = 1	Cr 193 SmE 196 SmA 209 I
119b	m = 0, n = 1	Cr 212 SmE (212) SmA 217 I
119c	m = 0, n = 2	Cr 182 SmE 185 SmA 189 I
119d	m = 1, n = 2	Cr 173 SmE 176 SmA 186 I
119e	m = n = 2	Cr 156 SmE 161 SmA 167 I

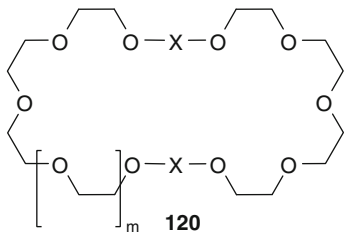

120

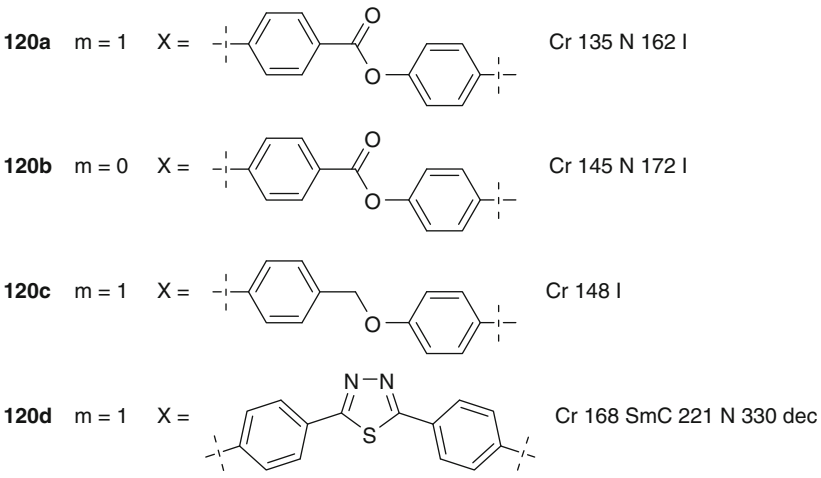

Scheme 67 Liquid crystalline cyclophane derivatives **120**

cyclization could also be observed. The replacement of the carboxylic acid groups by the flexible oxymethylene group in **120c** lead to the loss of mesogenity. Introducing a thiadiazole group can be a powerful tool for the induction of smectic C phases. As expected, **120d** exhibits a smectic C phase, followed by a nematic

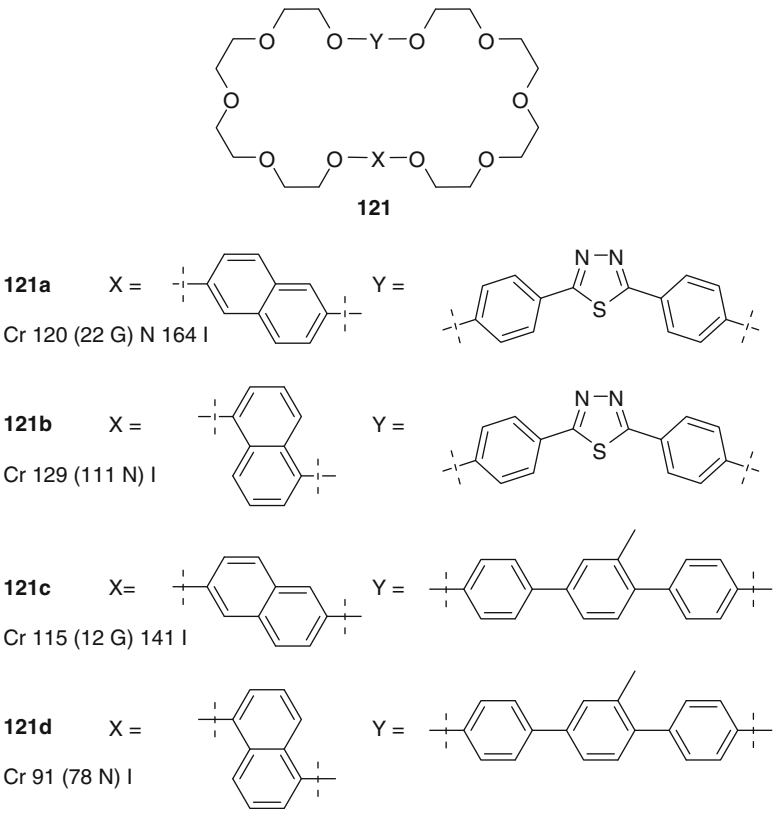

Scheme 68 Unsymmetrical substituted cyclophane derivatives **121**

phase at 221 °C. Clearing could not be observed due to decomposition above 330 °C.

The introduction of suitable mesogenic building blocks into macrocycles will generally have an enormous effect on the stability of mesophases. The reason results from the restricted flexibility of the linked calamitic units.

Tschierske also investigated derivatives **121** (Scheme 68) with different aromatic units in the macrocycle [137]. Besides the conventional thermotropic mesogens *p*-terphenyl or 2,5-diphenyl-1,3,4-thiadiazole, the non-mesomorphic naphthalene ring was included. The thiadiazoles are interesting compounds for electron-transfer interaction and for the templated synthesis of rotaxanes and catenanes. Despite the presence of the non-mesogenic naphthalenes, **121a–d** exhibit nematic phases with high clearing temperatures. The stability of the phases is dependent on the substitution pattern of the naphthalene unit. The 2,6-derivatives **121a**,**c** display higher mesophase stabilities than the corresponding 1,5-substituted derivatives **121b**,**d**. The nematic phases of **121a**,**c** can be supercooled and freeze in a nematic glassy state at 22 and 12 °C, respectively. For **121b**,**d** monotropic phases

Scheme 69 2,4,7-Trinitrofluorenone **122**

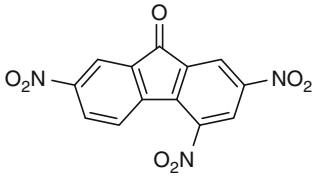

122

were found that did not show the nematic glassy state. Therefore, **121a**,**c** were the first glass-forming liquid crystalline cyclophanes.

Due to the electron-donating ability of naphthalene, compound **121a** was mixed with the electron acceptor 2,4,7-trinitrofluorenone **122** (TNF, Scheme 69) [137]. Upon mixing, a deep red color was observed. Under the POM, focal conic fan textures were observed, indicating a smectic A phase. While small amounts of TNF destabilize the nematic phase, larger amounts of it (~20 mol%) induce the smectic A phase. The attractive electron-acceptor/electron-donor interactions force the individual molecules to adopt a positional order which results in smectic A layers. Mixing of **121b–d** with TNF resulted in the same color but no smectic phases were induced. The reason can be seen in the twisted *p*-terphenyl structure and the 1,5-substitution pattern on the naphthalene ring.

Comparison of macrocyclic liquid crystals **123** based on triethylene glycol and 1-(4-hydroxy-4′-biphenylyl)-2-(4-hydroxyphenyl)butane with varied degree of polymerization with their open-chain analogs **124** (Scheme 70) showed that macrocyclization overrides the established polymer effect in the formation and stabilization of liquid crystalline phases [138]. Contrary to what was thought in the past, the cyclic – and not the linear – architecture is the most powerful way to design molecular and macromolecular liquid crystals. It was found that for higher numbers of *z*, the *anti* conformer is found more often than the *gauche* counterpart. First, on increasing *z*, the cyclic **123** evolve from amorphous to liquid crystalline and back to amorphous. Second, an odd-even dependence of the isotropization temperature as a function of the ring size (i.e., the degree of polymerization) is observed. This is surprising because one would expect an odd-even effect with respect to the spacer chain length – not to the degree of polymerization. The main difference between the odd and even series of *z* in **123** is that in the odd series there is permanently one unit of **125** in the fold of the ring, resulting in a lower rigidity. The presence of the **125** unit in the fold is responsible for the odd-even effect which is not encountered in the linear liquid crystalline polymers **124**. This unusual behavior can lead to a design of nematic crown ethers with a predetermined placement of binding sites.

Crown ether binaphthyl derivatives **128–131** (Scheme 71) were synthesized and investigated by Akagi [139]. Compounds **128–131** were used to induce chiral nematic phases (N*) in liquid crystals. It was found that the helical twisting power increased with decreasing ring size. Helical polyacetylenes were synthesized in the N* phases. It was found that the interdistance between the fibril bundles of the helical polyacetylene was equal to the half-helical pitch of the N* liquid

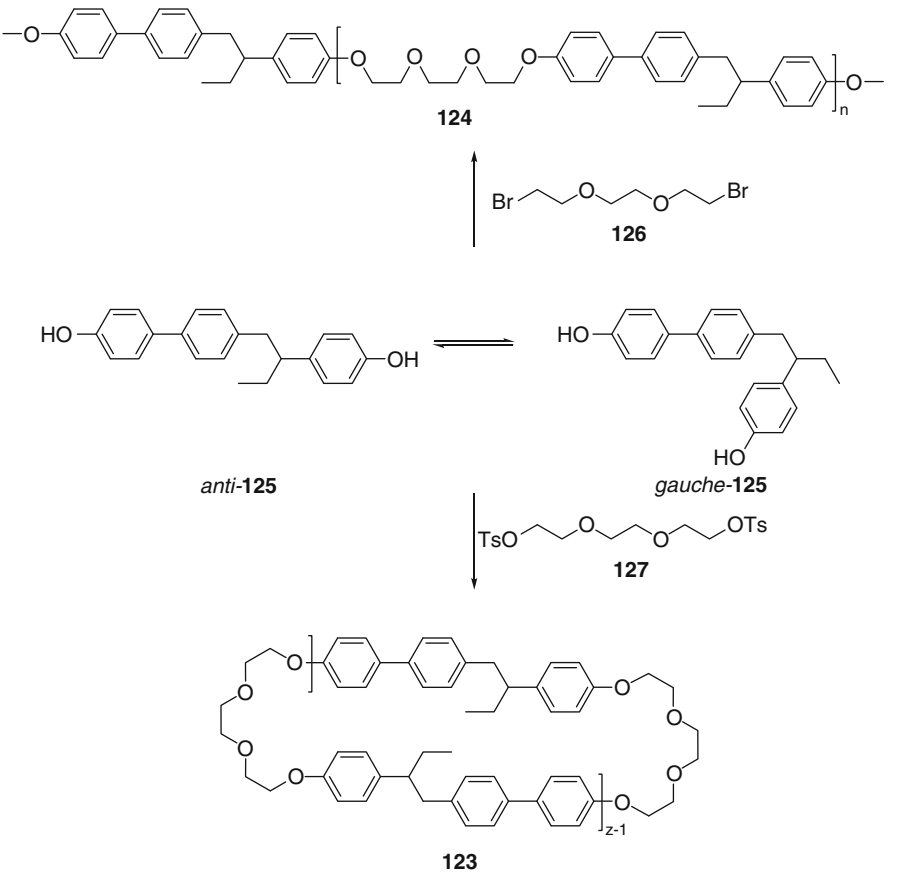

Scheme 70 Cyclic (**123**) vs linear (**124**) liquid crystalline polymers

crystal and the screw direction of the fibrils was opposite to that of the N* liquid crystal. Chiral dopants are promising in gaining control over the screwed structure of polyacetylenes.

2.8 Metallomesogens

The term "metallomesogen" is often used when a (transition) metal is complexed (by coordinative bonds between the *crown heteroatoms* and the metal center) by a crown ether. These compounds were discussed in the previous sections as "complexed crown ethers" (instead of "metallomesogens") together with their uncomplexed precursors. In this section, mesogens with a covalent bond between

Scheme 71 Axial chiral crown-like binaphthyl derivatives **128–131**

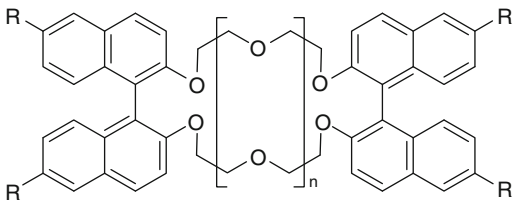

R-**128**, *S*-**129** n = 1
R-**129**, *S*-**129** n = 2
R-**130**, *S*-**130** n = 3

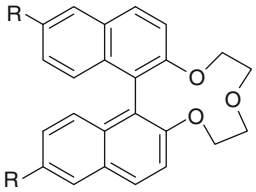

R-**131**

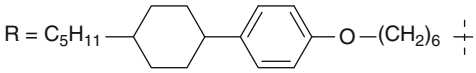

the metal and a *carbon atom that is not part of the crown ether macrocycle* will be discussed.

Tschierske synthesized the "butterfly" mesogens **132–134** (Scheme 72, Table 9). These compounds are based on a macrocyclic crown-like *para*-cyclophane ring containing two 2-phenylpyrimidine units. O*rtho*-palladation and subsequent treatment with substituted half-disks like β-diketones gave the desired dinuclear palladium complexes with 4 (**132**), 8 (**133**), and 12 (**134**) peripheral alkyl chains [127].

All uncomplexed *para*-cyclophanes show monotropic nematic phases upon cooling. For complex **132** with four alkyl chains, a fan-like texture was observed which corresponds to a smectic A phase (Table 9). Compound **134b** shows a mosaic-like texture (Fig. 20) typical for columnar mesophases. The columnar hexagonal phase could be unambiguously confirmed by temperature-dependent X-ray experiments as in the small angle regime of an aligned sample of **134b** a regular hexagon could be detected (Fig. 21).

Surprisingly, **133** with eight alkyl chains was not liquid crystalline (Table 9). With increasing number of alkyl chains a transition from a lamellar to a columnar organization of the molecules takes place. Due to the planar geometry around the Pd(II) centers linked by the macrocycle it is reasonable to assume that the molecules self-assemble in columnar phases. However, a certain number of chains are necessary to surround the molecules completely and to obtain columnar phases.

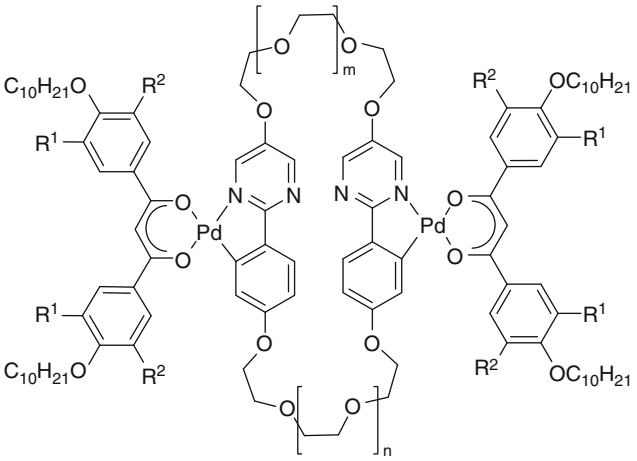

132, 133, 134

Scheme 72 *Ortho*-palladated "butterfly" mesogens **132–134**

Table 9 Mesomorphic properties of **132–134**

Compound	*m*	*n*	R^1	R^2	Phase transitions
132	3	1	H	H	Cr 197 SmA 207 I
133	3	1	$OC_{10}H_{21}$	H	Cr 137 I
134a	3	1	$OC_{10}H_{21}$	$OC_{10}H_{21}$	Cr 110 Col_h 178 I
134b	1	2	$OC_{10}H_{21}$	$OC_{10}H_{21}$	Cr 108 Col_h 211 I
134c	1	3	$OC_{10}H_{21}$	$OC_{10}H_{21}$	Cr 110 Col_h 208 I

Fig. 20 Polarized light optical micrograph of the Col_h phase of **134b** at 103 °C. Reproduced by permission of The Royal Society of Chemistry from [127]

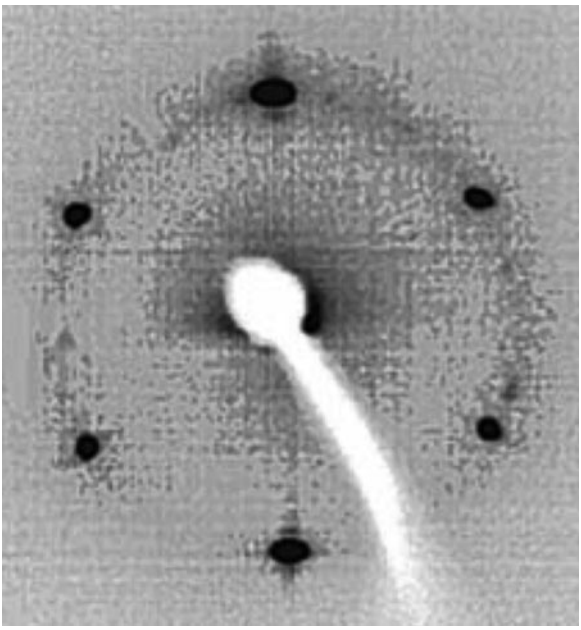

Fig. 21 Small-angle X-ray diffraction pattern of an aligned sample of **134b** at 110 °C. Reproduced by permission of The Royal Society of Chemistry from [127]

If this is not possible, the columnar order gets lost (**133**) or smectic layers are favored (**132**).

With an increasing number of linking polyether chains, the melting and clearing points increase (Table 9) as expected due to the increased rigidity of the molecules. Compounds **132**, **134** are interesting for further research and might open new possibilities to build well-defined structures containing transition metals and ion channels in close proximity to each other embedded in insulating surroundings.

Espinet synthesized imine-substituted benzo[15]crown-5 ethers which were not liquid crystalline. After orthopalladation and anion exchange, dinuclear chloride-bridged complexes **135** (Scheme 73) were obtained [140]. The dinuclear complexes exhibit enantiotropic smectic A phases. The smectic phase ranges of the series increase with increasing chain length in a range of 3 K (**135a**) to 62 K (**135b**). A problem of **135** is the high clearing temperature; the compounds start to decompose after three heating cycles.

In order to obtain mesophases with lower clearing temperatures and broader phases, the number of side chains was increased and the symmetry decreased by exchanging one ligand with a substituted β-diketone carrying two dodecyl chains [140]. The desired effect could be observed: the isotropization temperatures were significantly broadened and the mesophases gained in stability (37 K for **136a**, 65 K for **136b**, Scheme 74).

The mesogenic behavior of $KClO_4$ complexes was also studied, but none of the complexes $KClO_4$·**135** and $KClO_4$·**136** were liquid crystalline and melted accompanied by decomposition [140].

Scheme 73 Liquid crystalline Pd-organic compounds **135**

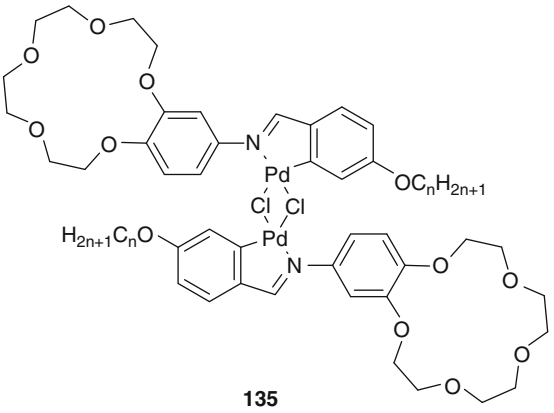

135

135a	n = 4	Cr 220 SmA 223 I
135b	n = 12	Cr 170 SmA 232 I

Scheme 74 Unsymmetrical Pd complexes **136** with improved mesogenic properties

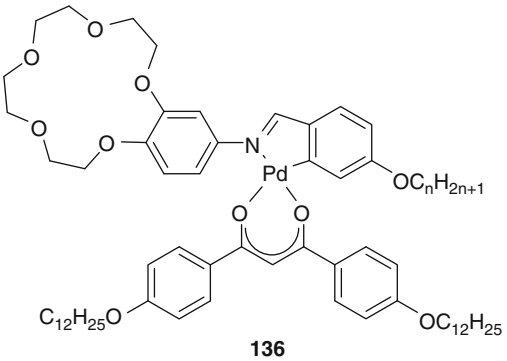

136

136a	n = 4	Cr 86 SmA 123 I
136b	n = 12	Cr 70 SmA 135 I

Similar *ortho*-palladated complexes **137**, **138** (Scheme 75) were presented by Espinet and Coco [141].

All the Pd complexes show mesomorphic behavior. Although one might expect a columnar arrangement, due to the presence of the high number of alkyl chains in the periphery, enantiotropic smectic C phases were observed for **137a** and **138a** (Table 10) as deduced from POM and X-ray results. Complexes **137b** and **138b**, in contrast, show monotropic behavior (Table 10). The present phase could not be identified unambiguously. Complexation with $KClO_4$ produces an important change in the mesomorphic properties. Compared with the parent complexes, the potassium adducts have increased clearing temperatures and mesophase ranges (Table 10). Also, all potassium complexes are enantiotropic liquid crystals. Complexation makes the molecules more polar, the crown ethers become more

Scheme 75 Palladated complex **137**, **138** containing two dibenzo[18]crown-6 units

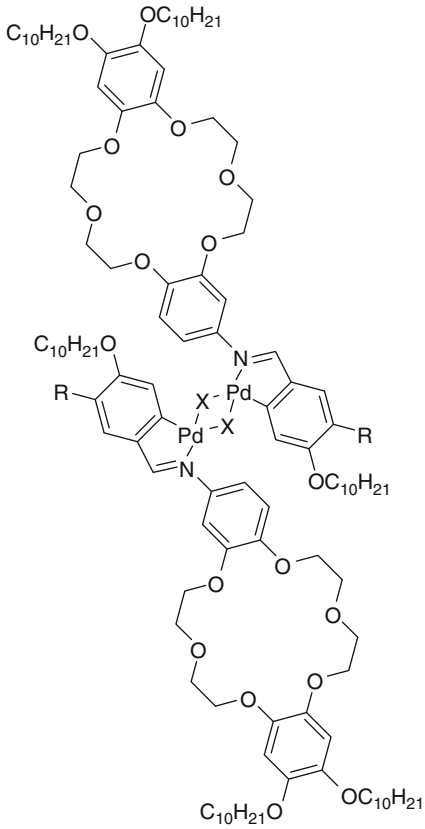

137, 138

Table 10 Mesomorphic properties of **137**, **138**

Compound	R	X	Phase transitions
137a	H	OAc	Cr 108 SmC 122 I
$KClO_4$·**137a**	H	OAc	G 82 SmC 193 I
137b	$OC_{10}H_{21}$	OAc	I 77 M_X 44 G
$KClO_4$·**137b**	$OC_{10}H_{21}$	OAc	Cr 94 M_X 147 I
138a	H	Cl	Cr 109 SmC 200 I
$KClO_4$·**138a**	H	Cl	G 85 SmC 179 I
138b	$OC_{10}H_{21}$	Cl	I 139 M_X 90 Cr
$KClO_4$·**138b**	$OC_{10}H_{21}$	Cl	G 110 M_X 207 I

rigid and, probably, the molecule gains in width. Combined with the improved microsegregation, the increased transition temperatures and phase stability ranges were explained.

Espinet also investigated liquid crystalline gold(I) complexes (Scheme 76) of crown ether isocyanides **139** [142].

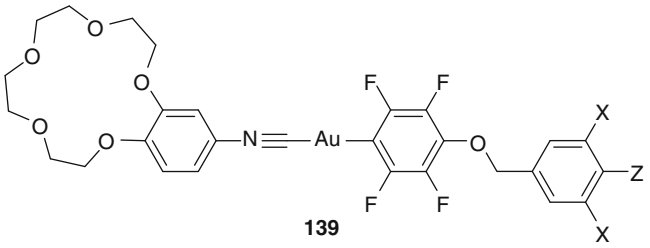

139

Scheme 76 Liquid crystalline Au(I) isocyanide complexes **139**

Table 11 Liquid crystalline properties of **xx**

Compound	X	Z	Phase transitions
139a	H	$OC_{10}H_{21}$	I 37 SmC 2 G
139b	H	$OC_{12}H_{25}$	I 42 SmC
139c	$OC_{10}H_{21}$	$OC_{10}H_{21}$	I 55 SmC
139d	$OC_{12}H_{25}$	$OC_{12}H_{25}$	I 17 M_X 15 Cr

Complexes **139** exhibit monotropic liquid crystalline phases upon cooling from the isotropic phase (Table 11). Complexation with $KClO_4$ destroys the liquid crystalline properties. In the solid state as well as in the mesophase, and even in the isotropic liquid at moderate temperatures, the complexes show luminescence (which is surprising and has been rarely observed) which is visible with the naked eye for **139b**,**d** under a UV-vis chromatography lamp at 298 K. The luminescence properties make **139** interesting for use as sensors or light-emitting diodes.

In summary, metallomesogens of crown ethers are interesting compounds that combine a variety of properties: (1) appropriate metal centers can show luminescence, (2) all properties can be tuned by the addition of alkaline metal salts to the crown ether, and (3) ordered, liquid crystalline phases are possible. With these hybrid materials, interesting applications can be foreseen in the near future.

3 Concluding Remarks

In the last few sections we have shown that liquid crystalline crown ethers are very versatile compounds. In this relatively young field of research, a huge variety of compounds has already been synthesized and studied.

When synthesizing a liquid crystalline crown ether, one has many building blocks readily at hand. The type of crown ether can be chosen from a variety of commercially available or simple to synthesize structures and many mesogenic side groups ranging from rod- to taper- and disc-shaped moieties are accessible. It is possible to create molecules with more than one crown or more than one mesogenic group. Other functionalities, such as dyes or phthalocyanines, can also be part of the mesogen. The final products can be complexed with a variety of main group,

transition, or rare earth metal salts leading to a change of the mesogenic properties. According to the mesogen and the chosen salt, mesophases can be induced, stabilized, or disfavoured. This gives the possibility of fine-tuning liquid crystalline properties "on demand" by an external stimulus (salt complexation) while leaving the molecular structure itself unchanged.

Interesting properties and applications have been reported so far. Liquid crystalline crowns can be used as sensors for salts or even chirality. Luminescence can be observed when choosing appropriate metals for complexation. Supramolecular structures such as channels and wires are readily available. Combined with polymerizable side groups, matrix- or membrane-bound supramolecular structures can be obtained.

The huge versatility of the molecular structures combined with the unique properties makes liquid crystalline crowns interesting compounds for future research. Combination of selective ion complexation, ion conductivity, or even electric conductivity within the substituents gives rise to materials for use in biological or electronic devices. However, much has to be done to develop such systems and to understand fully the properties of liquid crystalline crowns.

References

1. Frängsmyr T (1992) Nobel lectures in chemistry 1981–1990. World Scientific, Singapore
2. Lehn JM (1995) Supramolecular chemistry: concepts and perspectives. Wiley-VCH, Weinheim
3. Lehn JM (1996) Comprehensive supramolecular chemistry. Pergamon, Oxford
4. Cram D (1997) Container molecules and their guests. Royal Society of Chemistry, Cambridge
5. Lehn JM, Malthête J, Levelut AM (1985) J Chem Soc Chem Commun 1794–1796
6. He GX, Wada F, Kikukawa K, Matsuda T (1987) J Chem Soc Chem Commun 1294–1296
7. He GX, Wada F, Kikukawa K, Shinkai S, Matsuda T (1990) J Org Chem 55:541–548
8. Akopova OB (2006) J Struct Chem 47:120–129
9. Blake AJ, Bruce DW, Fallis IA, Parsons S, Richtzenhain H, Ross SA, Schröder M (1996) Philos Trans R Soc London, Ser A 354:395–414
10. Boden N, Movaghar B (1998) Handbook of liquid crystals. Wiley-VCH, Weinheim
11. Gennes PGD, Prost J (1995) The physics of liquid crystals. Oxford University Press, Oxford
12. Brown G (1971) A review of the structure and physical properties of liquid crystals. Butterworths, London
13. Laschat S, Baro A, Steinke N, Giesselmann F, Hägele C, Scalia G, Judele R, Kapatsina E, Sauer S, Schreivogel A, Tosoni M (2007) Angew Chem 119:4916–4973; Angew Chem Int Ed 46:4832–4887
14. Pedersen CJ (1967) J Am Chem Soc 89:7017–7036
15. Pedersen CJ (1970) J Am Chem Soc 92:391–394
16. Pedersen CJ (1988) Angew Chem 100:1053–1059
17. Pedersen CJ (1988) Science 241:536–540
18. Bradshaw J (1997) J Inclusion Phenom Macrocyclic Chem 29:221–246
19. Patai S (1980) Chemistry of ethers, crown ethers, hydroxyl groups and their sulphur analogues. Wiley, Chichister

20. Tsukanov AV, Dubonosov AD, Bren VA, Minkin VI (2008) Chem Heterocycl Comp 44:899–923
21. Minkin VI, Dubonosov AD, Bren VA, Tsukanov AV (2008) Arkivoc IV:90–102
22. Kralj M, Tušek-Božić L, Frkanec L (2008) ChemMedChem 3:1478–1492
23. Grigoras M, Stafie L (2010) Supramolecular Chem 22:237–248
24. Walkowiak W, Kozlowski CA (2009) Desalination 240:186–197
25. Urs MSR, Surendranath V (1983) Mol Cryst Liq Cryst 99:279–284
26. Gallardo H, Silva FC (1987) J Chem Soc Perkin Trans 2 319–321
27. He GX, Wada F, Kikukawa K, Shinkai S, Matsuda T (1990) J Org Chem 55:548–554
28. Shinkai S, Shimamoto K, Manabe O, Sisido M (1989) Makromol Chem Rapid Commun 10:361–366
29. Shinkai S, Nishi T, Ikeda A, Matsuda T, Shimamoto K, Manabe O (1990) J Chem Soc Chem Commun 303–304
30. He Y, Xie M, Li L, Liao L (1997) Mol Cryst Liq Cryst 304:165–169
31. Jiang Q, Li L, Xie M, Ran J (1997) Mol Cryst Liq Cryst 302:1311–1319
32. Leblanc K, Berdague P, Bayle J, Judeinstein P, Rault J (2000) Chem Commun 1291–1292
33. Blake AJ, Bruce DW, Danks JP, Fallis IA, Guillon D, Ross SA, Richtzenhain H, Schröder M (2001) J Mater Chem 11:1011–1018
34. Percec V, Rodenhouse R (1989) Macromolecules 22:4408–4412
35. Ungar G, Percec V, Rodenhouse R (1991) Macromolecules 24:1996–2002
36. Hsiue G, Wen J, Hsu C (1991) Makromol Chem 192:2243–2254
37. Rodenhouse R, Percec V (1991) Polym Bull 25:47–54
38. Rodenhouse R, Percec V (1991) Makromol Chem 192:1873–1879
39. Percec V, Rodenhouse R (1991) J Polym Sci Part A Polym Chem 29:15–28
40. Percec V, Johansson G, Rodenhouse R (1992) Macromolecules 25:2563–2565
41. Percec V, Johansson G (1993) J Mater Chem 3:83–96
42. Shibaev V, Medvedev A, Bobrovsky A (2008) J Polym Sci Part A Polym Chem 46:6532–6541
43. Shinkai S, Minami T, Kusano Y, Manabe O (1983) J Am Chem Soc 105:1851–1856
44. Shinkai S, Ogawa T, Kusano Y, Manabe O, Kikukawa K, Goto T, Matsuda T (1982) J Am Chem Soc 104:1960–1967
45. Nishi T, Ikeda A, Matsuda T, Shinkai S (1991) J Chem Soc Chem Commun 339–341
46. Shinkai S, Nishi T, Matsuda T (1991) Chem Lett 437–440
47. Vögtle F, Knops P (1991) Angew Chem 103:972–974; Angew Chem Int Ed 30:958–960
48. Kimura K, Kawai Y, Oosaki S, Yajima S, Yoshioka Y, Sakurai Y (2002) Anal Chem 74:5544–5549
49. Oosaki S, Yajima S, Kimura K (2007) Anal Sci 23:963–967
50. Feng R, Tian Y, Chen H, Huang Z, Zeng Z (2010) Electrophoresis 31:1975–1982
51. Schröter JA, Tschierske C, Wittenberg M, Wendorf JH (1997) Angew Chem 109:1160–1163; Angew Chem Int Ed 36:1119–1121
52. Plehnert R, Schröter JA, Tschierske C (1998) J Mater Chem 8:2611–2626
53. Plehnert R, Schröter JA, Tschierske C (1998) Langmuir 14:5245–5249
54. Tschierske C (1998) J Mater Chem 8:1485–1508
55. Kaller M, Tussetschläger S, Fischer P, Deck C, Baro A, Giesselmann F, Laschat S (2009) Chem Eur J 15:9530–9542
56. Leblanc K, Berdague P, Judeinstein P, Bayle JP, Guermouche MH (2001) Liq Cryst 28:265–269
57. Sinha N, Ramanathan KV, Leblanc K, Judeinstein P, Bayle JP (2002) Liq Cryst 29:449–457
58. Ziessel R, Camerel F, Donnio B (2009) Chem Rec 9:1–23
59. Rodenhouse R, Percec V, Feiring AE (1990) J Polym Sci Part C Polym Lett 28:345–355
60. Xie M, Peng M, Jiang Q, Hu Z, Wang X (1996) Liq Cryst 21:461–467
61. Pannell KH, Yee W, Lewandos GS, Hambrick DC (1977) J Am Chem Soc 99:1457–1461
62. Zhang S, He K, Zheng S, Tang S, Zhang X, Li Z (2004) Chin J Chem 22:395–399

63. Parikh VB, Menon SK (2008) Mol Cryst Liq Cryst 482:71–83
64. Xie M, Qin J, Hong F, Wang L (1991) Mol Cryst Liq Cryst 209:309–318
65. Heiney PA, Stetzer MR, Mindyuk OY, DiMasi E, McGhie AR, Liu H, Smith ABI (1999) J Phys Chem B 103:6206–6214
66. Xie M, Liu S, Liu G, Li L, Jiang Q (1996) Liq Cryst 21:313–316
67. Tuffin RP, Toyne KJ, Goodby JW (1995) J Mater Chem 5:2093–2104
68. Tuffin RP, Toyne KJ, Goodby JW (1996) J Mater Chem 6:1271–1282
69. Neve F, Ghedini M, Levelut A, Francescangeli O (1994) Chem Mater 6:70–76
70. Neve F, Ghedini M (1994) J Incl Phenom Macrocycl Chem 15:259–272
71. Belarbi Z, Sirlin C, Simon J, Andre JJ (1989) J Phys Chem 93:8105–8110
72. Miwa H, Kobayashi N, Ban K, Ohta K (1999) Bull Chem Soc Jpn 72:2719–2728
73. Ban K, Nishizawa K, Ohta K, van de Craats AM, Warman JM, Yamamoto I, Shirai H (2001) J Mater Chem 11:321–331
74. Qi M, Liu G (2003) ChemPhysChem 4:605–608
75. Nakai T, Ban K, Ohta K, Kimura M (2002) J Mater Chem 12:844–850
76. Qi M, Liu G (2003) J Phys Chem B 107:7640–7646
77. Binnemans K, Sleven J, De Feyter S, De Schryver FC, Donnio B, Guillon D (2003) Chem Mater 15:3930–3938
78. Suarez S, Mamula O, Scopelliti R, Donnio B, Guillon D, Terazzi E, Piguet C, Bunzli JG (2005) New J Chem 29:1323–1334
79. Suárez S, Imbert D, Gumy F, Piguet C, Bünzli JG (2004) Chem Mater 16:3257–3266
80. Suárez S, Mamula O, Imbert D, Piguet C, Bünzli JG (2003) Chem Commun 1226–1227
81. Blake AJ, Bruce DW, Fallis IA, Parsons S, Schröder M (1994) J Chem Soc Chem Commun 2471–2473
82. Richtzenhain H, Blake AJ, Bruce DW, Fallis IA, Li W, Schröder M (2001) Chem Commun 2580–2581
83. Percec V, Rodenhouse R (1989) Macromolecules 22:2043–2047
84. Percec V, Johansson G, Heck J, Ungar G, Batty SV (1993) J Chem Soc Perkin Trans 1 1411–1420
85. Johansson G, Percec V, Ungar G, Abramic D (1994) J Chem Soc Perkin Trans 1 447–459
86. Ungar G, Batty SV, Percec V, Heck J, Johansson G (1994) Adv Mater Opt Electron 4:303–313
87. Tomazos D, Out G, Heck JA, Johansson G, Perce V, Möller M (1994) Liq Cryst 16:509–527
88. Percec V, Heck J, Johansson G, Tomazos D, Kawasumi M, Ungar G (1994) J Macromol Sci A 31:1031–1070
89. Percec V, Heck J, Johansson G, Tomazos D, Kawasumi M, Chu P, Ungar G (1994) Mol Cryst Liq Cryst 254:137–196
90. Percec V, Johansson G, Ungar G, Zhou J (1996) J Am Chem Soc 118:9855–9866
91. Jung H, Kim SO, Hudson SD, Percec V (2002) Appl Phys Lett 80:395–397
92. Percec V, Cho W, Ungar G, Yeardley DJP (2002) Chem Eur J 8:2011–2025
93. Gitsov I, Ivanova PT (2000) Chem Commun 269–270
94. Steinke N, Frey W, Baro A, Laschat S, Drees C, Nimtz M, Hägele C, Giesselmann F (2006) Chem Eur J 12:1026–1035
95. Steinke N, Jahr M, Lehmann M, Baro A, Frey W, Tussetschläger S, Sauer S, Laschat S (2009) J Mater Chem 19:645–654
96. Steinke N (2007) Neuartige columnare Flüssigkristalle mit Kronenether-Einheit als zentralem Baustein. Mensch & Buch Verlag, Berlin
97. Beginn U, Zipp G, Möller M (2000) Chem Eur J 6:2016–2023
98. Beginn U, Zipp G, Möller M (2000) Adv Mater 12:510–513
99. Beginn U, Zipp G, Mourran A, Walther P, Möller M (2000) Adv Mater 12:513–516
100. Beginn U, Zipp G, Moller M, Johansson G, Percec V (1997) Macromol Chem Phys 198:2839–2852
101. Percec V, Zipp G, Johansson G, Beginn U, Moeller M (1997) Macromol Chem Phys 198:265–277

102. Beginn U, Zipp G, Möller M (2000) J Polym Sci Part A Polym Chem 38:631–640
103. Malthête J, Poupinet D, Vilanove R, Lehn J (1989) J Chem Soc Chem Commun 1016–1019
104. Mertesdorf C, Ringsdorf H (1989) Liq Cryst 5:1757–1772
105. Lattermann G (1989) Liq Cryst 6:619–625
106. Lattermann G (1990) Mol Cryst Liq Cryst 182:299–311
107. Lattermann G, Schmidt S, Gallot B (1992) J Chem Soc Chem Commun 1091–1092
108. Tatarsky D, Banerjee K, Ford WT (1990) Chem Mater 2:138–141
109. Idziak SHJ, Maliszewskyj NC, Heiney PA, McCauley JP, Sprengeler PA, Smith AB (1991) J Am Chem Soc 113:7666–7672
110. Malthête J, Levelut A, Lehn JM (1992) J Chem Soc Chem Commun 1434–1436
111. Mori A, Yamamoto E, Kubo K, Ujiie S, Baumeister U, Tschierske C (2010) Liq Cryst 37:1059–1065
112. Liebmann A, Mertesdorf C, Plesnivy T, Ringsdorf H, Wendorff JH (1991) Angew Chem 103:1358–1361; Angew Chem Int Ed 30:1375–1377
113. Lattermann G, Schmidt S, Kleppinger R, Wendorff JH (1992) Adv Mater 4:30–33
114. Schmidt S, Lattermann G, Kleppinger R, Wendorff J (1994) Liq Cryst 16:693–702
115. Mertesdorf C, Ringsdorf H, Stumpe J (1991) Liq Cryst 9:337–357
116. Hirose T, Tanaka S, Aoki Y, Nohira H (2000) Chem Lett 1290–1291
117. Yan J, Tang R, Zhang B, Zhu X, Xi F, Li Z, Chen E (2009) Macromolecules 42:8451–8459
118. Kaller M, Staffeld P, Haug R, Frey W, Giesselmann F, Laschat S (2011) Liq Cryst 38:531–553
119. Schultz A, Laschat S, Saipa A, Giesselmann F, Nimtz M, Schulte JL, Baro A, Miehlich B (2004) Adv Funct Mater 14:163–168
120. Kaller M, Deck C, Meister A, Hause G, Baro A, Laschat S (2010) Chem Eur J 16:6326–6337
121. Steinke N, Kaller M, Nimtz M, Baro A, Laschat S (2010) Liq Cryst 37:1139–1149
122. Li J, He Z, Gopee H, Cammidge AN (2010) Org Lett 12:472–475
123. van Nostrum CF, Picken SJ, Nolte RJM (1994) Angew Chem 106:2298–2300; Angew Chem Int Ed 33:2173–2175
124. van Nostrum CF, Picken SJ, Schouten A, Nolte RJM (1995) J Am Chem Soc 117:9957–9965
125. van der Pol JF, Neeleman E, Zwikker JW, Nolte RJM, Drenth W, Aerts J, Visser R, Picken SJ (1989) Liq Cryst 6:577–592
126. Nolte RJM (2006) Liq Cryst 33:1373–1377
127. Hegmann T, Neumann B, Kain J, Diele S, Tschierske C (2000) J Mater Chem 10:2244–2248
128. Engelkamp H, Middelbeek S, Nolte RJM (1999) Science 284:785–788
129. Samorí P, Engelkamp H, de Witte P, Rowan AE, Nolte RJM, Rabe JP (2001) Angew Chem 113:2410–2412; Angew Chem Int Ed 40:2348–2350
130. Boamfa M, Christianen P, Engelkamp H, Nolte R, Maan J (2004) Adv Funct Mater 14:261–265
131. Yilmaz F, Atilla D, Ahsen V (2004) Polyhedron 23:1931–1937
132. Akopova OB, Logacheva NM, Baulin VE, Tsivadze AY (2008) Russ J Gen Chem 78:2118–2124
133. Wang R, Liu W, Chen Y, Zuo J, You X (2009) Dyes Pigm 81:40–44
134. Wright JD, Roisin P, Rigby G, Nolte RJ, Cook MJ, Thorpe SC (1993) Sens Actuators B Chem 13:276–280
135. Ashton PR, Joachimi D, Spencer N, Stoddart JF, Tschierske C, White AJP, Williams DJ, Zab K (1994) Angew Chem 106:1563–1566; Angew Chem Int Ed 33:1503–1506
136. Joachimi D, Ashton P, Sauer C, Spencer N, Tschierske C, Zab K (1996) Liq Cryst 20:337–348
137. Neumann B, Joachimi D, Tschierske C (1997) Adv Mater 9:241–244
138. Percec V, Turkaly PJ, Asandei AD (1997) Macromolecules 30:943–952
139. Akagi K, Guo S, Mori T, Goh M, Piao G, Kyotani M (2005) J Am Chem Soc 127:14647–14654
140. Arias J, Bardají M, Espinet P (2006) J Organomet Chem 691:4990–4999
141. Coco S, Cordovilla C, Espinet P, Gallani J, Guillon D, Donnio B (2008) Eur J Inorg Chem 1210–1218
142. Arias J, Bardají M, Espinet P (2008) Inorg Chem 47:3559–3567

http://www.springer.com/978-3-642-27590-6

Liquid Crystals
Materials Design and Self-assembly
Tschierske, C. (Ed.)
2012, XII, 412 p., Hardcover
ISBN: 978-3-642-27590-6